MRI for Technologists

4712-402 MRI of the Body

PROGRAM INFORMATION

MRI for Technologists is a training program designed to meet the needs of radiologic technologists entering or working in the field of magnetic resonance imaging (MRI). These units are designed to augment classroom instruction and on-site training for radiologic technology students and professionals planning to take the review board examinations, as well as to provide a review for those looking to refresh their knowledge base in MR imaging.

Original Release Date: **March 2014**
Review Date: **June 2018**
Expiration Date: **April 1, 2021**

This material will be reviewed for continued accuracy and relevance. Please go to www.icpme.us for up-to-date information regarding current expiration dates.

OVERVIEW

The skill of the technologist is the single most important factor in obtaining good quality diagnostic images. A successful MRI examination is the culmination of many factors under the direct control of the technologist.

MRI of the Body introduces the learner to elements of MRI important for performing high-quality diagnostic studies of the body. Significant advances in MR hardware and software have contributed to the significant growth of body MRI in recent years. Acquisition times are sufficiently short to be performed within a single breath-hold, and the majority of MR protocols can be completed in less than 30 minutes.

EDUCATIONAL OBJECTIVES

After completing this educational material, the reader should be able to:

General Approach to Body MRI

- Explain the major challenges of body MRI
- Discuss methods for reducing or eliminating artifacts seen in body MRI
- Describe coil selection and image reconstruction

MR Angiography of the Body

- Discuss the advantages and disadvantages of noncontrast-enhanced time-of-flight techniques in vascular imaging
- Explain the role of gadolinium-based contrast agents in vascular imaging
- Discuss the advantages and disadvantages of different bolus timing methods
- Identify the advantages of contrast-enhanced image acquisition

Liver

- Develop a protocol for liver MRI
- Identify benign and malignant liver disease processes
- Develop protocols for imaging of the biliary ducts and gallbladder
- Describe the role of hepatocyte-specific gadolinium-based contrast agents

Adrenal Glands and Kidney

- Describe the basic imaging requirements for the adrenal glands and kidneys
- Name the major MR findings for each organ

Small Bowel

- Describe the signs and symptoms of inflammatory bowel disease and the two major types of pathology
- Explain the preparation required for MR enterography
- Discuss the major applications and findings for MR enterography

Female Pelvis

- Name the primary MRI findings of the female pelvis, including pelvic floor weakness
- Discuss obstetrical and fetal imaging when exposure to ionizing radiation must be avoided
- Respond appropriately to the patient given the sensitive nature of the female pelvic MRI exam

Bladder

- Describe the role of MRI as an adjunct to ultrasonography for bladder imaging
- Discuss imaging techniques required for visualization of the bladder and bladder wall

Prostate

- Identify the anatomy and function of the prostate gland
- Explain the basic sequences for prostate imaging
- Describe MRI prostate findings and the utility of MRI-guided prostate biopsy
- Respond appropriately to the patient given the sensitive nature of the prostate MRI exam

Anal-rectal Area

- Identify the main anatomical structures of the anal-rectal area
- List the major imaging parameters for evaluating anorectal cancer
- Discuss the advantages of MRI vs CT in visualizing anorectal cancer
- Name typical MRI findings of the anal-rectal area

EDUCATIONAL CREDIT

This program has been approved by the American Society of Radiologic Technologists (ASRT) for 5.0 ARRT Category A continuing education credits.

HOW TO RECEIVE CREDIT

Estimated time to complete this activity is 5 hours. The posttest and evaluation are required to receive credit and must be completed online.

- In order to access the posttest and evaluation, enroll in the online course at icpme.us
- Read the entire activity.
- Log in to your account at icpme.us to complete the posttest and evaluation, accessible through the course link in your account.
- A passing grade of at least 75% is required to be eligible to receive credit.
- You may take the test up to three times.
- Upon receipt of a passing grade, you will be able to print a certificate of credit from your online account.
- Your credit certificate will remain in your account as a permanent record of credits earned at icpme.us

FACULTY

Thomas Schrack, BS, ARMRIT
Manager, MR Education and Technical Development
Fairfax Radiological Consultants
Fairfax, VA

Currently serving as Manager of MR Education and Technical Development at Fairfax Radiological Consultants in Fairfax, VA, Thomas Schrack served as Adjunct Faculty Instructor for Northern Virginia Community College from more than 10 years, teaching MR physics and clinical procedures. He serves on the Board of Examiners of the American Registry of Magnetic Resonance Imaging Technologists (ARMRIT) and in 2013 was elected to the Board of Directors. Mr. Schrack is also the Co-Founder and Program Director of the Tesla Institute of MRI Technology, a school offering certification in MRI for radiologic technologists and others interested in entering the field of MRI.

Mr. Schrack is the author of *Echo Planar Imaging: An Applications Guide,* GE Healthcare, 1996, and contributing author, *Magnetic Resonance Imaging in Orthopaedics & Sports Medicine* with David Stroller, MD, 1997. Working with International Center for Postgraduate Medical Education, Mr. Schrack has authored or co-authored several units of the *MRI for Technologists* series, including *MRI Systems and Coil Technology, MR Image Postprocessing and Artifacts, Patient and Facility Safety in MRI, MRI Contrast Agent Safety, Advanced MRI Neurological Applications, MRI of the Brain and Spine, Musculoskeletal MRI, Clinical Magnetic Resonance Angiography, MRI of the Body, and Cardiac MRI.*

Mr. Schrack is a graduate of The Pittsburgh NMR Institute, James Madison University, and Northern Virginia Community College.

Lisa K. Wall, BS, RT (R)(MR)(CV)
Senior Applications Specialist
Duke Hospital Systems
Duke University School of Medicine
Department of Radiology
Durham, NC

Ms. Wall is Senior Applications Technologist at Duke University Hospital's MRI Unit. Ms. Wall graduated from Elon University with a BS in Radiology Technology and shortly thereafter joined the staff at Duke, where she has worked in MRI for the past 20 years.

ACKNOWLEDGMENTS

Our thanks to both Mr. Schrack and Ms. Wall for their updates of this material, as well as to Stephen Dashnaw, ARMRIT, Director of Imaging Services at Columbia University Medical Center in New York for his review of the content. Peter Caravan, PhD, and Alexander Guimaraes, MD, PhD, from Massachusetts General Hospital, Harvard Medical School contributed the material on gadolinium-based contrast agents and potential risks to patients, for which we are grateful.

SPONSORED BY

icpme
Your Partner in Medical Education

SUPPORTED BY AN EDUCATIONAL GRANT FROM

BAYER
Bayer HealthCare
Pharmaceuticals

DISCLAIMER

Participants have an implied responsibility to use the newly acquired information to enhance patient outcomes and their own professional development. The information presented in this activity is not meant to serve as a guideline for patient management. Any procedures, medications, or other courses of diagnosis or treatment discussed or suggested in this activity should not be used by clinicians without evaluation of their patient's conditions and possible contraindications on dangers in use, review of any applicable manufacturer's product information, and comparison with recommendations of other authorities.

FDA Drug Safety Communication: FDA warns that gadolinium-based contrast agents (GBCAs) are retained in the body; requires new class warnings

https://www.fda.gov/Drugs/DrugSafety/ucm589213.htm Accessed June 14, 2018.

05-16-2018 Update

In addition to approving the updated prescribing information concerning the gadolinium retention safety issues described in the Drug Safety Communication below, FDA has also approved new patient Medication Guides for all GBCAs.

Health care professionals and patients can access the patient Medication Guides according to the GBCA drug name* on the Medication Guides webpage, or the latest prescribing information by searching in Drugs@FDA.

All MRI centers should provide a Medication Guide the first time an outpatient receives a GBCA injection or when the information is substantially changed. In general, hospital inpatients are not required to receive a Medication Guide unless the patient or caregiver requests it. A health care professional who determines that it is not in a patient's best interest to receive a Medication Guide because of significant concerns about its effects may direct that it not be provided to that patient; however, the Medication Guide should be provided to any patient who requests the information.†

*The brand names of the GBCAs can be found in Table 1 below.
†For more information on distribution of Medication Guides, see the Guidance Document, the Drug Info Rounds Video, or the Code of Federal Regulations at 21 CFR 208.26.

This is an update to the FDA Drug Safety Communication: FDA identifies no harmful effects to date with brain retention of gadolinium-based contrast agents for MRIs; review to continue issued on May 22, 2017.

12-19-2017 Safety Announcement

The U.S. Food and Drug Administration (FDA) is requiring a new class warning and other safety measures for all gadolinium-based contrast agents (GBCAs) for magnetic resonance imaging (MRI) concerning gadolinium remaining in patients' bodies, including the brain, for months to years after receiving these drugs. Gadolinium retention has not been directly linked to adverse health effects in patients with normal kidney function, and we have concluded that the benefit of all approved GBCAs continues to outweigh any potential risks.

However, after additional review and consultation with the Medical Imaging Drugs Advisory Committee, we are requiring several actions to alert health care professionals and patients about gadolinium retention after an MRI using a GBCA, and actions that can help minimize problems. These include requiring a new patient Medication Guide*, providing educational information that every patient will be asked to read before receiving a GBCA. We are also requiring manufacturers of GBCAs to conduct human and animal studies to further assess the safety of these contrast agents.

GBCAs are used with medical imaging devices called MRI scanners to examine the body for problems such as cancer, infections, or bleeding. GBCAs contain gadolinium, a heavy metal. These contrast agents are injected into a vein to improve visualization of internal organs, blood vessels, and tissues during an MRI, which helps health care professionals diagnose medical conditions. After being administered, GBCAs are mostly eliminated from the body through the kidneys. However, trace amounts of gadolinium may stay in the body long-term. Many GBCAs have been on the market for more than a decade.

Health care professionals should consider the retention characteristics of each agent when choosing a GBCA for patients who may be at higher risk for gadolinium retention (see Table 1 listing GBCAs). These patients include those requiring multiple lifetime doses, pregnant women, children, and patients with

inflammatory conditions. Minimize repeated GBCA imaging studies when possible, particularly closely spaced MRI studies. However, do not avoid or defer necessary GBCA MRI scans.

Patients, parents, and caregivers should carefully read the new patient Medication Guide* that will be given to you before receiving a GBCA. The Medication Guide explains the risks associated with GBCAs. Also tell your health care professional about all your medical conditions, including:

- If you are pregnant or think you might be pregnant
- The date of your last MRI with gadolinium and if you have had repeat scans with gadolinium
- If you have kidney problems

There are two types of GBCAs based on their chemical structures: linear and macrocyclic (see Table 1 below). Linear GBCAs result in more retention and retention for a longer time than macrocyclic GBCAs. Gadolinium levels remaining in the body are higher after administration of Omniscan (gadodiamide) or OptiMARK (gadoversetamide) than after Eovist (gadoxetate disodium), Magnevist (gadopentetate dimeglumine), or MultiHance (gadobenate dimeglumine). Gadolinium levels in the body are lowest after administration of Dotarem (gadoterate meglumine), Gadavist (gadobutrol), and ProHance (gadoteridol); the gadolinium levels are also similar across these agents.

*The Medication Guide will be posted once it is approved.

Table 1. FDA-Approved GBCAs*

Brand name	Generic name	Chemical Structure
Dotarem†	gadoterate meglumine	Macrocyclic
Eovist	gadoxetate disodium	Linear
Gadavist†	gadobutrol	Macrocyclic
Magnevist	gadopentetate dimeglumine	Linear
MultiHance	gadobenate dimeglumine	Linear
Omniscan‡	gadodiamide	Linear
OptiMARK‡	gadoversetamide	Linear
ProHance†	gadoteridol	Macrocyclic

*Linear GBCAs result in more gadolinium retention in the body than macrocyclic GBCAs.
†Gadolinium levels remaining in the body are LOWEST and similar after use of these agents.
‡Gadolinium levels remaining in the body are HIGHEST after use of these agents.

To date, the only known adverse health effect related to gadolinium retention is a rare condition called nephrogenic systemic fibrosis (NSF) that occurs in a small subgroup of patients with pre-existing kidney failure. We have also received reports of adverse events involving multiple organ systems in patients with normal kidney function. A causal association between these adverse events and gadolinium retention could not be established.

We are continuing to assess the health effects of gadolinium retention in the body and will update the public when new information becomes available. We are requiring the following specific changes to the labeling of all GBCAs:

- A *Warning and Precaution*
- Changes related to gadolinium retention in the *Adverse Reactions, Pregnancy, Clinical Pharmacology*, and *Patient Instructions* sections

We urge patients and health care professionals to report side effects involving GBCAs or other medicines to the FDA MedWatch program.

Tom Schrack, BS, ARMRIT
Fairfax Radiological Consultants
Fairfax, VA

4712-402
GENERAL APPROACH TO BODY MRI

After completing this section, the reader should be able to:

- Explain the major challenges of body MRI
- Discuss methods for reducing or eliminating artifacts seen in body MRI
- Describe coil selection and image reconstruction

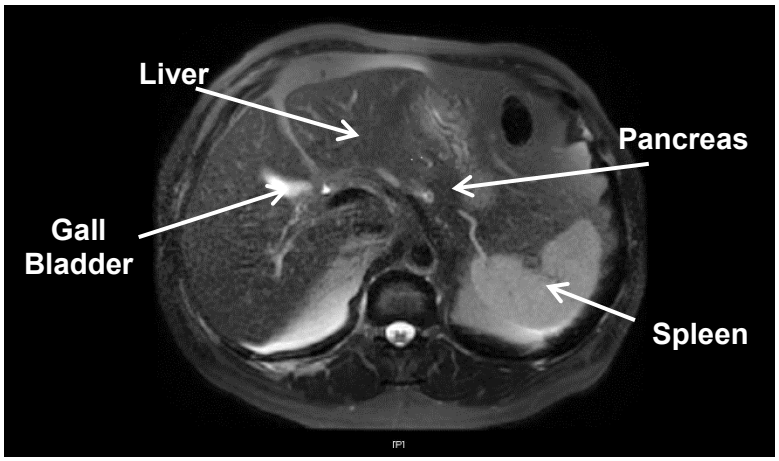

Figure 1. Axial T2W breath-held image of the liver; also visualized is the spleen, part of the pancreas, and gallbladder stem.

OVERVIEW

In recent years, magnetic resonance imaging (MRI) of the body has enjoyed its greatest relative growth in the number of procedures performed compared to neurological and musculoskeletal MRI applications. This growth is attributed to numerous factors, including significant advances in MR hardware and software.

Early MR systems were unable to acquire images in the body rapidly enough to eliminate artifacts associated with respiration and other physiologic motion. With state-of-the-art scanners and scanning techniques, acquisition times of most body sequences are sufficiently short to be performed during a single breath-hold, which eliminates most motion artifacts. As a result, the majority of these stream-lined body MR protocols can be completed in less than 30 minutes. See **Figures 1-4** for examples of a typical abdominal MRI exam for evaluation of the liver.

For the purposes of this material, *MRI of the Body* refers to any MR imaging in the abdomen and pelvis.

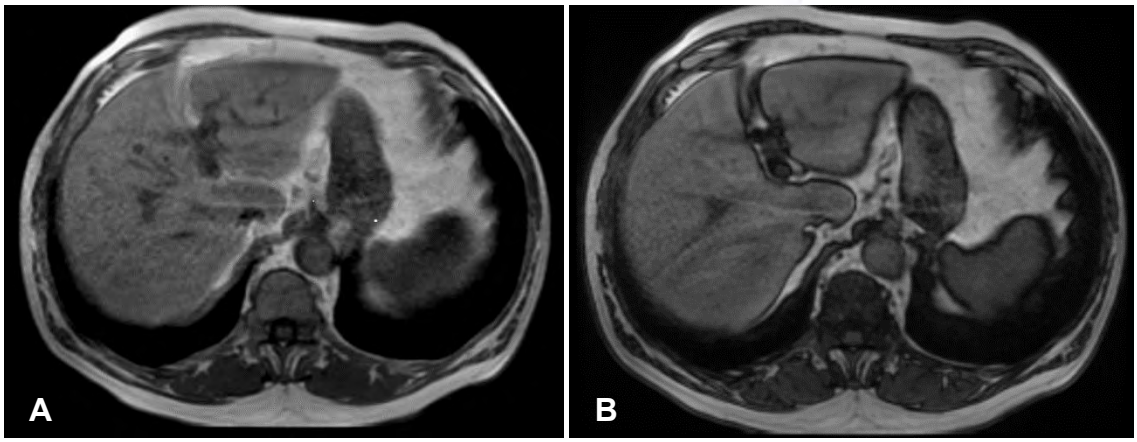

Figure 2. (A) Axial in-phase gradient echo of the abdomen. (B) Axial out-of-phase gradient echo. Same location as (A). Note the characteristic "India ink" effect or outlining of organs along fat/water interfaces in the out-of-phase.

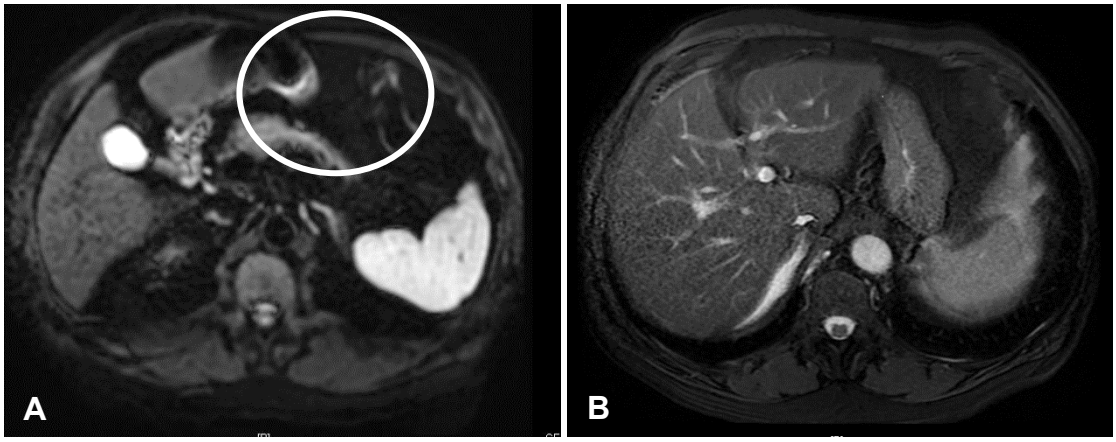

Figure 3. (A) Axial diffusion-weighted image of the abdomen. Note increased susceptibility of the anterior border of the liver and anterior abdominal wall (circle). (B) Axial FIESTA fat-suppressed image.

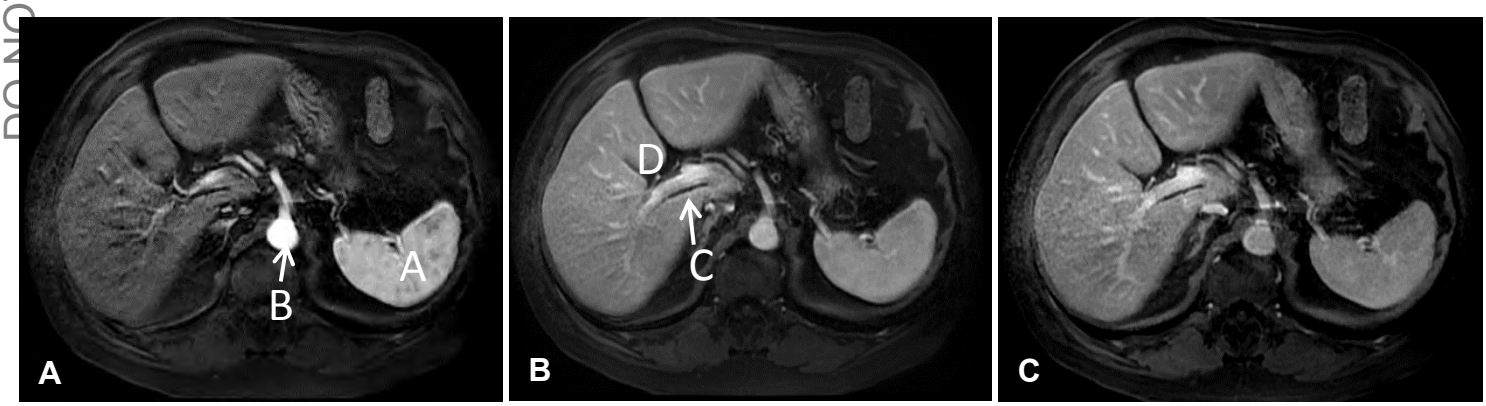

Figure 4. Dynamic tri-phasic postcontrast 3D T1W. (A) Arterial phase approximately 20 seconds postcontrast. Note mottled appearance of the spleen and contrast-filled abdominal aorta. (B) Venous phase, approximately 1 minute postcontrast. Note lack of mottling of the spleen, contrast update by the liver and contrast filling of the portal vein. (C) Delayed phase approximately 3 minutes postcontrast. Tri-phasic liver imaging is useful in differentiating cancerous liver lesions from hemangioma.

A - Spleen
B - Abdominal Aorta
C - Portal Vein
D - Liver

Benefits and Challenges of Using MRI

Although computed tomography (CT) and ultrasound (US) have benefited from technological advances over the last several years, in many spheres of diagnosis body MRI remains the most sensitive and specific diagnostic imaging tool available (**Figure 5**). Although patients undergoing CT or US exams may require a more definitive study using magnetic resonance imaging, MRI is increasingly used for first-line imaging.

Body MRI generally requires more scan time than most other imaging modalities. Because of the nature of collecting MR data, it has been difficult to acquire a diagnostic image in what might be considered a “fast” imaging time. In the early days of MRI, obtaining a single image in less than a minute was considered a marvel, despite the severely compromised image quality. These long imaging times, for example, six to eight minutes to acquire axial images of the entire brain, could be tolerated for many applications because the patient only had to lie still for a painless, albeit long and noisy, imaging exam. Body applications, however, were altogether different.

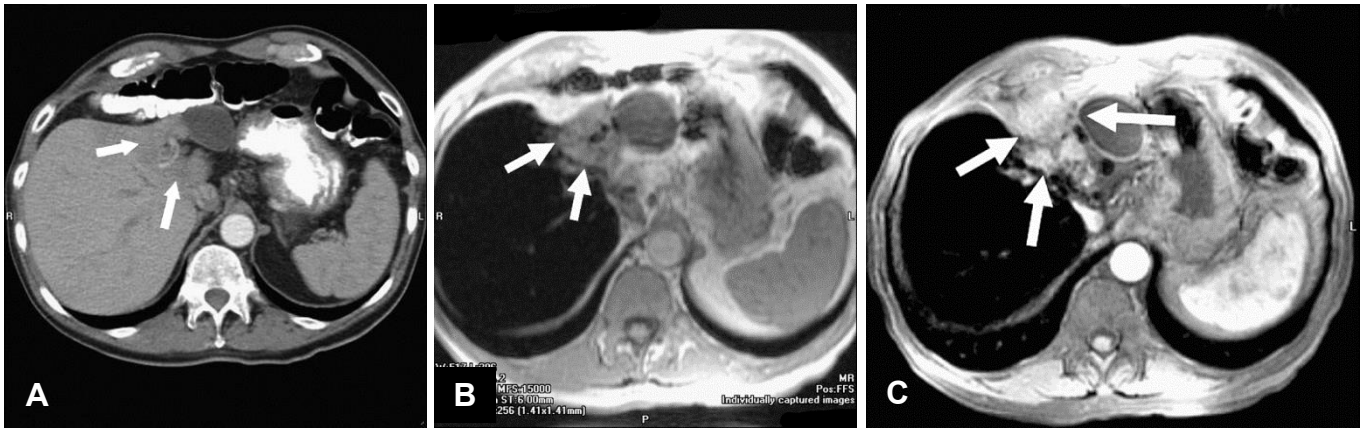

Figure 5. (A) Axial contrast-enhanced liver CT depicts a subtle abnormality of the medial segment of the left lobe of the liver (arrows). (B) Axial precontrast T1-weighted gradient-echo MR image. (C) Postcontrast T1W image. Arrows depict a malignant cholangiocarcinoma.

For many years, body imaging using MRI suffered from challenges typically not problematic for other areas of the body. Because of respiratory, cardiac, and bowel motion, MR systems lacked the hardware and software to scan rapidly enough to acquire meaningful images. Much of body MR imaging was of poor quality, requiring patients to remain in the magnet bore for excessively long periods even by MR standards. With the addition of gadolinium-enhanced contrast sequences, the exam became intolerably long. Respiratory **artifacts** severely affected image quality. Compromises in imaging matrix, slice thickness, and **signal-to-noise ratio** (SNR) in favor of speed left images pixilated with noise and with poor **spatial resolution**.

For all its promise in other applications, MRI was not valued as a diagnostic tool in body applications until the mid-1990s when high-speed gradients and advanced pulse sequences were developed.

ADVANCES IN GRADIENT SPEED AND PULSE SEQUENCING

Gradient Speed

The gradients of any MRI machine are the "engine" that determines the overall performance of an MRI system. A gradient is an induced, additional magnetic field that adds to or takes away from the main magnetic field, B_0. Gradients alter the magnetic field along a strict spatial coordinate, and their purpose is to change the resonant frequency of any excited protons. When electrical current is induced in the gradient coil in the direction of B_0, the main magnetic field strength will increase as well. If the current is induced in the *opposite* direction of B_0, the main magnetic field strength will decrease. The back-and-forth switching of the gradient fields is the source of the acoustic noise heard during an MR scan.

There are three pairs of gradients in every MR machine: two in the *x*-direction, two in the *y*-direction, and two in the *z*-direction. The range that a gradient field can change from high to low is referred to as **gradient amplitude**, which is measured in milliTesla per meter (mT/m). The time required for a gradient to reach its specified amplitude is referred as its **rise time**, most often in microseconds (μs – one-millionth of a second).

Slew rate is the term used to describe the performance of the gradients with regard to their amplitude and rise time. Gradient slew rate is measured in Tesla/meter/sec (T/m/sec). The higher the slew rate, the greater the overall performance of the MR system.

High slew rate gradients allow for more slices per repetition time (TR), resulting in shortened acquisition times. High slew rate gradients also reduce echo spacing in fast/turbo spin echo sequences (FSE/TSE), improving image quality.

Advanced Pulse Sequences

Advanced pulse sequences (pulse sequence database or PSDs) collect MR data quickly, reducing acquisition times so that 3D imaging is now routine. Other pulse sequences provide effective methods of reducing or even eliminating breathing artifacts, and these are discussed later in detail.

Phased-array Technology

High-channel phased-array coils specifically designed for chest, abdominal, and pelvic imaging yield high SNR and coverage that eliminates the need for in-room coil repositioning. Today most MRI body applications are optimized so that few precontrast pulse sequences are required, and these are typically breath-held sequences. Postcontrast imaging can now be sufficiently rapid to acquire dynamic contrast uptake images with high **temporal resolution** in a 3D acquisition. While not all body applications require contrast-enhanced imaging, its use is no longer an impediment to successful body imaging.

In the material that follows, the use and special characteristics of typical pulse sequences are presented. The newer techniques in body imaging such as parallel imaging, fast steady-state techniques, ultrafast T2W techniques, and fast 3D T1 methods will be discussed.

The anatomical areas of MR body imaging included in this material are:

- Liver
- Adrenal Glands and Kidneys
- Small Bowel
- Female Pelvis
- Bladder
- Prostate
- Anal-rectal

ISSUES UNIQUE TO BODY MRI

Body MRI presents unique challenges compared to other MRI applications. These challenges include respiratory and cardiac motion, **peristalsis**, and magnetic susceptibility effects of tissue-air interfaces. Each of these challenges affects images differently, but each can be minimized or resolved using artifact-reduction methods.

Respiratory Motion Artifacts

It is well recognized that any motion of imaged anatomy invariably contains a cascading artifact across the image known as a **ghost**. Motion artifacts occur in any MR image when the position of protons changes relative to the gradient field from one phase-encoding step to the next. The resulting phase-encoding errors cause misplaced signal in the phase-encoding direction (**Figure 6**).

Respiratory motion usually presents the most visible of motion ghosts compared to jerk motion, which occurs sporadically. Moreover, respiratory motion artifacts are compounded by changes in breathing depth and rate. While it is optimal to eliminate respiratory motion artifacts completely by suspension of breathing, there are beneficial pulse sequences with a duration longer than a breath-hold. Fortunately, several strategies exist to reduce or eliminate respiratory motion.

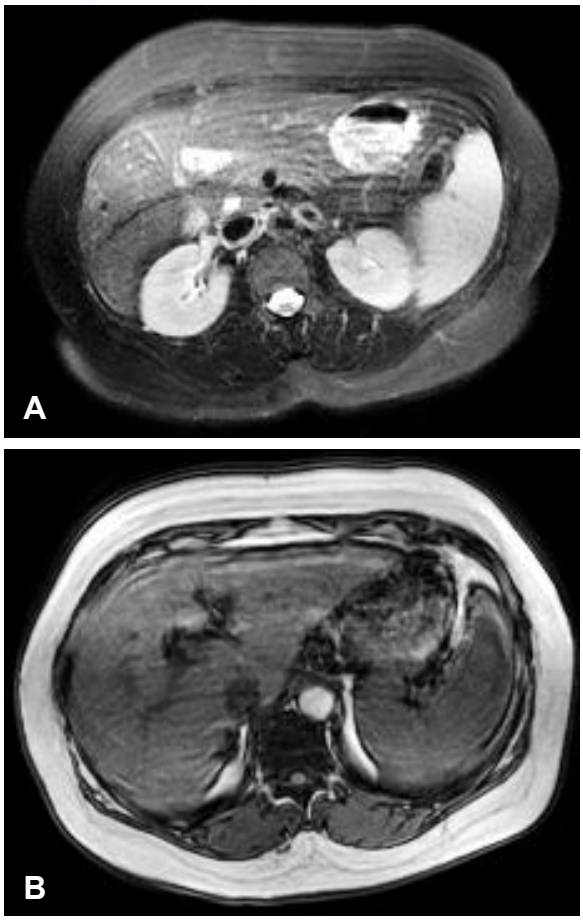

Figure 6. 53-year-old female with a limited ability to breath-hold during liver imaging. (A) Axial T2-weighted fat suppression. (B) Axial T1-weighted spoiled gradient echo. Total breath-hold time was 0:22 and 0:26 seconds, respectively. The line-like artifacts throughout the images are the result of excessive respiratory motion.

Strategies to Reduce or Eliminate Respiratory Motion

Respiratory-ordered Phase Encoding

With respiratory-ordered phase encoding, respiratory bellows are placed around the patient's abdomen to record the patient's breathing rate and depth of inspiration/expiration, called a respiratory waveform (**Figure 7**). For each phase-encoding step, the respiratory position is recorded. After the scan is completed, the data are shuffled to correspond as closely as possible to the position of the abdomen. This "respiratory compensation method" reduces the number and intensity of respiratory ghosts without increasing scan time. While this method is only somewhat effective, it represents one of the earliest advances in body imaging.

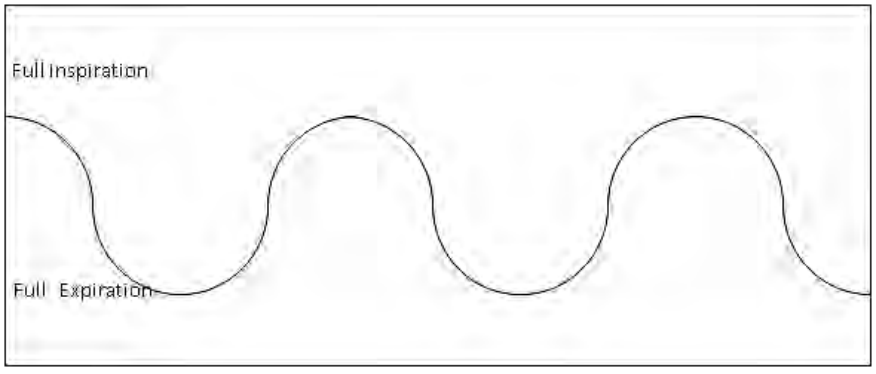

Figure 7. Respiratory waveform generated by the expansion and contraction of respiratory bellows placed around the patient's abdomen.

Increasing Signal Averaging

Because they are random, respiratory ghosts can be treated as noise rather than as true signal. One method for reducing noise is to significantly increase the SNR by increasing the number of signal averages (NEX or NSA), effectively decreasing the intensity of the respiratory ghosts into the noise floor of the image. The obvious downside to this method is the greatly increased scan time.

Fat Saturation and Fat Saturation Techniques

Respiratory ghosts are highly visible when they arise from the bright signal of subcutaneous fat primarily located in the anterior abdominal wall. Ghosts from tissue of very low-signal intensities are typically not visible because their lower signal intensity falls below the noise floor. Therefore, if the high intensity fat signal is suppressed, the ghosts can be converted to low-signal intensity and become less intrusive by falling below the noise floor.

One method for suppressing fat signal is to place pre-saturation pulses into the anterior abdominal wall, the largest contributor of respiratory ghosts. However, the pre-saturation bands must be carefully placed so as to not saturate important structures. Pre-saturation bands cannot be shaped to the curvature of a patient's abdomen or be used to suppress fat signal deeper within the abdomen. Additionally, pre-saturation pulses increase **specific absorption rate** (SAR), which can reduce the numbers of slices per TR and ultimately increase scan time.

Chemical saturation is the other method for suppressing fat. Fat protons are excited just prior to slice excitation, thereby saturating the fat signal throughout the entire image. While this method is effective in reducing the intensity of respiratory ghosts, it also reduces the overall SNR on the image. However, high-intensity "non-fat tissues" can still exhibit ghosting. Alternatively, chemical fat saturation also increases SAR and ultimately scan time.

Gradient Reorientation

Like any motion artifact, respiratory ghosts run in the phase-encoding direction. In an axial body image, the anterior-to-posterior direction is the default direction for phase encoding and thus the ghosts appear to cascade through the image in that direction. Re-orienting or "swapping" the phase-encoding and frequency-encoding directions so that phase runs in the right-to-left direction forces the ghosts to run in that direction. It should be noted that this method does not reduce the number or intensity of the respiratory ghosts but only changes their direction.

Respiratory Triggering

As in the respiratory-ordered phase-encoding method, **respiratory triggering** also employs the application of bellows, although the data collection scheme is vastly different and far more effective. In respiratory triggering, an FSE/TSE is used to generate a respiratory waveform. Instead of noting the most active part of the respiratory cycle as in respiratory-ordered phase encoding, the system registers the most **quiescent** part of the respiratory cycle or **end-expiratory phase**. During this period of the cycle, the system collects numerous lines of ***k*-space** (**Figure 8**). No data are collected during the remainder of the cycle when there is maximum abdominal motion.

It is essential that the patient breathes at a consistent rate when respiratory triggering is being employed. The effective TR is determined by the patient's respiratory rate, and therefore the effective TR is always relatively high, making T1-weighted imaging impractical. For non-breath-held methods, respiratory triggering is nonetheless a highly effective method for near-elimination of respiratory ghosts.

Navigator-based sequences have been developed that track the motion of the diaphragm, allowing data acquisition during the end-expiratory phase without the use of respiratory bellows.

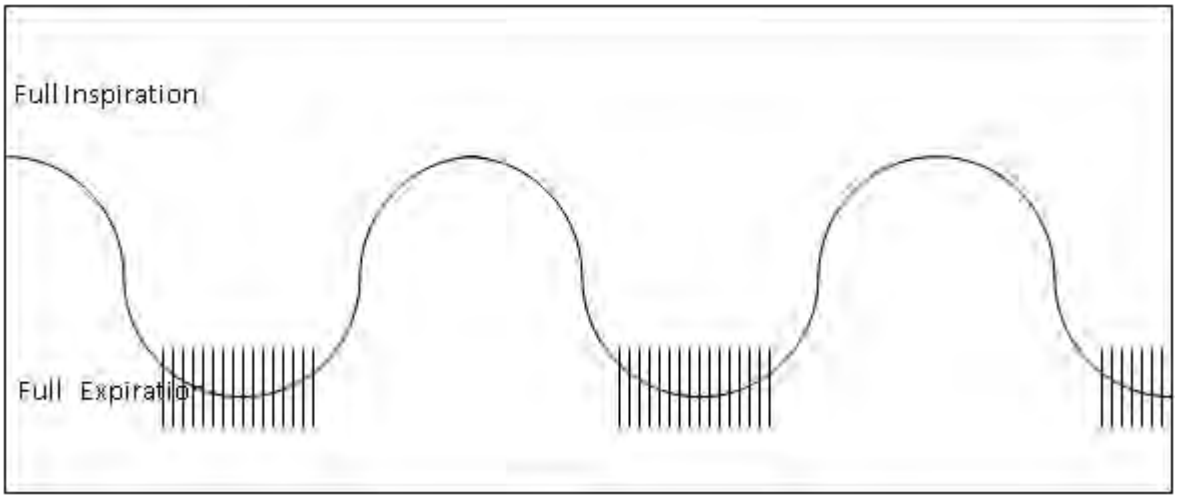

Figure 8. Respiratory triggering. Respiratory waveform monitored by the MR system uses the most quiescent period of the respiratory cycle to trigger and launch data acquisition. *k*-space reordering is applied so that the most accurately sampled data points fall into the center of *k*-space, providing the least artifact in the area of greatest SNR.

Parallel Imaging

Parallel imaging is a highly useful imaging technique in body imaging and most often used as a means to reduce acquisition times. This technique does not specifically reduce artifacts common in body imaging but when used effectively shortens scan times sufficiently to further ensure the patient can hold their breath long enough to prevent respiratory artifacts. With **echo planar imaging** (EPI)-based diffusion-weighted sequences — a commonly used sequence in body imaging — parallel imaging can reduce echo-spacing times dramatically, resulting in decreased geometric distortion in the diffusion-weighted images. Echo spacing is discussed later.

Parallel imaging is the name given to a class of sequences that shortens acquisition times by calculating sensitivity maps of the individual elements of a phased-array coil. The sensitivity maps are used to under-sample areas of *k*-space and thereby greatly reduce acquisition times. The under-sampled data, however, causes **aliasing** of the signal. Several reconstruction techniques exist to "unwrap" the aliased imaged into an artifact-free image acquired in substantially less time. Depending on the number and arrangement of individual phased-array coil elements, the reduction in acquisition time can be decreased by a factor of 1.5 – 4.

It is said that "nothing in MRI is free," meaning that any change in one parameter will have a detrimental effect on another.

It is said that "nothing in MRI is free," meaning that any change in one parameter will have a detrimental effect on another. This is also true with parallel imaging. The "cost" of parallel imaging is a reduction in signal-to-noise ratio. The greater the acceleration, the greater the loss of SNR. Given this caveat, parallel imaging is used cautiously in some applications that require extremely high spatial resolution, like musculoskeletal imaging. Most body imaging protocols use large **fields-of-view** (FOV) and fairly thick slice acquisitions. Because these parameters typically provide an abundance of SNR, any loss of SNR using parallel imaging is usually of little consequence.

Parallel imaging techniques are referred to by different names according to manufacturer:

Philips Healthcare	GRAPPA® and SENSE®
GE Healthcare	ASSET® and ARC®
Siemens Medical	iPAT®

Susceptibility Effects

Magnetic susceptibility refers to the ability of a tissue to become magnetized. Interfaces between tissue and air and the presence of metal can generate magnetic field gradients and significantly alter the local magnetic field. The change in magnetic field alters the resonant frequency, which leads to dephasing of spins. In regions of altered magnetic susceptibility, the net effect causes dephasing of spins, yielding significant signal loss and dropout. The field gradients created may result in geometric distortions in the images.

Methods for reducing magnetic susceptibility effects in body MRI are limited. Because the technologist has no control over the field strength of the system, manipulation of the pulse sequence must balance the reduction of susceptibility effects with the tissue contrast, resolution, and SNR requirements of the exam.

Primary sources of magnetic susceptibility effects in the body include tissue-air interfaces near the diaphragm and compact bone-tissue interfaces. Excessive susceptibility in these areas can lead to image distortion near the interface and increased signal dephasing that results in very low SNR in that area. These distortions and areas of signal loss are exacerbated by higher field strengths, lower slew rate gradients (which result in longer echo-spacing times), and the widespread use of **gradient echo** (GRE) and **diffusion-weighted imaging** (DWI) pulse sequences (**Figure 9**).

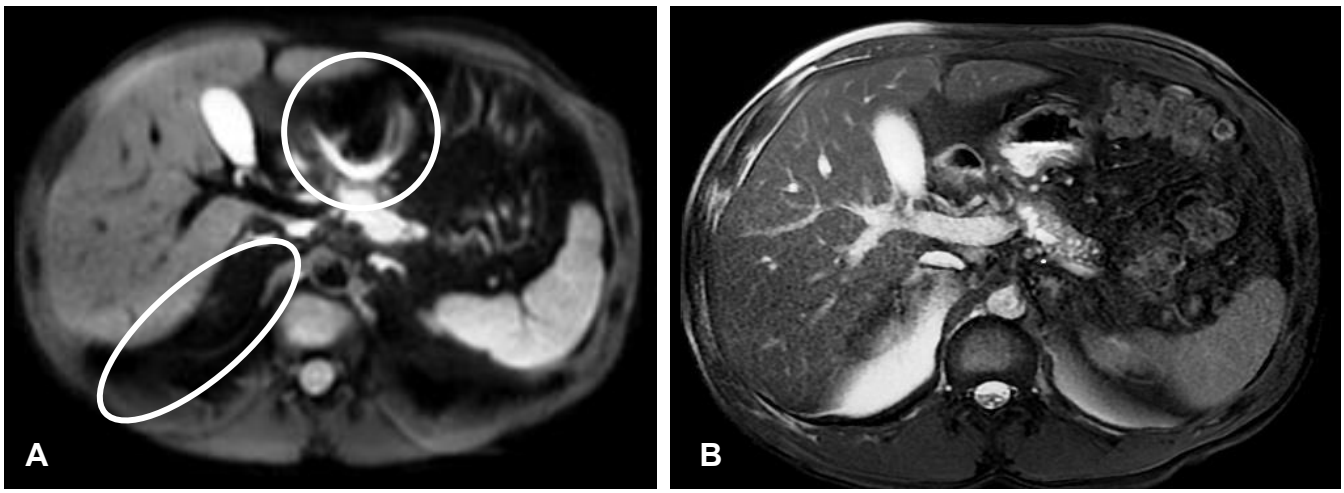

Figure 9. Axial liver images of a 43-year-old male. (A) Single-shot echo planar imaging DWI with a *b*-value of 200. (B) Same location using FIESTA. Note the amount of image distortion in the DWI image (circles). This distortion, referred to as geometric distortion, is an example of the sensitivity of EPI to magnetic susceptibility effects such as tissue-air interfaces, compact bone-tissue interfaces, or susceptibility effects caused by the presence of metal, for example, orthopaedic implants. In EPI and gradient-echo imaging techniques, these areas of magnetic susceptibility cause high degrees of dephasing and image "bending" or distortion. Nevertheless, DWI of the liver can be highly sensitive to liver pathologies and motion-free due to the ultrafast imaging speed of EPI.

Methods for reducing magnetic susceptibility effects in body MRI are limited. Because the technologist has no control over the field strength of the system, manipulation of the pulse sequence must balance the reduction of susceptibility effects with the tissue contrast, resolution, and SNR requirements of the exam.

Echo Spacing

In an echo-train type pulse sequence like FSE/TSE and EPI, the time between successive echo read-out gradient pulses is termed **echo spacing** (ESP). The duration may be milliseconds or microseconds depending on the sequence. Regardless of the sequence, any increase in ESP increases the variance of T2 decay within *k*-space. This increased variance results in several predictable effects. In FSE/TSE, blurring will increase. In an EPI sequence such as DWI, an increase in ESP results in greater geometric distortion (**Figure 10**). In both sequences where there is a tissue-air interface, the area of susceptibility effect is greatly increased.

Reducing the ESP can be accomplished by increasing the **receiver bandwidth** (RBW), reducing frequency-encoding steps and to some extent increasing the field-of-view. Associated disadvantages are decreased SNR when increasing RBW and decreased spatial resolution when decreasing frequency encoding and increasing FOV. Nonetheless, effective balancing of the advantages and disadvantages are attainable as demonstrated in the protocol tables for body applications following the end of this material.

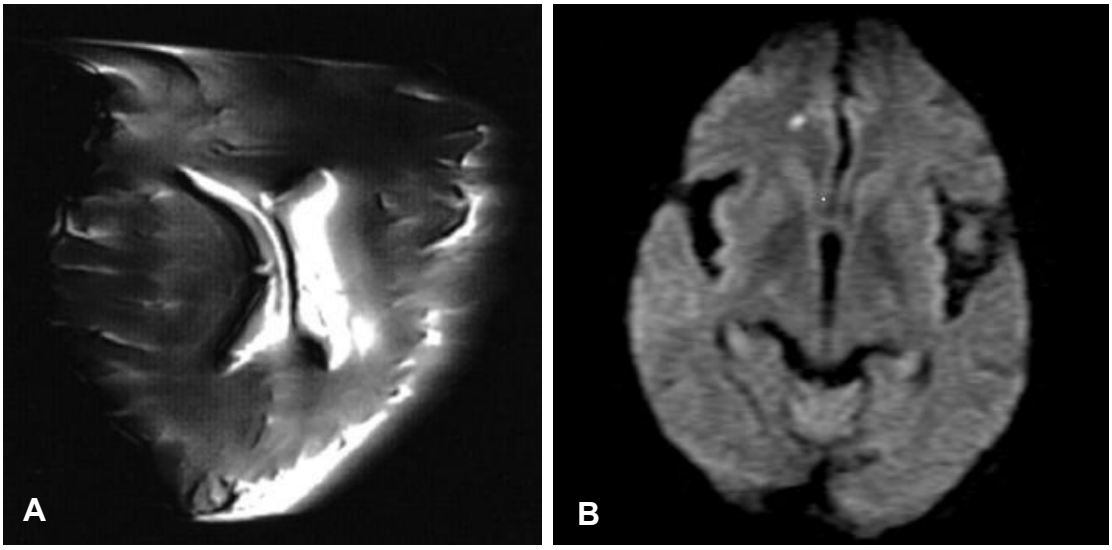

Figure 10. Examples of how reducing echo spacing can reduce geometric image distortion. (A) Axial single-shot echo planar imaging of the brain. The extreme distortion in the image is is due to parameters purposely selected to demonstrate the effects of significantly increased ESP on image quality. These parameters include low slew rate gradients, high spatial matrix, small field of view, and narrow receive bandwidths. (B) Axial SS-EPI image of the brain that demonstrates greatly reduced geometric distortion due to reductions in ESP.

GRADIENT-ECHO SEQUENCES VS SE/FSE/TSE SEQUENCES

Spin echo–based (SE) sequences are less affected by susceptibility artifacts because the dephasing effects of the field changes are rephased by 180° **radiofrequency** (RF) refocusing pulses. In contrast, gradient echo-based and echo-planar sequences may experience large areas of signal loss and dropout from the field changes and dephasing effects because of gradient-echo refocusing pulses. In rare instances, these sequences may be completely unusable. It may appear, then, that using a GRE or EPI sequence for imaging the body would be less than ideal.

However, GRE and EPI sequences have been some of the most effective methods for obtaining fast abdominal imaging in the time of a breath-hold. These sequences very quickly provide the requisite SNR, tissue contrast, and spatial resolution. The vast majority of body MRI applications employ an effective combination of GRE and FSE/TSE sequences.

Effective Use of Local Gradient Shimming

There is no more important parameter for producing high image quality than magnetic field homogeneity. Even if all other components of the MRI system are optimized, their value is negated if magnetic field homogeneity is poor, and therefore it is essential that the scan operator makes judicious use of local gradient **shimming** for any body imaging. Shimming further reduces susceptibility effects and maximizes the SNR for any given pulse sequence and its parameters.

There is no more important parameter for producing high image quality than magnetic field homogeneity.

SURFACE COIL SELECTION AND USE

The **surface coil** is a well-known and common accessory in MRI. A surface coil is nothing more than a receiving antenna that collects the signal from excited protons and then carries that signal back into the radiofrequency receiver subsystem for conversion into *k*-space. Ultimately, this signal information generates a matrix of **voxels** that are reconstructed to become the anatomical image.

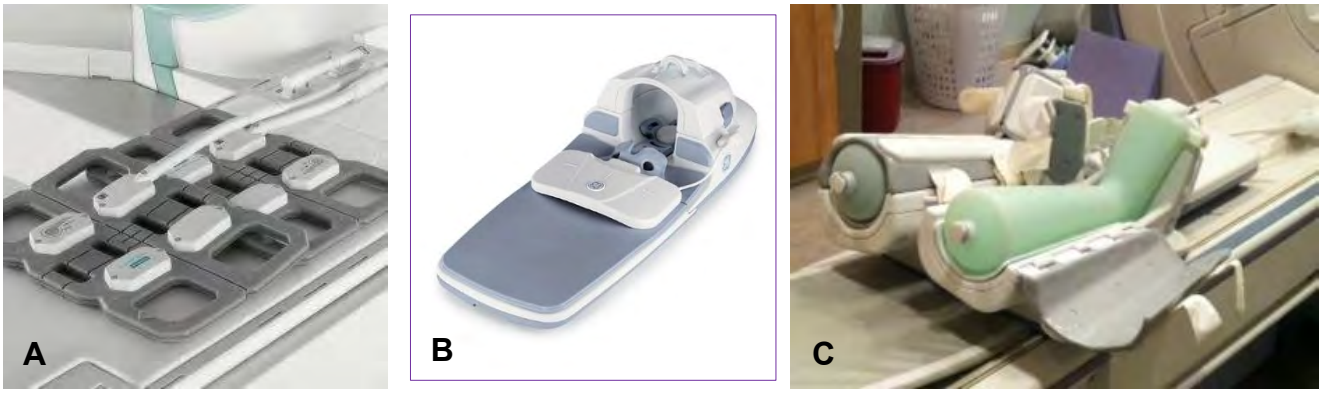

Figure 11. (A) 16-channel body array coil. (B) 32-channel head-spine array coil. (C) 32-channel bilateral lower leg coil. *Courtesy of GE Healthcare.*

Surface coils generally refer to the family of coils that act as receive-only coils and are designed for a specific anatomical part of the body. There are many different types of surface coils, including transmit, receive, and single-coil and multi-coil designs. Surface coils are made in all shapes and sizes, depending on the area of interest (**Figures 11-14**).

Surface coil development has benefitted all MR applications but has had the greatest impact on body imaging. The most significant of these advances was the development of phased-array coils.

Phased-array Coils

All other factors remaining the same, the smaller the coil size, the better the SNR; the trade-off is that the smaller the coil size, the smaller the detection area. The earliest coil used in MR for body imaging was the inserted transmit/receive coil that makes up the bore of the magnet. This is referred to as the "body coil" because it is as large as the typical body of a patient. While coverage was excellent, SNR was inadequate as the sheer size of the coil length was as much as six feet!

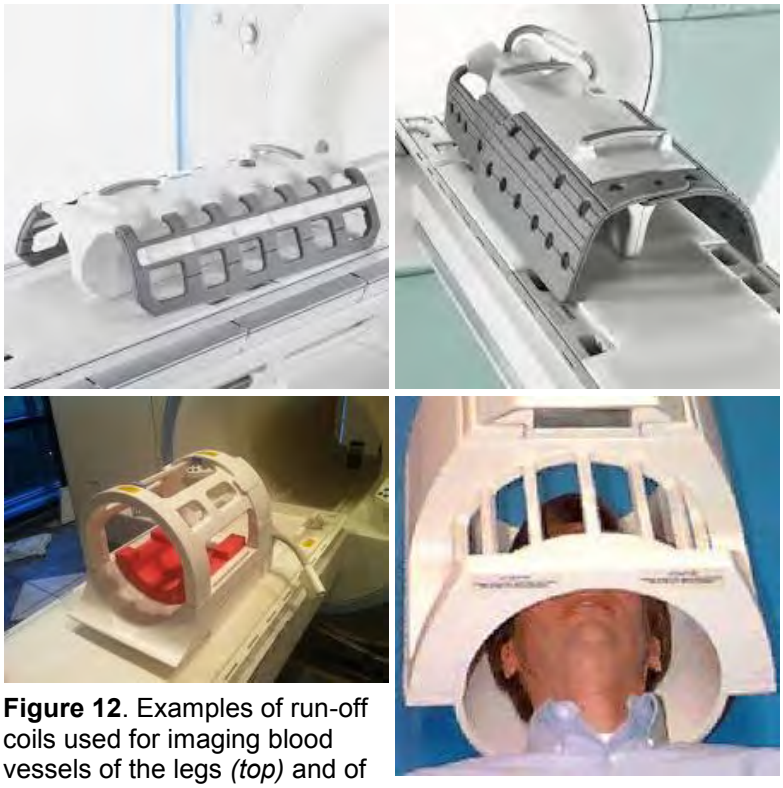

Figure 12. Examples of run-off coils used for imaging blood vessels of the legs *(top)* and of head coils *(bottom).*

Courtesy of Siemens Healthcare, GE Healthcare, and Philips.

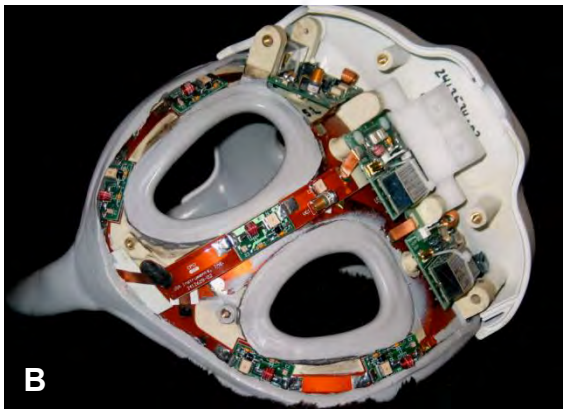

Figure 13 *(top)*. (A) Shoulder array coil with cover. (B) Shoulder array coil without cover.

Figure 14 (*bottom).* (A) 16-channel body array coil. (B) 8-channel head array coil

Figures courtesy of GE Healthcare and Siemens Healthcare.

The development of localized abdominal surface coils greatly improved SNR compared to the bore insert but still lacked the SNR boost that other applications were enjoying due to their much smaller size. Phased-array coil technology changed all of that.

In the mid-1990s, **phased-array coil** technology revolutionized MR. The benefit was so evident that today there is no MR system manufactured that does not include a phased-array coil system as standard hardware.

Stated simply, phased-array coil technology uses the SNR boost of a small surface coil and "strings" together several smaller coils to obtain the coverage of a larger coil. The key is for each local coil, called a "coil element," to have a dedicated receiver channel that collects the signal from that coil only.

The early iterations of phased-array coil technology used four receivers and coils that contained six to eight elements or channels. With four receivers in the RF cabinet, these multi-channel coils could utilize up to four to six of the six to eight elements in the coil. For example, a phased-array coil designed for the spine might consist of six elements. The user could select the top two channels for cervical spine imaging, the middle four channels for thoracic spine imaging, and the bottom three channels for lumbar spine imaging. Note that the total number of coil elements used at one time is never greater than the number of receivers present in the RF cabinet. For body imaging, the first phased-array design was comprised of two coil elements anteriorly and two posteriorly.

Today MR systems routinely have 16-32 receivers, and phased-array coils can contain an even greater number of elements. Body arrays are often large enough to permit imaging of the abdomen and pelvis without the need to move the coil, resulting in a greater number of smaller elements providing high SNR over a large imaging area. However, all of this imaging power does not come without some trade-offs.

IMAGE RECONSTRUCTION

The image reconstruction process, referred to as **Fast Fourier Transform** (FFT), is a highly mathematical computation. Converting *k*-space data into image data that are then projected as **pixels** onto a display screen requires robust processing power. The reconstruction of the image is done by the "array processor" engine. In phased-array architecture, each receiver produces its own image, with the final image a composite of the images from all of the receivers. If there is only one array processor for four receivers, the time to reconstruct and display one composite image will be four times longer than if the data were acquired from only one receiver. If there are eight receivers, reconstruction time will be eight times longer. In other words, if the time to reconstruct the data from one receiver is one second, it will require eight seconds of reconstructive time if eight receivers are used.

This may seem of little consequence until we review a real-world example: If the time to reconstruct 60 images is one minute using one receiver, using eight receivers would result in an image construction time of eight minutes, significantly increasing reconstruction time. To address this issue, MR systems employ high-speed parallel-array processors. Like personal computers that use dual processors, parallel-array processors contain two or more processors that operate in tandem, resulting in far faster processing times for image reconstruction and display.

Likewise, continued development of faster processors also aids in keeping reconstruction times reasonable.

IMAGING AT 3.0T

3.0 tesla MRI systems are far more prevalent today than they ever have been. The obvious benefit of 3.0T systems versus lower field strength systems of 1.5T or less is the greatly increased inherent SNR in all imaging applications. Body imaging at 3.0T can be highly diagnostic, however, 3.0T imaging does not come without caveats, particularly with body applications.

As a general rule, as magnetic field strength goes up, so does an increase in magnetic susceptibility artifacts and the visibility of respiratory motion artifacts. With this in mind, body imaging at 3.0T field strength can be challenging when scanning in areas sensitive to magnetic susceptibility effects such as the diaphragm and compact bone-tissue interfaces.

SUMMARY

Because of the unique challenges of body imaging, body applications have lagged behind other MR applications. These challenges included overcoming respiratory motion artifacts, extremely long scan times, and susceptibility effects.

Body MR imaging continues to improve with the advanced development of key components of the MR system. These developments include faster, more powerful gradient subsystems; improved software such as parallel imaging; and the development of phased-array coil technology. MRI body imaging remains a significant contributor in the diagnosis and staging of body-related pathologies and disease processes.

NOTES

Tom Schrack, BS, ARMRIT
Fairfax Radiological Consultants
Fairfax, VA

MR ANGIOGRAPHY OF THE BODY

After completing this section, the reader should be able to:

- Discuss the advantages and disadvantages of noncontrast-enhanced time-of-flight techniques in vascular imaging
- Explain the role of gadolinium-based contrast agents in vascular imaging
- Discuss the advantages and disadvantages of different bolus timing methods
- Identify the advantages of contrast-enhanced image acquisition, as well as the potential risks of using gadolinium-based contrast agents
- List signs and symptoms of reactions to gadolinium-based agents and treatment recommendations

OVERVIEW

MR **angiography** (MRA) continues to be one of the most common applications in MR imaging in general and in body applications in particular. As recently as the mid-2000s, advanced MRA was far from customary. Outside of routine intracranial MRA imaging, more advanced MRA imaging such as contrast-injected carotid vessels and MR peripheral runoffs were fraught with pitfalls, including difficult set-up and variable results. More powerful gradients and more sophisticated software, specialized coils, and faster reconstruction processors have all made MRA fast and easy to prescribe by the technologist, resulting in more consistent, highly diagnostic images.

VASCULAR IMAGING:
NONCONTRAST-ENHANCED TIME-OF-FLIGHT TECHNIQUES

The use of a gadolinium-based contrast agent (GBCA) for imaging the vascular system changed the way MRA examinations were performed. Until the mid-1990s, the vast majority of MRA scanning was done using noncontrast-enhanced 2D or 3D **time-of-flight** (TOF) imaging (**Figures 15 and 16**). With these techniques, the scanning sequence uses a gradient echo series in the plane most perpendicular to the flow direction of interest. For example, if the carotid arteries are the vessels of interest, the scan plane is typically in the axial direction, perpendicular to the flow as the carotid arteries run inferior to superior. In this example, TOF imaging would create contrast in the image based on the flow-related enhancement of flowing blood into an axial slice plane where magnetization of the blood is at its greatest. The resultant images show darker (non-flowing) stationary tissues against very bright (flowing) blood. Images are then postprocessed into **maximum intensity projections** (MIP) in a 3D display.

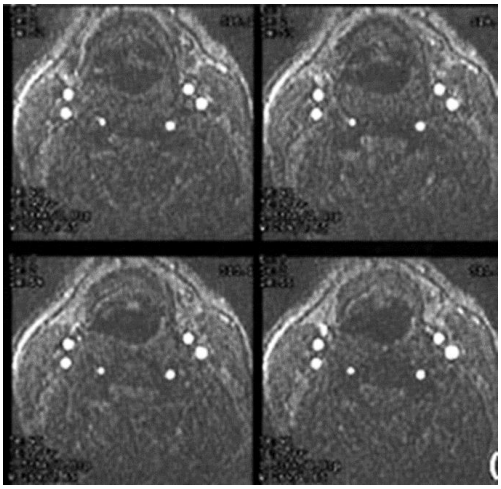

Figure 15. Axial TOF source images acquired perpendicular to the carotid and vertebral arteries. A short TR and a high flip angle ensure heavy saturation of stationary tissues while providing maximum flow-related enhancement of the carotid and vertebral arteries. These source images are then postprocessed into a 3D MIP projection.

Figure 16. 3D TOF collapsed MIP projection of the intracranial arteries. This time-of-flight image takes advantage of the flow-related enhancement of the fast-flowing blood. The individual source images are displayed as a singular MIP projection to visualize the entire vasculature.

While 2D and 3D TOF imaging is robust, it is not without disadvantages:

- TOF can overestimate the degree of stenosis
- Flow that is not perpendicular to the imaging plane can become saturated with RF energy, appearing dark and falsely resembling a stenotic vessel
- Flow that is slow may become saturated with RF and appear dark
- Long scan times (4-6 minutes for 2D TOF and 6-9 minutes for 3D TOF) increase the risk of patient motion and blurred images
- Specific to body applications, images of the lower extremities are often badly smeared due to naturally occurring **tri-phasic flow** velocities, where arterial flow moves in three distinct phases: fast forward, short reverse, then fast forward.

VASCULAR IMAGING:
THE ROLE OF GADOLINIUM IN CONTRAST-ENHANCED IMAGING

The introduction of gadolinium-based contrast agents in vascular imaging dramatically altered the methods used to perform most MRA examinations. Because gadolinium is **paramagnetic**, it does not rely on flow-related enhancement to provide strong (bright) signal, and the scan plane orientation is no longer required to be perpendicular to the flow. The use of ultrafast 3D gradient echo sequences significantly reduces scan times while increasing resolution. Finally, the occurrence of tri-phasic flow is no longer a factor because gadolinium does not saturate with RF energy and therefore emits little to no absorbed RF energy (saturated tissues, like stationary soft tissue in a TOF sequence, emit little signal and appear dark on the image). The technical challenge of using a contrast agent is in delivering the bolus of contrast material so that the bolus arrives precisely at the time of image acquisition.

Specific Bolus Detection Techniques

MRI is a versatile imaging modality, capable of analyzing signal data in near real-time. The ability to perform real-time data processing is extremely useful in MRA for determining when the contrast bolus arrives at the region of interest.

Methods for predicting or detecting the arrival of a bolus of contrast material into the vessel of interest typically fall into one of three categories:

- Manual Timing
- Computer-aided Detection
- Visual Detection

Manual Timing

Manual timing is very effective for determining the arrival of the bolus. This timing method allows facilities without dedicated bolus detection software to acquire a high-quality MRA.

The technologist sets up a scanning series so that a single slice is prescribed to be imaged multiple times. This multiphase series is performed while a small amount of contrast (1-2mL) is injected over a period of two seconds. After the series is complete, the technologist reviews the images to determine which image has the greatest degree of signal contrast in the vessel of interest by using a region of interest (ROI) tool that displays the actual pixel values of the contrast agent entering the vessel.

Once a specific image is identified as having the greatest degree of signal contrast, the technologist calculates the time required for the bolus to arrive in the ROI by looking at the time stamp on the image.

For the technologist, the challenge of predicting or detecting the arrival of the bolus using manual timing is to correctly calculate the bolus arrival time. An obvious disadvantage is that the small amount of contrast agent used in the test bolus can linger in the venous system and obscure arterial vessels. But, to be sure, a well-timed, manually calculated bolus series is indistinguishable from the more automated methods.

Computer-aided Detection

This automated bolus detection method requires the technologist to prescribe a small volume area of interest (20mm x 20mm x 20mm) on a **scout image** – such as the abdominal aorta for renal MRA – and the fully prescribed area to be scanned when the contrast agent is delivered. The scanner begins the imaging sequence, analyzing the pixel intensity from the small volume of contrast media, often called the "tracker" (**Figure 17**). Once the system determines the average pixel value of the volume, that is, the baseline of pixel values, the technologist injects the contrast. The system will continue to monitor the tracker volume.

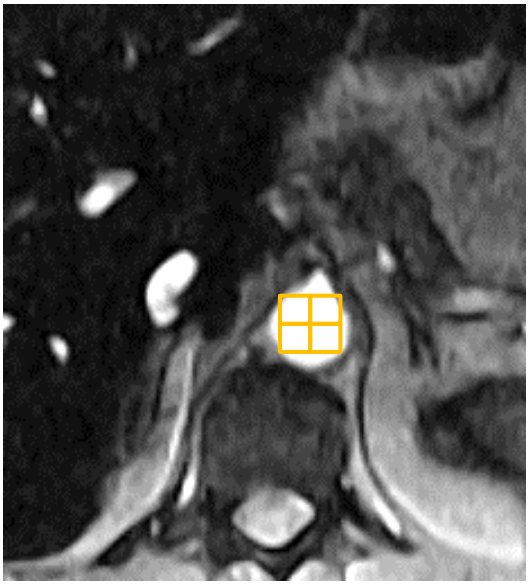

Figure 17. Axial image showing abdominal aorta with a graphically prescribed 3D "tracker" pulse cube. The area inside the cube is monitored in real time for rapid increases in pixel signal intensity resulting from gadolinium in-flow. When a set threshold of signal increase is reached, data acquisition of the 3D MRA begins.

When the bolus arrives in the region of interest, the pixel values from the tracker quickly increase in dramatic fashion, signaling the MR system that the bolus has arrived. The system then launches the ultrafast gradient echo sequence for the contrast-enhanced MRA series (**Figure 18**).

Automated computer-aided bolus detection methods are highly effective, and produce excellent contrast-enhanced MRA studies. The technique is automated, with little outside intervention and no manual calculations required. There is no contamination of the images from small amounts of test bolusing in the venous system.

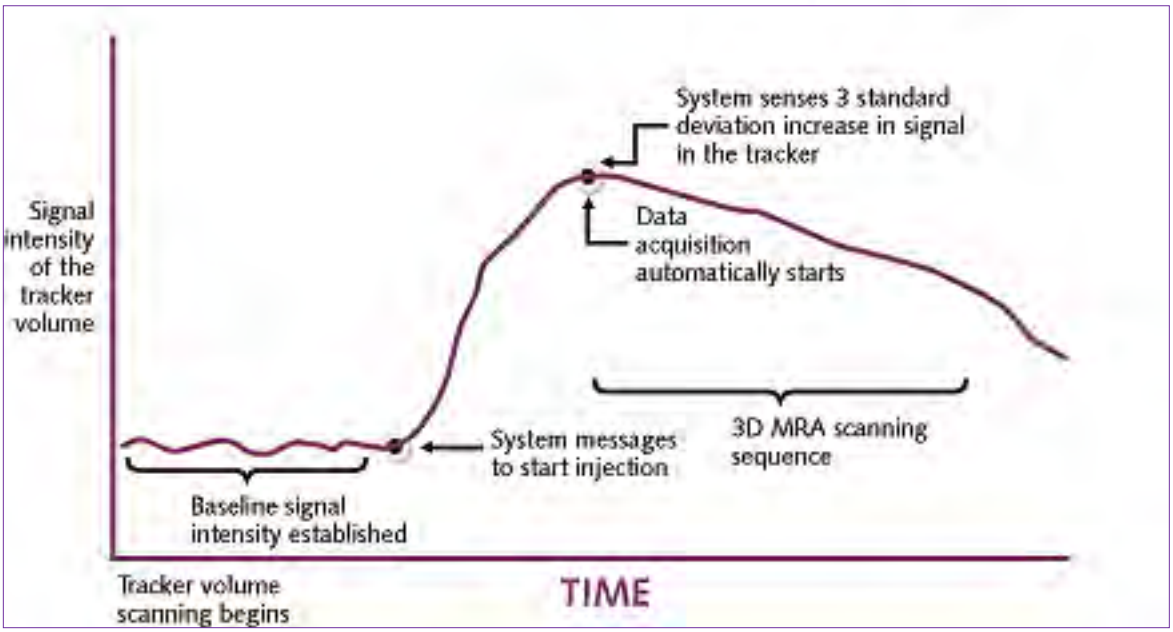

Figure 18. Time course of events in an automated bolus detection technique.

The challenge of the automated computer-aided bolus detection method is that it requires precise placement of the tracker volume. If the tracker is misplaced or the patient moves between the time of placement and the time the actual scan begins, the bolus may not be detected or may be detected too late, yielding non-diagnostic images. Also, the central *k*-space line of the MRA sequence must first be filled to meet the arrival of the contrast bolus.

Visual Detection

Visual detection methods combine the best of manual timing and computer-aided techniques. Visual detection integrates the real-time display of image data from the automated computer-aided bolus detection with the visual cues of the manual timing method. Visual detection is often referred to as “fluoro-triggered” MRA. The area of interest is scanned at first with a very low resolution technique so that the images are displayed in near real-time — thus, the use of the term “fluoro” as in real-time x-ray imaging. The contrast agent injection is made during the display of the images in real time, and the technologist can often watch the patient’s breathing during an abdominal MRA. The technologist visually inspects the images to note the arrival of the contrast bolus. Once the bolus is seen, the technologist switches the imaging parameters in real-time to a higher resolution scan to produce excellent contrast-enhanced angiographic results.

The advantage of the visual method is that the technologist is in control of the start of the scan, eliminating the need for a test bolus, and breathing commands can be tailored to individual needs. The only potential drawback is that the technologist must be vigilant in watching the images in order to track the arrival of the bolus. Again, the central *k*-space lines first need to be sampled in order to meet the arrival of the contrast bolus.

Ultrafast Scanning Can Eliminate Bolus Timing

Imagine scanning so fast that:

- entire 3D volumes are acquired as fast as a single slice.
- one simply prescribes the required 3D volume of interest and then tells the system how many times to scan this volume.
- the course of a bolus of contrast is captured as it progresses through the vasculature of interest.
- it does not matter when the bolus arrives because the scanner is already acquiring the data before, during, and after peak enhancement.
- this technique takes no longer than the typical 3D time-of-flight sequence.

Ultrafast scanning is now used on many high-end MR scanners. Referred to by various manufacturer names (GE – TRICKS; Siemens – TWIST, TREAT; Philips – 4D-TRAK), this rapid scanning technique has found its way into the mainstream. It requires very fast and high performance gradients to rapidly acquire the data in addition to very fast array processor reconstruction engines. In less than five minutes, 1,000 or more individual images can be acquired, making ultrafast reconstruction processors an absolute asset.

The technologist prescribes the 3D volume of interest of, for example, the patient's lower legs, and determines the number of times the volume will be scanned. Each of these scans is referred to as a "phase." The technologist must then balance the spatial resolution with the necessary temporal resolution, that is, how fast each 3D volume must be acquired.
Recall that as spatial resolution increases, temporal resolution decreases. Once the parameters are set, the technologist simply administers the contrast agent and begins the scan at the same time as the injection. Typically within a matter of seconds, each 3D volume is acquired and quickly reconstructed and processed into a MIP that is displayed on the screen while the subsequent 3D volume is acquired. Each 3D MIP displays an increasing, then decreasing amount of contrast material in the vasculature (**Figure 19**).

STEPPING TABLES

Stepping tables, also called mobile MR tables, are widely available on newer MR systems and are usually standard equipment on high-field magnets. The primary application for a stepping table is to provide an automated method for performing the MR peripheral runoff exam. In this application, a bolus of contrast material is injected and then, through careful timing, the patient is imaged in stations to essentially chase the bolus from the mid-abdominal aorta to the feet.

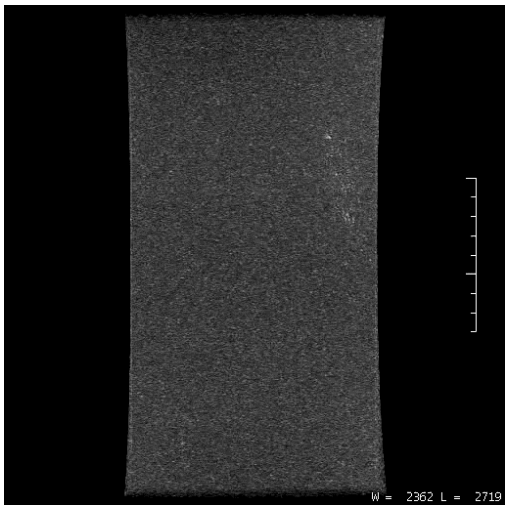

Figure 19. MOVIE Extremely rapid multi-3D slab MRA acquisition of the right upper arm of a 32-year-old female to evaluate several arteriovenous malformations.

To view this movie, click here: YouTube.com/ICPMEducation.

The automated stepping table is motorized and controlled remotely from the MR console without need for intervention in the scan room. The scan operator can reposition the table and perform multiple scans directly from the scan console without entering the scan room or repositioning the table or the patient, increasing patient safety and comfort.

Application to Peripheral Runoff MRA

A complete peripheral MRA runoff can be acquired using a single bolus of contrast material. The patient is initially positioned at the first anatomic station. After the localizer scan is obtained and the areas of interest are prescribed, the GBCA is injected and the first set of arterial images is acquired. Next the table is moved a specific distance, typically 30–45 cm to center the patient towards the lower extremities, and the acquisition is repeated. The process continues until images from all three stations are acquired, including the feet and ankles (**Figure 20**). Next the table motion is reversed, and venous images are obtained at each of the three stations.

A complete angiographic set can be acquired using a single contrast bolus and within two to three minutes. The entire process, including patient positioning, obtaining the localizer scan, and then imaging at each anatomic station for both arterial and venous images can often be completed in 15-20 minutes and cover 75–150cm of anatomy.

Figure 20. MR peripheral runoff exam. Note the coverage from above the renal arteries to the level of the feet. Also note the boundaries between "stations" indicating the three levels of scanning: upper abdomen (upper station), lower pelvic and femoral areas (middle station), and the lower legs (lower station).
Courtesy of F. Scott Pereles, MD.

Acquisition of such a large field-of-view without repositioning the patient is most efficiently performed using an appropriate set of coils. Dedicated peripheral vascular coils are available from a variety of vendors. Alternatively, multiple coils covering the anatomy of interest can be applied simultaneously by manually switching the coil used at each station. Some MR systems are capable of automatically switching to the coil set covering the current anatomic station. Other examinations that take advantage of a stepping table for an extended field-of-view include abdominal and pelvic vascular imaging and whole body imaging for metastatic surveys (**Figure 21**).

Continuous Table Movement

Advances in technology have made it possible to allow the table to continuously advance during image acquisition. The advantage of a constantly moving table is the continuous data acquisition throughout the entire runoff exam. In addition, the speed of the automatic table advance can be adjusted to track the movement of the contrast bolus. This ensures that the timing of the images at each location is precise, allowing visualization of the arterial phase (first postcontrast phase) and preventing **venous contamination**.

SUMMARY

MR angiography remains a very useful application. A typical MRI facility routinely performs MRA examinations every day for many different body areas. The use of intravenous contrast- enhancement is often preferred when imaging areas other than the intracranial vessels.

When performing contrast-enhanced MR angiography, the beginning of data acquisition must be precisely timed to coincide with the arrival of the contrast bolus. Understanding the various timing methods and the capabilities and limitations of the particular MRI system is essential for perfecting the techniques for this important examination.

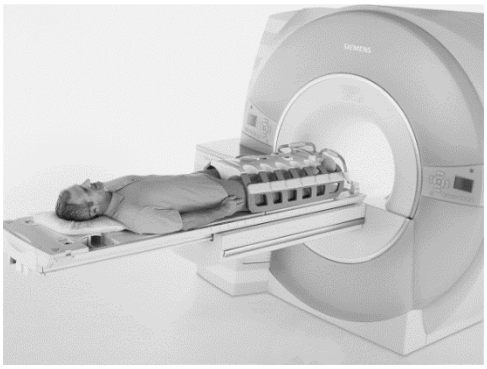

Figure 21. Example of a runoff coil used for imaging blood vessels of the legs. Abdominal imaging can be done with a separate coil or the inherent body coil.

Courtesy of Siemens Healthcare.

Lisa K. Wall, BS, RT (R)(MR)(CV)
Duke University Hospital
Durham, NC

Liver MRI

After completing this section, the reader should be able to:

- Develop a protocol for liver MRI
- Identify benign and malignant liver disease processes
- Develop protocols for imaging of the biliary ducts and gallbladder
- Describe the role of hepatocyte-specific gadolinium-based contrast agents

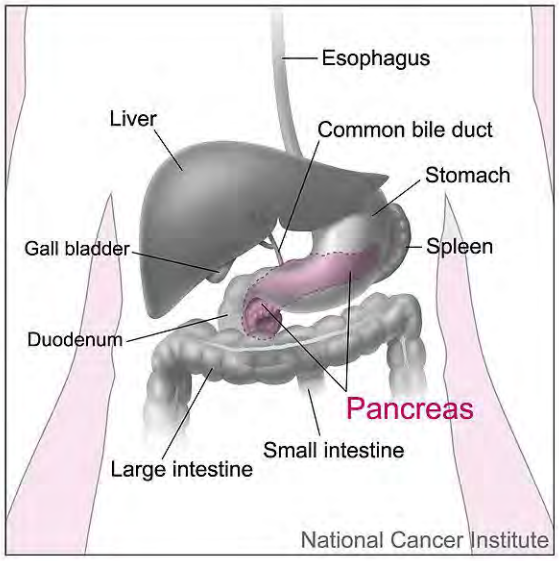

Figure 25. Anterior view of the abdominal viscera and nearby organs. Liver MRI protocols cover the liver from just above the diaphragm to a point in the mid to lower abdomen, yielding enough coverage to include all of the right liver margin, which can extend up to 20cm or more.

Available at: Wikimedia Commons.

OVERVIEW

MR imaging of the liver has become an important and relevant diagnostic tool. Liver MRI is most commonly used to evaluate an indeterminate focal hepatic lesion detected on other imaging studies as well as for imaging patients with contraindications to the iodinated contrast media used in CT scanning. Liver MRI is more sensitive and accurate for detection and characterization of focal lesions than either CT or ultrasound.

Advances in contrast agents, faster pulse sequences, larger scanner bores, and MR **elastography** are examples of how liver MRI is becoming more technologically sophisticated and clinically valuable. When imaging the liver, the pancreas and hepatobiliary structures are included because of their correlation with each other in both function and location (**Figures 25 and 26**).

In order to perform liver MR well, the technologist must optimize the imaging protocol for the specific MR system used, understand the proper application of several basic MR sequences, and recognize the MR appearance of several common focal hepatic lesions. A basic liver MR protocol involves a good mixture of breath-hold and non-breath-hold sequences to demonstrate and differentiate abdominal tissue.

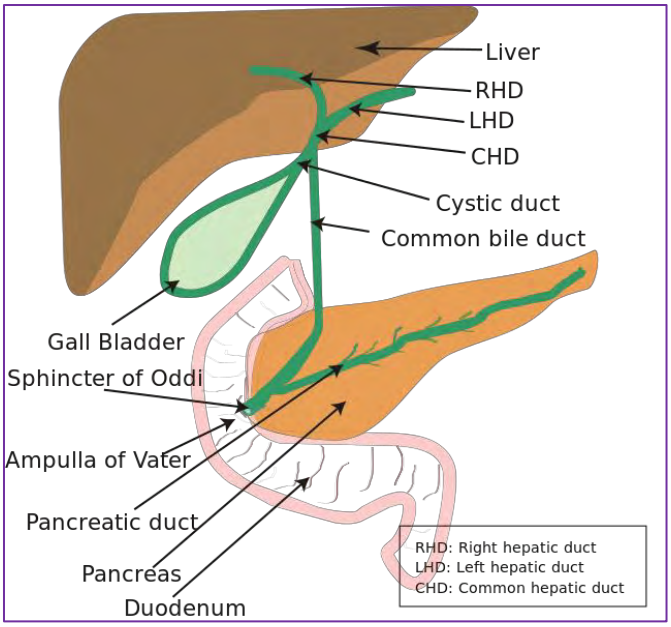

Figure 26. Anatomy of the hepatobiliary system.

Available at Wikiwand.

Liver MRI accurately detects and characterizes focal hepatic lesions. Specific sequences, such as T2-weighted FSE/TSE and inversion recovery (IR) sequences are highly sensitive for detecting lesions. Once visualized, lesions often can be accurately characterized as malignant or benign, cyst, or solid tumor, etc., based on appearance and relative signal intensity on T1W- and T2-weighted sequences. Administration of an intravenous gadolinium-based contrast agent increases both the **sensitivity** and **specificity** of MRI for detection and characterization of focal hepatic lesions. Common indications for liver MRI include:

- Evaluation of an indeterminate lesion
- Contraindication to CT contrast
- Evaluation of therapeutic response to chemotherapy or other therapy
- Normal CT or US but high clinical suspicion of lesion
- Metastatic disease staging
- Evaluation for liver transplant (recipient and living donors)
- Evaluation of the cirrhotic liver

LIVER IMAGING REPORTING AND DATA SYSTEM

The **Liver Imaging Reporting and Data System** (LI-RADS®) was created by the American College of Radiology to standardize the reporting and data collection of CT and MR imaging for hepatocellular carcinoma (HCC).[13]

The ACR has designated five assessment categories[14]

- **LR1**: Definitely benign
- **LR2**: Probably benign
- **LR3**: Intermediate Probability for HCC
- **LR4**: Probably HCC
- **LR5**: Definitely HCC

This method of categorizing liver findings for patients with cirrhosis or other risk factors for developing HCC allows the radiology community to apply consistent terminology and reduce imaging interpretation variability and errors. LI-RADS is also intended to enhance communication with referring clinicians and facilitate quality assurance and research.

LIVER MRI PROTOCOL DEVELOPMENT

Imaging Parameters

High-quality liver MRI studies can be a challenge to obtain because there are many external factors that can impact image quality. Breath-holding ability, the presence of **ascites**, anatomical variants, and language barriers are examples of potential challenges that technologists must manage in order to acquire high-quality scans. Well thought-out protocols, proper equipment, and patient education are crucial for successful imaging of the liver.

Currently, most MR centers use phased-array torso coils with multiple receiver channels that provide better SNR and the capacity for parallel imaging techniques. Special care should be taken to ensure that the liver and kidneys are placed in the center of the phased-array coil. Proper positioning of the patient in the coil is essential. If the liver is too close to the top edge on the localizer scan, signal intensity will drop off and fat saturation will not be optimal. If the patient is poorly positioned, assist in centering the region of interest in the bore of the magnet.

Patient Education

A good MRI liver protocol provides the patient with an opportunity to catch their breath and relax, especially prior to important breath-hold sequences. Non-breath-hold sequences also allow for **contiguous** slices throughout the abdomen without the misregistration that occurs when patients do not hold their breath in the same manner each time.

Instructing patients on how to hold their breath is one of the most important factors when educating patients about their liver MRI scans. While scanning on expiration provides the best replication of liver position, most patients are not able to hold their breath for more than 15 to 20 seconds on expiration. If the breath is held after inspiration, it is helpful to instruct the patient to breathe in, breathe out, breathe in again, and then hold their breath after two or three breaths to hyperventilate the patient for a longer breath-hold.

IMAGING PROTOCOLS

Liver MR imaging protocols typically employ a combination of T1- and T2-weighted images and dynamic contrast-enhanced imaging. Together they provide complementary information used for image interpretation. No one liver protocol can be used for every clinical situation — depending upon the complexity of the case and the clinical questions asked, additional sequences may be needed.

Many centers add a diffusion-weighted sequence for increased lesion detection. Recall that DWI measures the random motion of water molecules in the body. This free motion of water is inhibited in both the intracellular and extracellular spaces by increased cellularity and intact cell membranes, and thus this technique complements **morphological** information obtained by conventional MR imaging. Employing DWI for staging of metastatic lesions has been of particular interest since cell membranes in hypercellular tumor tissue serve as barriers to free diffusion in the intracellular and extracellular spaces (**Figure 27**).

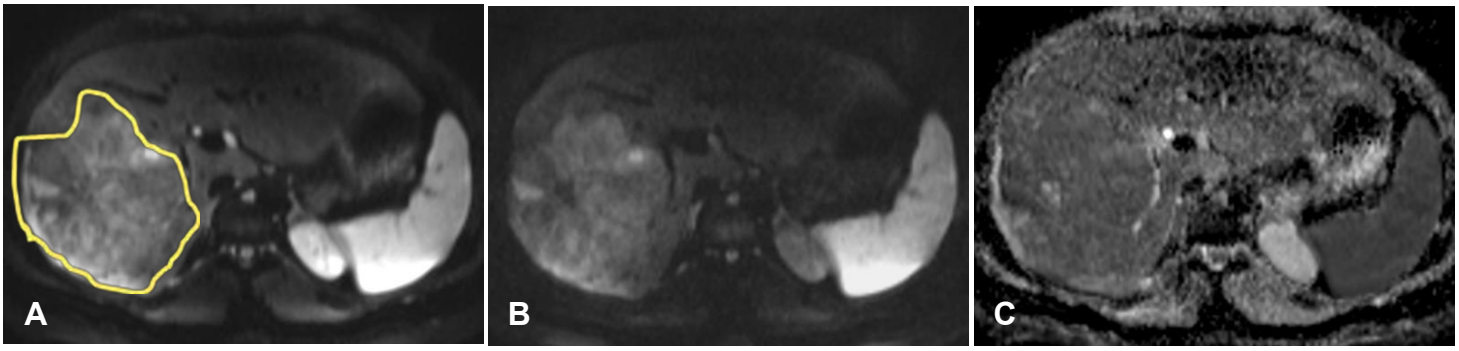

Figure 27. Large fibrolamellar mass seen on 3.0T axial diffusion-weighted images. (A) B-value=50. (B) B-value=800. (C) Apparent diffusion coefficient map.

Courtesy of Duke University Hospital.

The American College of Radiology recommends that liver imaging includes an axial T2-weighted sequence with fat saturation through the liver and spleen, axial T1W in- and out-of-phase gradient, and a 3D T1-weighted fat-saturated sequence for dynamic contrast imaging. Obtaining early arterial dynamic contrast enhancement of the liver is crucial for differentiating lesions, and there are several methods for determining the proper timing of contrast, which will be discussed later.

Axial In- and Out-of-Phase Imaging

In- and out-of-phase imaging is a vital tool for characterizing lesions on MR. Once the image weighting is set, tissue contrast is obtained by collecting image data at TE times when fat and water signals are in the same phase (in-phase) as well as in the opposed phase (out-of-phase).

Gradient echo sequences are used to generate a 3D, 2-point Dixon technique, which is acquisition of in- and out-of-phase sequences along with water-only and fat-only datasets and can be reconstructed once the scan is complete. By adding the raw data sets of in- and out-of-phase acquisitions, a water-only, T1-weighted image data set is obtained that can be used as a precontrast dynamic sequence, minimizing the number of breath-holds for a patient and thereby reducing the protocol time. If the raw datasets from the in- and out-of-phase vectors are subtracted, a fat-only image can be reconstructed. These fat-only images are useful for detection of small amounts of fat, like focal fatty infiltration and hepatic and adrenal adenomas.

When using in- and out-of-phase imaging, efforts should be made to use a sequence that allows both echoes to be acquired in the same breath-hold so that misregistration of slices is kept to a minimum. Additionally, in the 3.0T setting, it is important to acquire the first order pair of echoes (TE). Chemical shift cancellation artifacts are due to a difference in the resonant frequency between water and fat. This difference in resonant frequency is directly proportional to the main magnetic field strength, resulting in a difference of about 225 Hz at 1.5T or about 450 Hz at 3.0T. Thus, the echo time for obtaining in- phase and out-of-phase images needs to be adjusted at 3.0T as the frequency difference is twice as great compared to standard 1.5T MR systems. At 3.0T, fat and water protons are in phase at echo times of 2.2msec, 4.5msec, 6.7msec, and so on, with opposed phase at 1.1msec, 3.4msec, 5.6msec. 1.5T echo times should be 2.1msec for opposed-phase and 4.2msec for in-phase imaging (**Figure 28**).

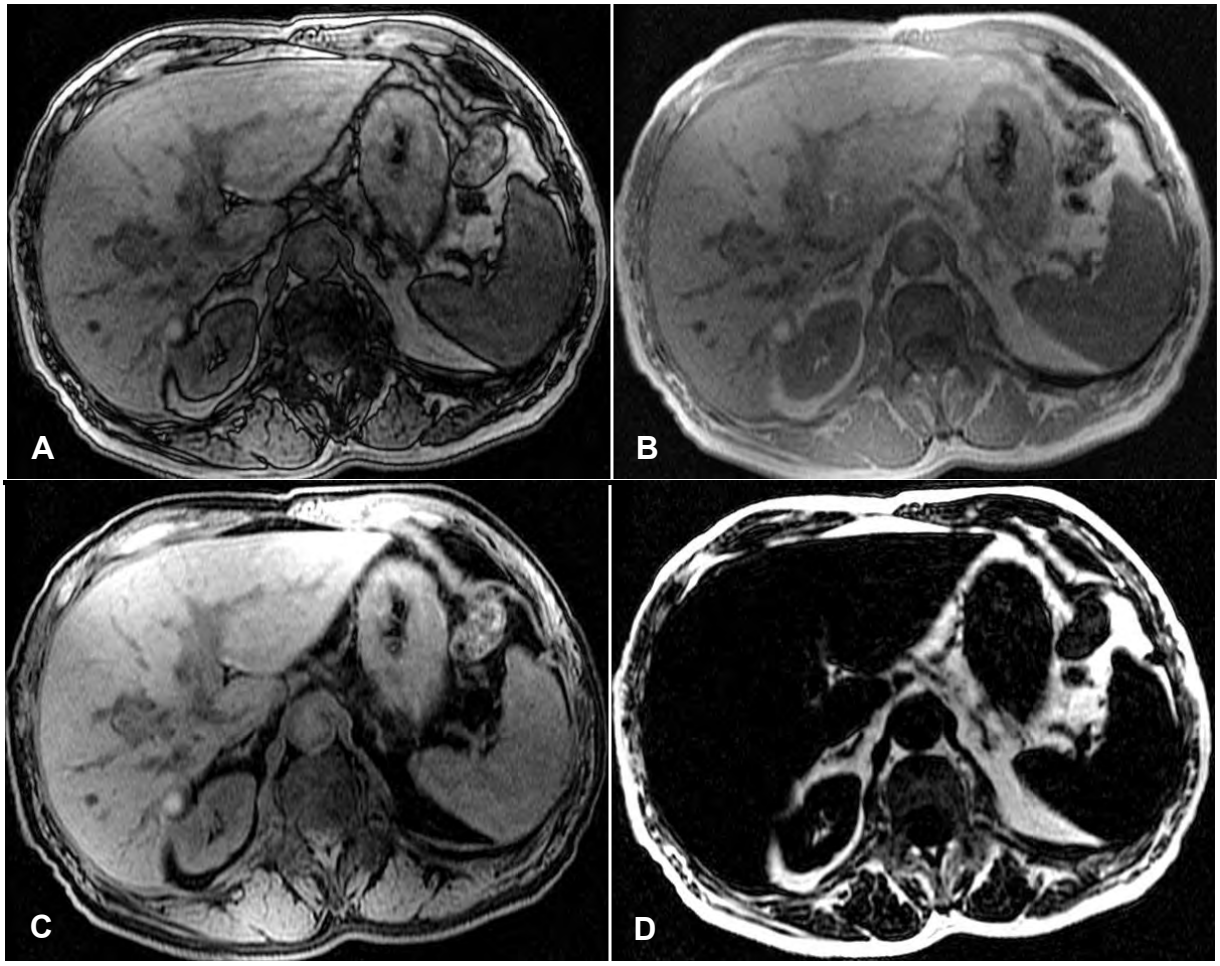

Figure 28. Axial 3-point Dixon in- and out-of-phase. (A) Out-of-phase. (B) In-phase. (C) Water only. (D) Fat only.

Courtesy of Duke University Hospital.

Axial T2-weighted Fast/Turbo Spin Echo

T2-weighted FSE/TSE or single-shot fast-spin echo (SSFSE) are routinely used in the liver for lesion detection and characterization (**Figure 29**). Again, the decision should be made regarding whether or not to breath-hold during this scan. This is a good opportunity to use a respiratory trigger or **navigator device** to trigger the scans according to a patient's respiratory cycle, especially for patients who have a difficult time holding their breath. Trigger and navigator placement are important for the success of this sequence. If the decision is made to breath-hold the T2-weighted images, educating the patient to breathe in the same manner is essential so that misregistration of slices is kept to a minimum and lesions are not missed because of inability to breath-hold consistently.

Dynamic Liver Imaging

Most liver exams require the use of a contrast agent to help differentiate cancer from **neoplasms,** which are atypical masses. Evaluation of arterial enhancement is crucial for proper diagnosis, and this process can be intimidating when approaching abdominal imaging. There are several methods by which to time the delivery of contrast to the liver, and each diagnostic center decides on the best delivery system based on their equipment and practices.

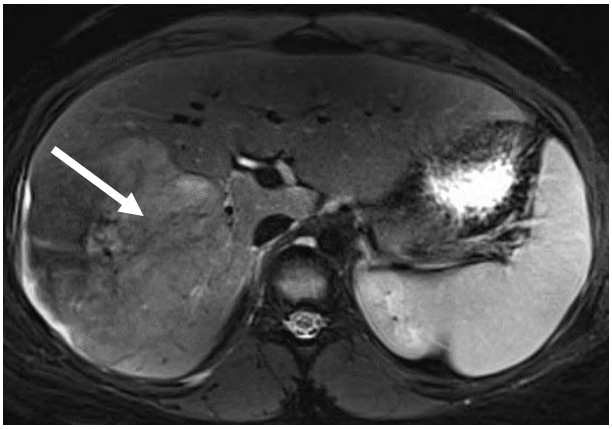

Figure 29. Axial T2W FSE with fat saturation demonstrating a large fibrolamellar carcinoma that encompasses virtually the entire right lobe.

Courtesy of Duke University Hospital.

Bolus Timing

When discussing contrast agent administration, it is important to note that healthy and unhealthy livers will enhance differently during the three postcontrast phases: the arterial, portal venous, and equilibrium phases.

The liver has a dual blood supply. In a healthy, well-functioning liver, 80% of the blood supply is via the portal vein and the remaining 20% by the hepatic artery. Thus the liver will enhance during the portal venous phase. Most liver tumors receive their blood supply through the hepatic artery and will enhance during the arterial phase.

Accurate timing of the arterial postcontrast phase can be performed by employing a quick circulation-time test prior to the start of the dynamic study. Many imaging centers use this technique for liver and pancreatic MRI. This “test-bolus” technique is commonly used to accurately time gadolinium-enhanced 3D MR angiograms and can also be performed to better time the arterial phase of contrast enhancement.

The disadvantage of using the test bolus technique is some loss of the total contrast dose and some background parenchymal enhancement of the liver tissue. To perform imaging with test bolus tracking, the technologist obtains a scout image, selecting a slice near the celiac artery. The test bolus, approximately 1-2mL of contrast, is injected with 20mL saline. A time-intensity graph is obtained to determine the time of peak intensity and therefore the delay time (**Figure 30**). The remaining bolus is then administered, and arterial phase imaging is initiated after the calculated time delay.

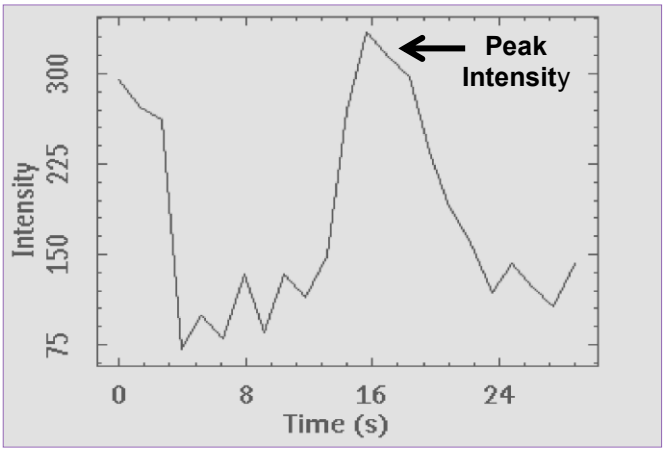

Figure 30. Time and intensity graph.

Bolus Tracking

Each manufacturer has different names for bolus tracking or computer-aided detection (CAD) of contrast media. To perform bolus tracking, the technologist obtains a scout image and selects the region of interest. Imaging begins when the ROI becomes **opacified**. The scan will either be auto-triggered when the intensity increases approximately 20% or manually when the technologist initiates the scan. Auto-triggered bolus tracking relies on proper placement of the bolus detection device, while manual triggering relies on the technologist's ability to recognize the arrival of contrast media.

Multiphase Dynamic Imaging

Multiphase dynamic imaging employs a lower spatial resolution sequence with several dynamic phases taken in rapid succession using a 3D T1-weighted, fat-saturated, fast-spoiled gradient sequence.

For example, there may be three acquisition phases, one every six to eight seconds. The peak of the early arterial phase as well as the late arterial phase are useful for the detection and characterization of focal liver lesions. While it can be a fairly long breath-hold, one or two phases should be sufficient for diagnosis if the patient cannot hold their breath for 24 seconds.

The dynamic timing of contrast arrival is straightforward: if a patient is under 60 years of age, use a **scan delay** of 15 seconds; if the patient is over 60 years of age, use a scan delay of 20 seconds. While this scan is often of lower spatial resolution, multiphase dynamic imaging is foolproof for obtaining excellent arterial contrast timing.

The advancement of parallel imaging and acceleration in both slice and frequency direction with higher acceleration rates allow for significantly reduced 3D breath-holds without affecting image resolution, coverage, or tissue contrast.

The dynamic timing of contrast arrival is straightforward: if a patient is under 60 years of age, use a scan delay of 15 seconds; if the patient is over 60 years of age, use a scan delay of 20 seconds

While proper dynamic enhancement is essential for accurate diagnosis of liver lesions, capturing high-resolution images of the hepatic vasculature system and parenchymal enhancement is also important. Once the initial arterial scan is complete, the next scan should be set up and ready to apply as soon as possible. Portal vein enhancement occurs approximately 45-75 seconds post-injection, so the imaging window of opportunity is small. The equilibrium state of the liver occurs approximately 90-120 seconds after administration of the contrast agent. The fast perfusion of the liver when using a GBCA requires a patient to do quite a bit of breath-holding, emphasizing the importance of using non-breath-hold sequences prior to the strenuous series of breath-holds that the patient must perform to acquire good dynamic images (**Figure 31**).

For detailed protocol information, see Sample Liver Protocol and Optional Liver Sequence at the end of this material.

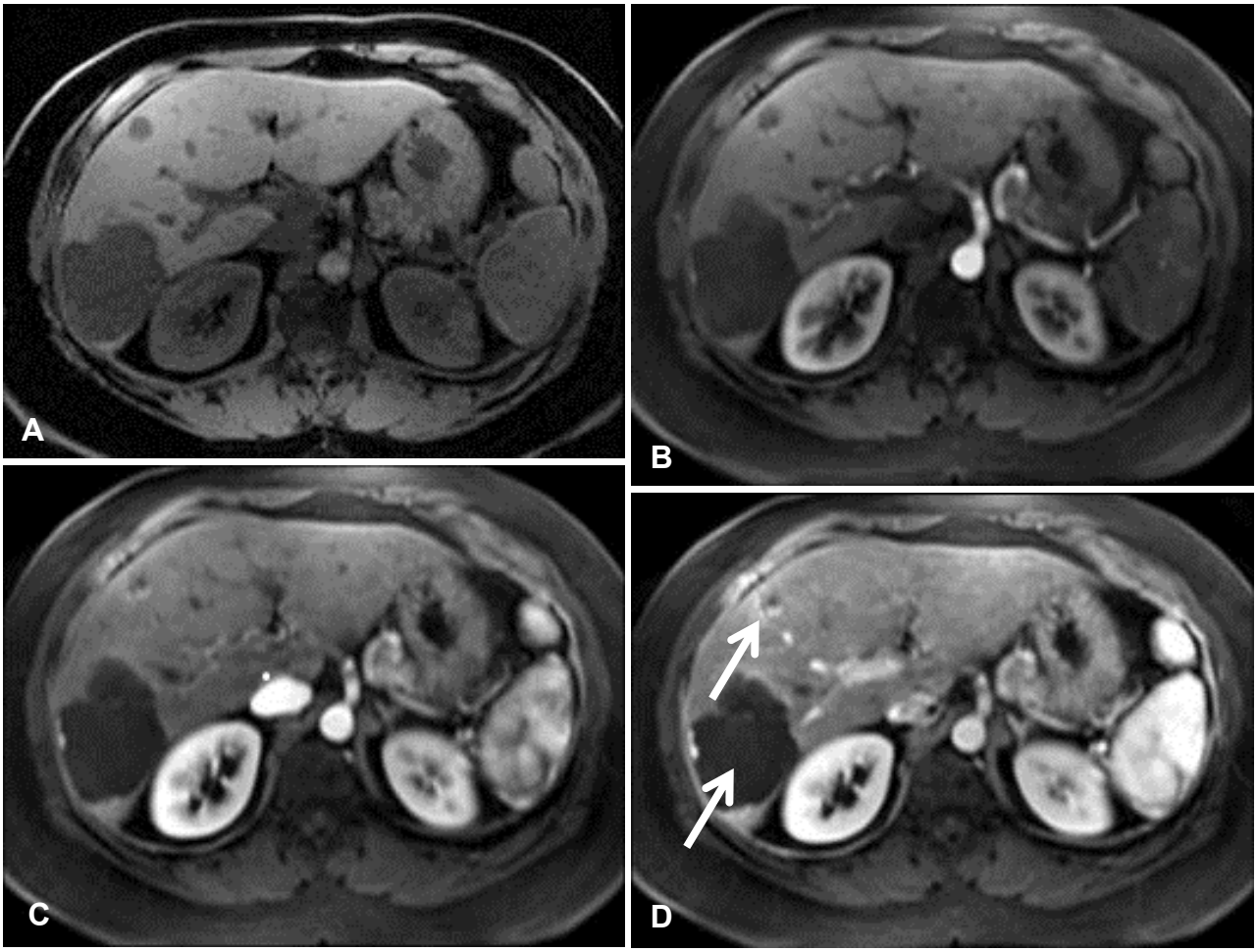

Figure 31. Multiphase dynamic imaging. (A) Precontrast. (B) First arterial phase. (C) Second arterial phase. (D) Third arterial phase. Two hemangiomas are seen in the right hepatic lobe (arrows).

Courtesy of Duke University Hospital.

LIVER-SPECIFIC GADOLINIUM-BASED CONTRAST AGENTS

Generally, most liver imaging requires the use of a gadolinium-based contrast agent to enhance liver **parenchyma** as the contrast between tumor tissue and the surrounding liver parenchyma is not great enough. Typically most agents are extracellular in nature, offering excellent parenchymal enhancement. These hepatocyte-specific agents have a high relaxivity, meaning a greater ability to shorten proton relaxation times and subsequently increase signal intensity on T1-weighted images.

LIVER MRI PROTOCOL TIPS

- Keep the exam as short as possible to reduce patient anxiety
- Keep each series as short as possible to reduce respiratory artifacts and slice misregistration
- Robust T2W and in-and-out-of-phase imaging reduces the number of breath-holds required while yielding optimal image quality
- For the contrast-enhanced series, be sure to acquire images during the unenhanced and arterial, portal venous, and equilibrium phases; remember that healthy and unhealthy liver will enhance differently
- Accurate timing of the arterial phase will ensure good visualization of liver pathologies in their appropriate phases
- A good mixture of breath-hold and non-breath-hold sequences will help differentiate liver tissue from abdominal tissue

Relaxivity is the mechanism that produces tissue contrast, allowing the radiologist to not only better visualize but to characterize abnormalities. Image quality is dependent upon the degree of relaxivity of the contrast agent, and gadolinium has proven to be efficient for producing relaxation in tissues in MRI.

Greater signal intensity results in better tissue contrast enhancement, which may lead to improved visualization. New contrast agents with hepatocellular properties are now available that may help with lesion detection and characterization. Eovist® (gadoxetate disodium, Bayer Healthcare Pharmaceuticals) was FDA-approved in 2008 and currently the only GBCA indicated for liver MRI for the detection and characterization of lesions in adults with known or suspected focal liver disease.

After Eovist administration, approximately half the dose is taken up by functioning **hepatocytes**, allowing for hepatocellular imaging after 20 minutes. Lesions with minimal or nonfunctioning hepatocytes generally will not take up Eovist, whereas lesions with functioning hepatocytes will take up the GBCA (**Figure 32**).

Another feature of Eovist is its dual elimination through both the renal and hepatobiliary systems. In healthy patients, approximately 50% of the dose is eliminated through the renal system and approximately 50% through the hepatobiliary system. This dual elimination mechanism has two important benefits for patients. First, it allows for rapid elimination in healthy patients and secondly, because of the dual excretion pathways, Eovist can still be eliminated even if one of the pathways is impaired, with no dosage adjustment required. Patients with impaired kidneys will eliminate a larger percentage of the dose through the hepatobiliary system.

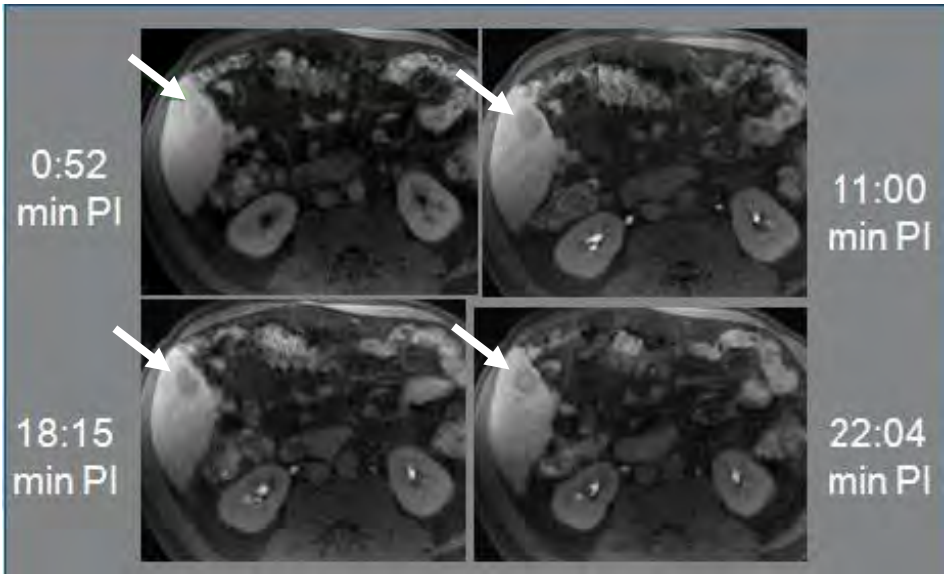

Figure 32. Patient with hepatitis C. Eovist-enhanced 3-phase dynamic series showing hypointense lesion. Note isointense appearance on 20-minute delay, which is necessary for complete lesion visualization (arrows).

Courtesy Duke University Hospital

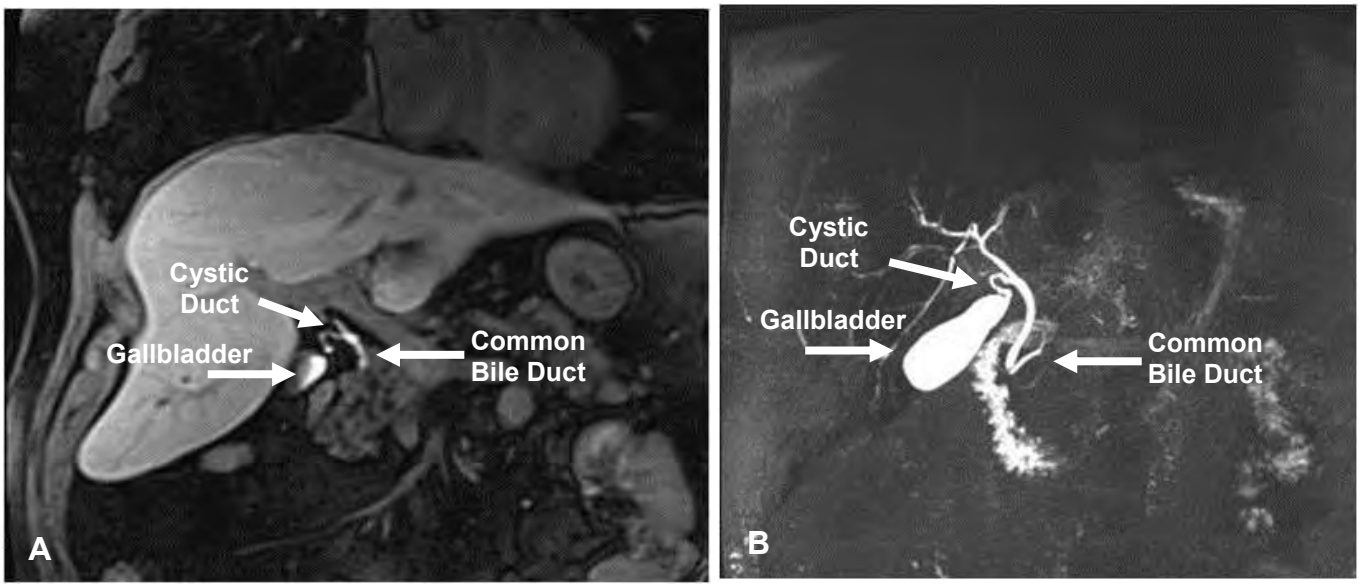

Figure 33. Comparison of T1W sequence to MRCP visualizing the gallbladder, common bile duct, and cystic duct. (A) Contrast-enhanced coronal T1W, 20-minute delay. (B) Noncontrast-enhanced coronal MRCP.

Courtesy Duke University Hospital

Due to the need for delayed imaging, protocol development is an important consideration when imaging with Eovist. T2 effects are not disturbed by administration of Eovist, allowing these sequences to be done after the injection of contrast. Once pre-contrast imaging is performed using Dixon and 3D T1-weighted sequences, Eovist can be injected and any further scans will help fill the 20-minute delay time necessary for Eovist to be taken up by functioning hepatocytes. Respiratory triggered T2W and diffusion-weighted imaging can be done postcontrast; however, any magnetic resonance cholangiopancreatography (MRCP) imaging should be done prior to administration of Eovist.

Because Eovist is a hepatocellular agent, it is excreted out the common bile duct (CBD) and when mixed with bile creates a negative contrast in the CBD and will not be well-visualized. Once 15-20 minutes has passed, a coronal 3D T1-weighted sequence will demonstrate the common bile duct and other biliary structures if the patient's **bilirubin** is not too high (**Figures 33 and 34**). If the bilirubin is too high, the bilirubin and Eovist will compete for the intracellular space, and Eovist will not excrete as quickly as in a liver with normal function.

Compared to other gadolinium-based contrast agents, Eovist has shown a significant improvement in detection of metastases and hepatocellular carcinoma, improved benign vs malignant lesion classification, and improvement in lesion detection, localization, and characterization.

As always, the patient should be thoroughly screened to ensure GBCA administration is not contraindicated.

A sample liver protocol using Eovist can be found at the end of this material.

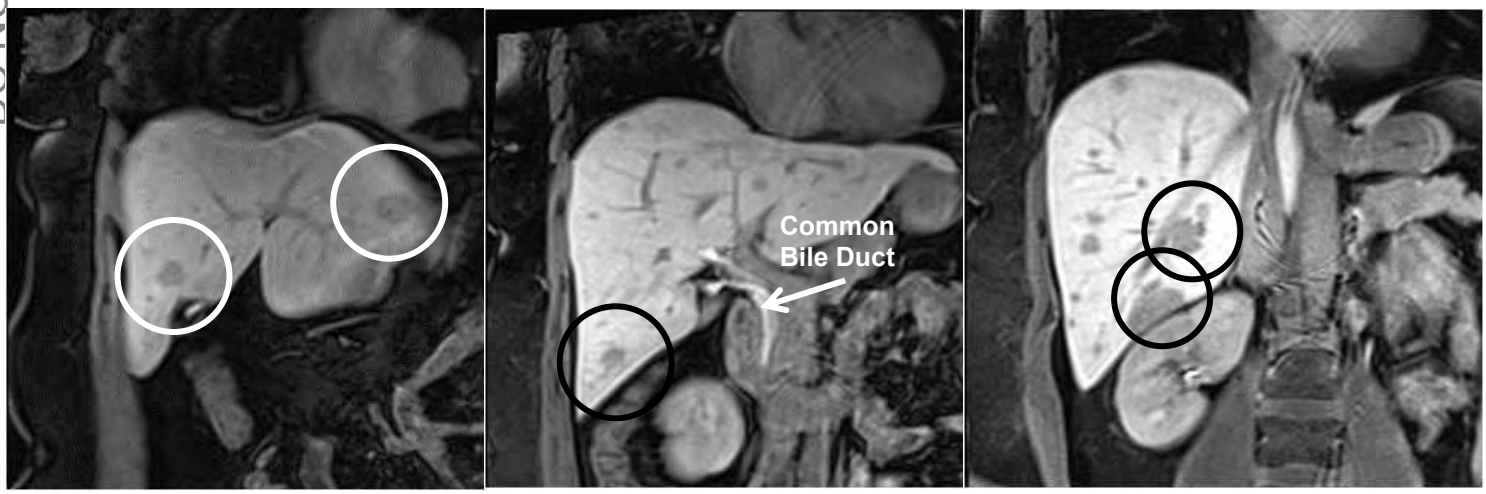

Figure 34. Coronal 3D T1W post-Eovist; note the appearance of several lesions and common bile duct.

Courtesy Duke University Hospital.

MRI FINDINGS — BENIGN

The liver is imaged to detect and characterize either **focal** diseases or **diffuse** processes. These can easily be separated into benign and malignant lesions or primary and secondary lesions. Most commonly encountered focal diseases include hemangiomas, cysts, focal nodular hyperplasia (FHN), hepatic adenoma, hepatocellular carcinoma, and metastatic neoplasms. Most common diffuse processes include cirrhosis, hemochromatosis, hemosiderosis, and hepatic steatosis.

Hemangiomas

Hemangiomas are common benign lesions that are clinically important only because they can be easily mistaken for malignant processes. Hemangiomas themselves seldom cause clinical problems, with the exception of giant hemangiomas, which can occasionally cause symptoms of pain or other discomfort when they become larger than 5.0cm.

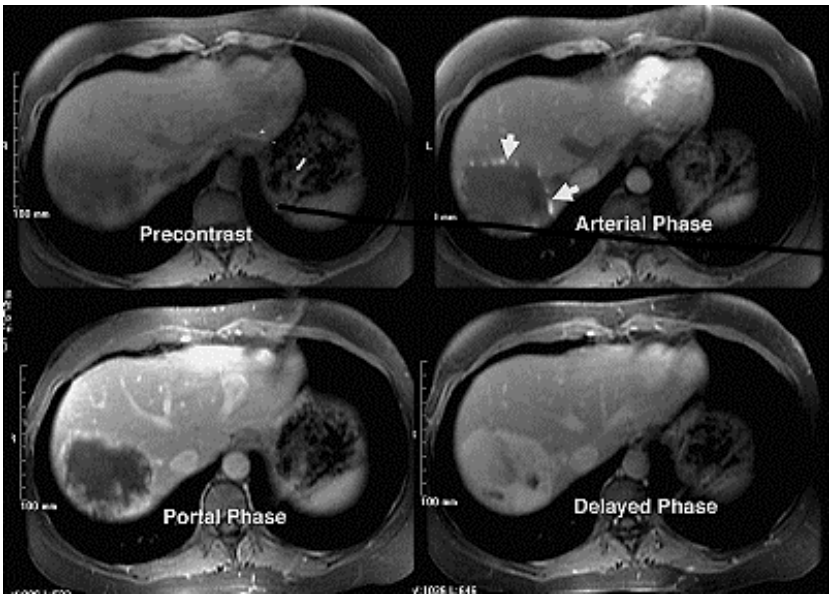

Figure 35. Dynamic pre- and postgadolinium-enhanced images of a liver hemangioma. The primary diagnostic criterion for liver hemangioma is the characteristic pattern of discontinuous peripheral nodular enhancement (arrows) with eventual complete or partial fill-in of the remainder of the lesion following gadolinium administration.

Courtesy of James P. Earls, MD, Fairfax Radiologic Consultants, Fairfax, VA

Hemangiomas are characteristically very high in signal intensity and sharply circumscribed on T2-weighted images. The primary diagnostic criterion is the characteristic pattern of contrast enhancement exhibited by hemangiomas following the administration of a GBCA. Hemangiomas depict characteristic discontinuous peripheral nodular enhancement with eventual complete or partial fill-in of the remainder of the lesion following contrast agent administration. The entire enhancement process may take less than one minute in some cases or several minutes for larger lesions; therefore, at least three to four postcontrast datasets are quickly acquired immediately following GBCA administration. The first two phases should be performed to coincide with the arterial and portal venous phases of perfusion (**Figure 35**).

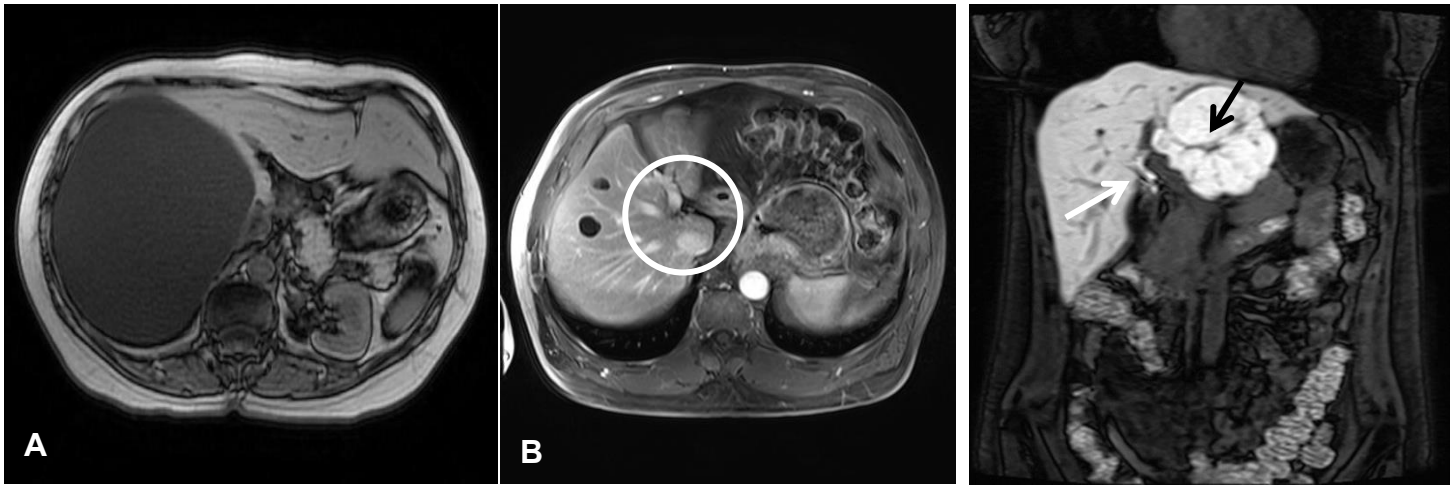

Figure 36 *(left***).** Liver cysts. (A) Axial 3D Dixon out-of-phase giant cyst without contrast. (B) Axial 3D T1W contrast-enhanced image demonstrates peripheral ring enhancement (circle) caused by compressed liver parenchyma around cyst.

Figure 37 *(right).* Coronal T1-weighted fat-saturated 3D gradient echo image acquired 20 minutes post-Eovist administration. A large FNH is seen in the left hepatic lobe, hyperintense compared to the rest of the liver and characterized by the central scar (black arrow). Also note the biliary excretion of the GBCA (white arrow).

Images courtesy Duke University Hospital.

Cysts

Liver **cysts** are benign lesions that can mimic neoplasms if not imaged correctly (**Figure 36**). Like hemangiomas, cycts are very bright on T2-weighted sequences and sharply circumscribed. Liver cysts usually can be characterized without the use of contrast enhancement, but when contrast is used, cysts will not enhance. Occasionally the adjacent liver tissue appears to enhance slightly more than the remainder of the liver parenchyma. This is not the cyst enhancing but may represent compressed normal liver that appears to enhance differently than the adjacent liver.

Focal Nodular Hyperplasia

Focal nodular hyperplasia is a benign and commonly encountered liver lesion. FNH is a collection of benign hepatocytes that derive most of their blood supply from the hepatic artery, while the remainder of the liver receives its supply predominantly from the portal vein. Because these lesions are comprised of normal hepatic tissue, they are often very subtle on unenhanced images, having T1W and T2W properties similar to normal hepatic parenchyma. In some lesions there may be a central region called a central scar or fibrovascular core that may be slightly darker than the liver on T1W and slightly brighter on T2W. Following gadolinium administration, FNH characteristically hyperenhances on the arterial phase and eventually **equilibrates** with the remainder of the liver on later phases of enhancement. Using a contrast agent with hepatocellular properties can help characterize these lesion types since FNH typically demonstrates a popcorn-like enhancement pattern on delayed imaging (**Figure 37**).

Hepatic Adenomas

Hepatic adenomas are clinically important benign lesions because they tend to bleed and cause symptoms; in rare instances, hepatic adenomas can be serious. Hepatic adenomas are comprised of benign liver cells but are more disorganized than FNH and therefore are more heterogeneous than FNH on both unenhanced and enhanced images. Although some adenomas may appear as FNH, they sometimes contain blood or blood products, making them more detectable on MR and therefore more likely to be diagnosed (**Figure 38**). In a minority of cases, multiple hepatic adenomas, sometimes more than 10 or 20, appear simultaneously in a condition known as hepatic **adenomatosis** (**Figure 39**).

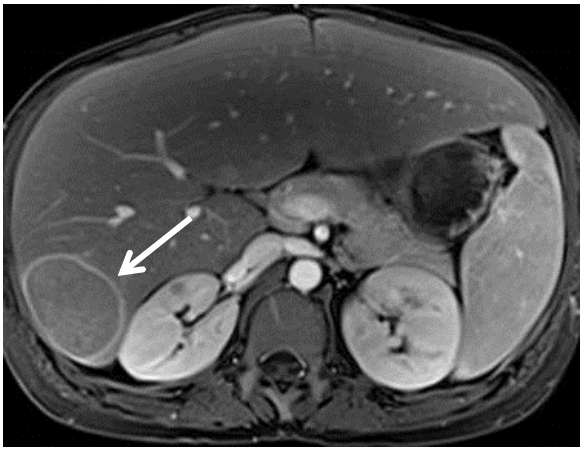

Figure 38. Hepatic adenoma. Note the capsular enhancement.

Courtesy of Duke University Hospital.

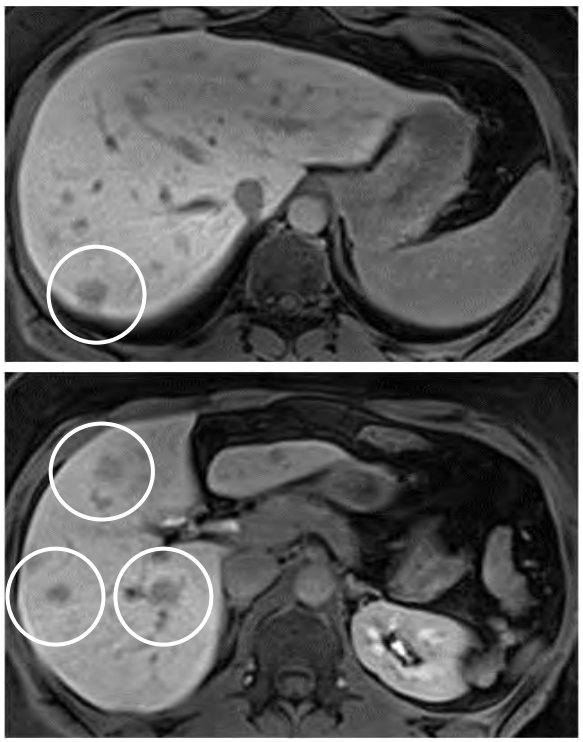

Figure 39. Example of adenomatosis. 3D T1W contrast-enhanced 20-minute delay showing multiple adenomas at different levels of the liver.

Courtesy of Duke University Hospital.

Hemochromatosis and Hemosiderosis

Hemochromatosis and hemosiderosis are both conditions where the liver contains too much iron. The iron causes T2* effects, leading to liver signal loss on all pulse sequences with the effect most pronounced on gradient echo images due to the lack of a refocusing pulse.

Hemochromatosis is a genetic disease in which the liver, pancreas, heart, and other organs accumulate excessive iron and can lead to the development of **hepatocellular carcinoma** in the liver.

Hemosiderosis is an overload of iron deposited in tissues that do not normally contain iron and is usually caused by multiple blood transfusions or chronic dialysis. Iron released by the blood cells is ingested by cells of the reticuloendothelial cell system (RES). The RES cells reside in the liver, spleen, and bone marrow and thus these areas will appear dark on MR imaging. The best pulse sequence for visualizing for iron storage is an in- and out-of-phase series where the signal intensity in the liver is markedly lower on the images with the longer echo time.

Hepatic Steatosis

Hepatic steatosis is a condition where fat is stored in the liver. Also known as fatty infiltration of the liver, steatosis can appear as a small focal area of liver involvement, regional or geographic involvement, lobar or parenchymal involvement.

There are many causes of hepatic steatosis, and it is a very common entity in the USA. Occasionally focal fatty infiltration or focal areas of normal liver that are spared from fatty infiltration in an otherwise fatty liver may be misdiagnosed as a focal neoplasm or other disease. The fatty areas have high signal intensity on non-fat saturated T1W and FSE T2W images. Because the liver in the region of fat has an intracellular mixture of fat and water, it loses a substantial amount of signal intensity on out-of-phase MR imaging techniques. This is an excellent indication for using the 3D 2-point Dixon gradient echo sequence described earlier.

Hepatitis

Hepatitis is usually caused by a viral infection and is characterized by irritation or swelling of liver cells causing inflammation of the liver. Worldwide, hepatitis viruses are the most common cause of the condition, but hepatitis can be caused by other infections, toxic substances (notably alcohol, certain medications, some industrial organic solvents, and plants), and autoimmune diseases.[15]

Hepatitis may occur with few or no symptoms but often leads to jaundice, poor appetite, and a general feeling of weakness and discomfort. Acute hepatitis resolves in less than six months; chronic hepatitis persists beyond six months.

The outcome of hepatitis depends heavily on the disease or condition that is causing the symptoms. Hepatitis A, which is caused by ingesting contaminated food or water or close contact with someone who is infected, may have no symptoms and the patient will recover without any long-term effects. Hepatitis C is considered one of the more serious forms of hepatitis and is usually acquired through contact with contaminated blood.

Depending on the type of hepatitis acquired, the subsequent chronic damage to the liver results in the replacement of healthy tissue by fibrotic tissue. The accumulation of fibrotic tissue prevents the liver from functioning properly and can result in the development of a cirrhotic liver or liver cancer, specifically hepatocellular carcinoma.

MRI FINDINGS — MALIGNANT

Metastatic Disease

A liver **metastasis**, also called secondary liver cancer, is a malignant tumor that has spread from another organ affected by cancer.

The liver is a common site for metastatic disease because of its dual blood supply. Metastatic tumors in the liver are much more common than cancer that starts in the liver (primary tumor). Almost any cancer can spread to the liver. Most metastases develop from colon or rectal cancers but can also originate in the gastrointestinal tract, breast, ovaries, lungs, and kidneys.[16]

Liver MRI is performed to stage liver cancer and is used to detect and characterize metastases or differentiate benign lesions from metastatic disease. Metastases are typically bright on T2-weighted images and darker than normal liver on T1-weighted images.

The challenge in liver MRI for metastatic disease is the high probability that a benign lesion can be misinterpreted as evidence of metastatic disease. The appearance of liver metastases on MRI can be variable, but MRI is typically found to be more sensitive than imaging on CT.

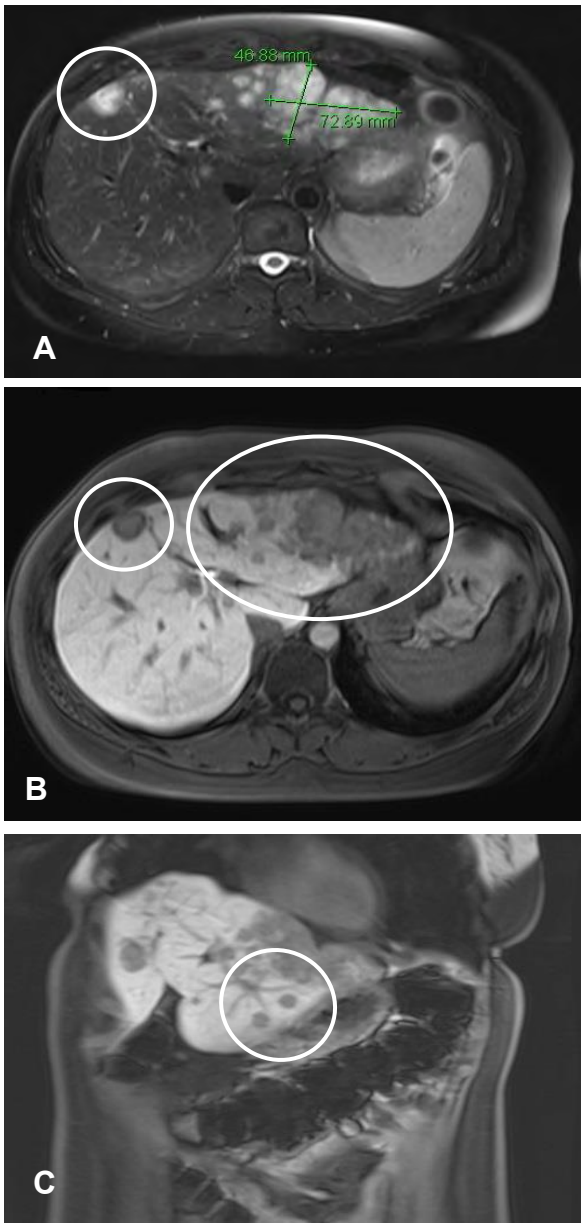

Figure 40. Breast cancer metastases. (A) Axial T2W demonstrating large lesion in left lobe (circle). (B) Axial 3D T1W 20-minute delay using Eovist; demonstrating hypointense large lesion and smaller lesion. (C) Coronal 3D T1W 20-minute delay using Eovist, demonstrating same lesions as Image B, and two additional lesions.

Courtesy of Duke University Hospital.

Metastases are typically bright on T2W and darker than normal liver parenchyma on T1-weighted images. Unlike hemangiomas or cysts, metastases are normally only moderately high in signal intensity and may be very heterogeneous in appearance, sometimes having a “target” or “bull’s-eye” appearance of higher central signal and layers of peripheral lower signal intensity on T2-weighted images.

Following GBCA administration, metastases may rapidly enhance on the arterial phase or they may show a ring of peripheral enhancement followed by partial or complete fill-in on delayed views (**Figure 40**).

Liver metastases are usually asymptomatic and generally are found during workups for malignancy. If metastases are advanced, the patient may experience localized tenderness, abnormal liver function tests, ascites, or a low-grade fever.

Cirrhosis

Cirrhosis is a disease that arises from continuous and prolonged injury to the liver. Common causes include chronic hepatitis B or C, alcohol abuse, or autoimmune disease. Because of repeated injury, the liver must continuously repair itself, creating many areas of fibrosis and regeneration of hepatocytes, which typically lead to a nodular pattern throughout the liver. The right lobe tends to atrophy while the **caudate lobe** becomes larger.

Cirrhosis is often associated with the development of ascites, enlargement of the spleen, development of larger collateral blood vessels throughout the abdomen (varices), and reversal of blood flow in the portal vein.

Imaging patients with cirrhosis can be a challenge because their breath-holding abilities may not be as good as in healthier patients. The ascites associated with cirrhosis can cause imaging artifacts, particularly on T2-weighted images and 3.0T imaging. At 3.0T, **dielectric effect** is more pronounced due to increasing field inhomogeneities in patients with ascites. Finally, the chronically damaged liver eventually becomes quite small, making it more difficult to image and detect lesions.

Hepatocellular Carcinoma

Hepatocellular carcinoma, or hepatoma, is a primary malignancy that arises from the liver. HCC is most commonly seen in patients with cirrhosis but occasionally arises in an otherwise normal liver. On imaging, HCC has varied appearances. Typically, these are solid masses that have a moderately high T2 signal intensity, and they enhance relatively quickly and heterogeneously following GBCA administration. Following contrast agent administration, the arterial phase images are of critical importance as some HCCs will only be evident on this phase and not detectable on any other phase of perfusion or on unenhanced images.

HCCs can be small and hypervascular, solid and homogeneous, encapsulated, necrotic, diffusely infiltrating, fat containing, or have small "daughter" HCCs along their margin. (**Figure 41**).

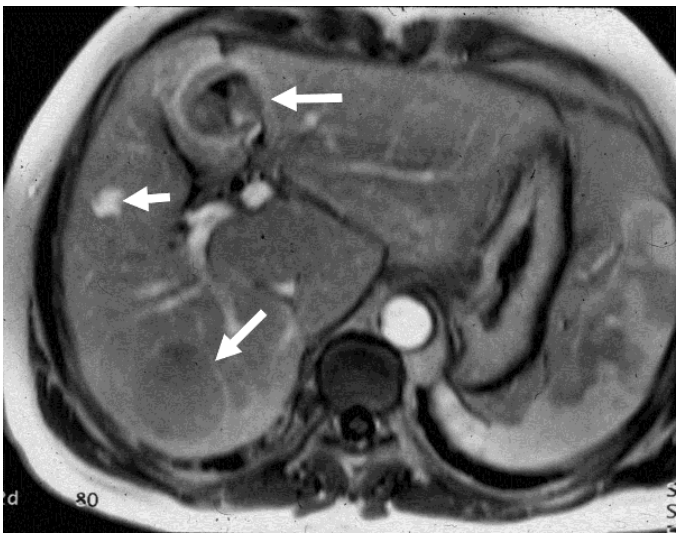

Figure 41. Hepatocellular carcinomas have numerous appearances on MRI. This gadolinium-enhanced T1W GRE image shows three HCCs (arrows), each with slightly different morphology.

Courtesy of James P. Earls, MD, Fairfax Radiologic Consultants, Fairfax, VA

MR CHOLANGIOPANCREATOGRAPHY

MRCP vs ERCP

Magnetic resonance cholangiopancreatography is a noninvasive test for evaluation of the bile ducts, gallbladder, and pancreatic duct. By using heavily T2-weighted sequences, the signal of static or slow-moving fluid-filled structures such as bile and pancreatic ducts is greatly increased, resulting in greater duct-to-background contrast. MRCP is comparable to invasive endoscopic retrograde cholangiopancreatography (ERCP) for diagnosis of extrahepatic bile duct and pancreatic duct abnormalities, such as stones, malignant obstruction, congenital anomalies, and chronic pancreatitis.

In most institutions, MRCP has become the first-line imaging tool for the biliary system, with ERCP reserved for therapeutic indications as ERCP is not without risk. ERCP patients can contract pancreatitis due to contrast injection into the pancreatic duct, which can result in hospitalization and occasionally serious complications.

Indications for MRCP

Indications for MRCP include unsuccessful ERCP, contraindication to ERCP, or a low index of suspicion that disease requiring endoscopic intervention is present (**Table 1**). Although ERCP is still the standard of reference for imaging the biliary system, there are specific advantages of MRCP over ERCP. MRCP is noninvasive, less expensive, uses no radiation, requires no anesthesia, is less operator-dependent and allows better visualization of ducts proximal to an obstruction and detection of extraductal disease. Therefore, the use of MRCP continues to grow as a diagnostic procedure.

	MRCP	ERCP
Indications	Unsuccessful or contraindication to ERCP	Aids in diagnosis of extrahepatic bile ducts and pancreatic abnormalities
Advantages	Noninvasive, less expensive, and uses no radiation Allows for better visualization of ducts proximal to an obstruction and extraductal disease Performed without contrast media	Patient is sedated and cooperative Allows for therapeutic intervention of obstructed bile ducts Generally more expensive
Disadvantages	Claustrophobia	Patient can contract pancreatitis from contrast agent administration

Table 1. Comparison of MRCP and ERCP.

Imaging Parameters for MRCP

MRCP protocols may vary between MR manufacturers and institutions. In general, MRCP is performed with ultrafast, heavily T2-weighted sequences using both 2D thick slab (single section) and 2D thin slice in the axial or coronal plane and coronal thin slice 3D respiratory-triggered fast-spin echoes.

The thick section coronal plane provides a cholangiographic display that mimics the appearance of the bile ducts on ERCP. One orthogonal coronal slab and two slabs angled plus and minus 20° are helpful in demonstrating the biliary anatomy. By examining these thick slab sequences, a determination can be made as to which slab best demonstrates the junction of the common bile duct and the pancreatic duct. Next, thin section sequences, usually 3mm slice thickness, can be set up to best evaluate the pancreatic duct and distal common bile duct. For patients who are not able to hold their breath, 3D respiratory-triggered sequences in a coronal plane can be very useful in MRCP evaluation.

Thick Slab MRCP

While the thick slab images more closely resemble conventional cholangiograms and are familiar to many clinicians, spatial resolution is degraded due to **volume averaging** effects. The single-shot fast-spin echoes (SSFSE, HASTE, etc.) are a more rapid MRCP sequence performed in a single breath-hold, thereby significantly reducing motion artifacts and increasing image quality. Because of less motion artifact with SSFSE, SNR increases compared with that of fast-spin echo MRCP.

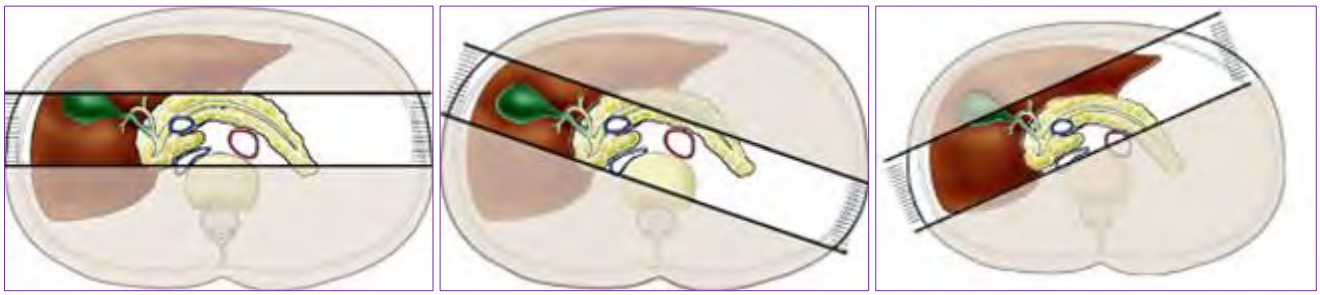

Figure 42. Thick slab MRCP. This series shows how the slices should be prescribed.

Used with permission of Martin Prince, MD, PhD.

The use of a breath-hold technique helps reduce artifacts from respiratory motion and section misregistration. The combination of rapid sequences and the torso phased-array coil or one of 8-channel array coils makes it possible to visualize ducts as small as 1mm in diameter. In addition, owing to the shorter spacing of the RF pulses, susceptibility artifacts from the intestine, surgical clips, catheters, and stents, for example, are reduced with the single-shot fast-spin echo sequence. **Figure 42** illustrates how slices should be prescribed for thick slab MRCP.

Thin Slice MRCP

3D, respiratory-triggered, thin slice acquisitions provide greater spatial resolution than thick slabs. Source images can be scrutinized to detect small filling defects and strictures easily missed on thick slab images. 3D acquisitions can be post-processed and MIP images obtained for 360° rotations of the entire biliary system. Proper respiratory triggering is essential for clear, high-resolution images. When using a navigator device, ensuring that the device is triggering appropriately is essential for obtaining good image quality. If using a respiratory belt, it is important that the waveform is reliable before starting the sequence. When using 2D thin slice imaging, patient education regarding proper breath-hold techniques is important. Misregistration is a common problem, so contiguous slices through the pancreas and gallbladder are preferable.

Additional sequences for MRCP protocols can be found at the end of this material.

MRI FINDINGS — MRCP

Choledocholithiasis

Choledocholithiasis (bile duct stones) is a common indication for MRCP, which is comparable to ERCP for detection of bile duct stones and superior to CT or ultrasound. Up to 25% of patients with acute **cholecystitis** (gallbladder stones and inflammation) have bile duct stones, and MRCP is often performed as part of the preoperative workup. Bile duct stones are readily identified as dark filling defects within the high-signal intensity bile fluid on MRCP (**Figure 43**). Stones as small as 2mm in diameter can be visualized. The accuracy of stone detection is improved with SSFSE techniques due to reduction of motion and susceptibility artifacts. Small stones may not cause secondary **dilatation** of the ducts and are best seen on source images. The differential diagnosis of filling defects in the bile ducts most commonly includes stones and air bubbles; however, neoplasms, blood clots, concentrated bile, metallic stents, flow voids, and susceptibility artifact from surgical clips must be ruled out.

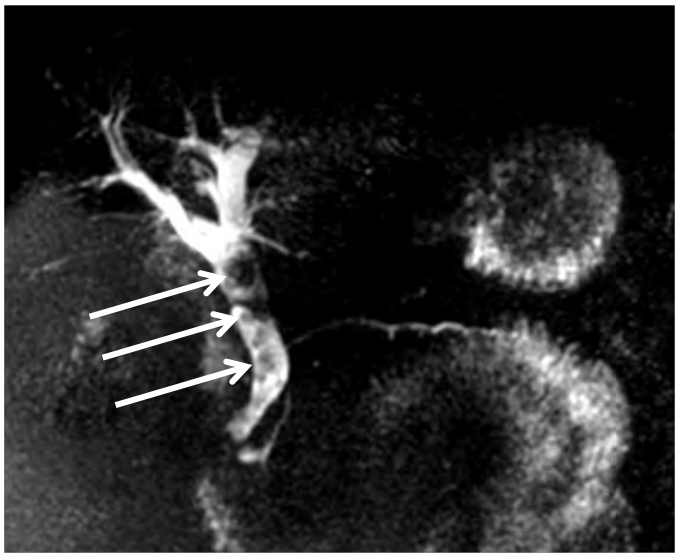

Figure 43. Common bile duct filled with multiple large and small stones. MRCP 3D T2W FSE.

Courtesy of Duke University Hospital.

Benign Strictures

Benign strictures are most commonly seen after an injury to the extrahepatic bile ducts during **cholecystectomy**, although other causes include infection, pancreatitis, stone passage, trauma, and **primary sclerosing cholangitis**. MRCP is comparable to ERCP for demonstrating the location and extent of strictures of the extrahepatic bile duct.

Congenital Anomalies

Congenital anomalies involve variations of the bile ducts from the commonly described anatomic pattern. MRCP is accurate for the diagnosis of **aberrant** hepatic ducts and cystic duct variants. Anatomic variants have high potential for injury during gallbladder removal. The most common anomalies are an aberrant right hepatic duct with insertion into the common hepatic duct or cystic duct, a long intramural cystic duct parallel to the common hepatic duct, or a cystic duct inserting medially on the common bile duct.

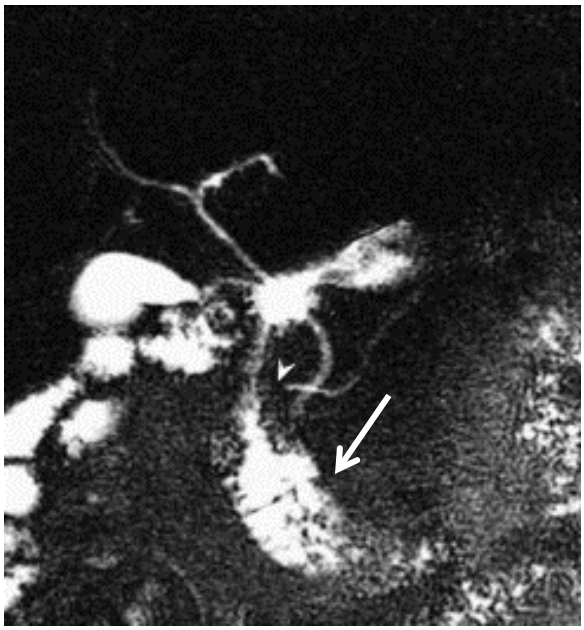

Figure 44. Pancreatic divisum. Depicts the dorsal and ventral pancreatic ducts of the body and tail draining through the minor papilla (arrow).

Used with permission of Martin Prince, MD, PhD.

Pancreas divisum, the most common anatomic variant of the pancreas, results from failure of fusion of the dorsal and ventral pancreatic ducts and may be associated with an increased prevalence of acute pancreatitis. MRCP has been shown to visualize pancreas divisum in almost all cases imaged with MR (**Figure 44**).

Primary Sclerosing Cholangitis

Primary sclerosing cholangitis, or PSC, is a disease of the bile ducts that causes inflammation and subsequent obstruction of bile ducts both at an intrahepatic and extrahepatic level (**Figure 45**). The inflammation impedes the flow of bile to the gut which can ultimately lead to cirrhosis, liver failure and liver cancer. Diagnosis typically is made in the setting of ERCP or MRCP. PSC appears as "beading" of the intrahepatic and extrahepatic bile ducts, both strictures and dilation. Primary sclerosing cholangitis is associated with **cholangiocarcinoma**, a cancer of the bile ducts inside and outside the liver. The lifetime risk for developing PSC in patients with cholangiocarcinoma is 10-15%[17].

Screening for cholangiocarcinoma in patients with primary sclerosing cholangitis is encouraged, but currently there is no consensus on which type of imaging modality or imaging intervals should be used.

Malignant Bile Duct Obstruction

Malignant bile duct obstruction is usually due to pancreatic neoplasms. Other causes include cholangiocarcinoma (bile duct cancer), metastases, and **lymphadenopathy**. Most malignant pancreatic neoplasms are **adenocarcinomas** that present as a focal mass in the pancreatic head. With MRCP, dilatation of both the pancreatic and bile ducts (the **double duct sign**) is highly suggestive of a pancreatic head malignancy. The addition of T1W- and T2-weighted sequences to MRCP improves specificity by allowing visualization of extraductal structures.

Chronic Pancreatitis

Chronic **pancreatitis** is a chronic inflammatory process of the pancreas that results in irreversible dysfunction and morphologic changes. The hallmark of this disease process is dilated side branches of the main pancreatic duct. Pancreatic **pseudocysts** are encapsulated collections of pancreatic fluid that can occur in association with acute or chronic pancreatitis. MRCP is more sensitive than ERCP for detection of pseudocysts because less than 50% of pseudocysts take up the contrast agent at ERCP. However, MRCP is less sensitive than ERCP for visualizing the site of communication with the pancreatic duct. High-signal intensity pseudocysts may obscure portions of the pancreatic and bile ducts; close scrutiny of the source images is necessary so that strictures or filling defects are not overlooked.

SUMMARY

Liver MRI continues to be a dynamic field. With significant advances in software and hardware, coils with higher receiver channels, and hepatobiliary-specific contrast agents, the quality of liver and pancreatic imaging has improved sufficiently to become the standard of care. With state-of-the-art scanners and parallel imaging techniques, the acquisition time for most liver sequences are short enough to be performed with breath-holds, resulting in exam times of less than 30 minutes.

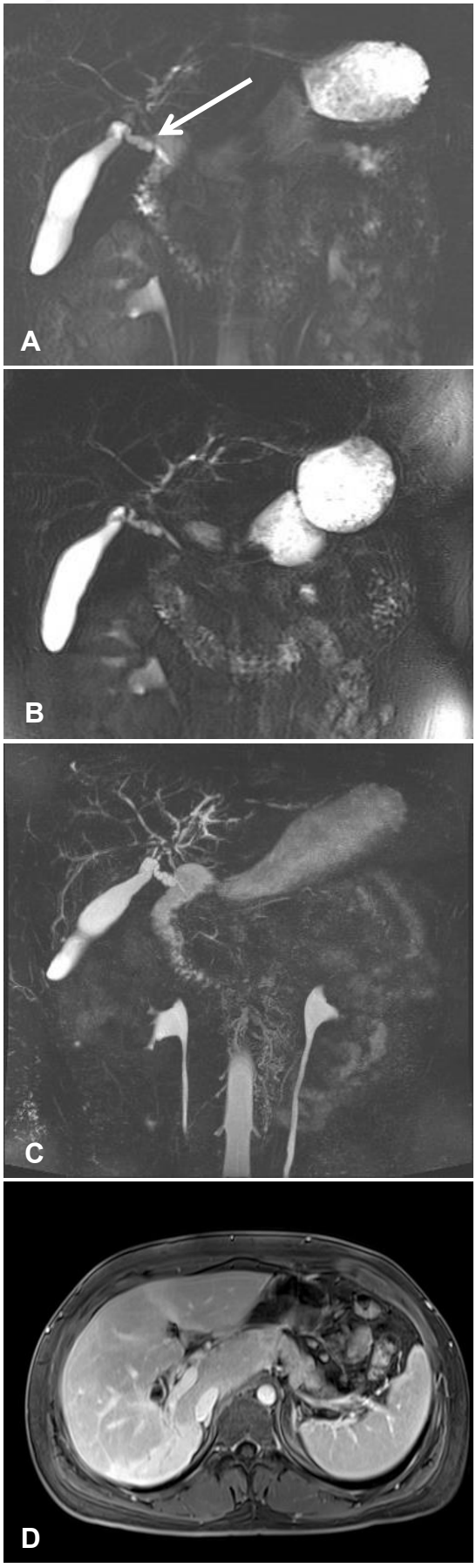

Figure 45. Primary sclerosing cholangitis. (A) Coronal 3D SSFSE (thick slab 60mm), demonstrating bead-like appearance of central CBD. (B) Oblique coronal 3D SSFSE; demonstrates same finding but from another projection. (C) Coronal 3D respiratory-triggered T2W again demonstrating a bead-like appearance of the central CBD. (D) Axial 3D contrast-enhanced T1W showing fibrotic enhancement of liver parenchyma, commonly associated with PSC.

Courtesy of Duke University Hospital.

Tom Schrack, BS, ARMRIT
Fairfax Radiological Consultants
Fairfax, VA

MRI OF THE ADRENAL GLANDS AND KIDNEYS

After completing this section, the reader should be able to:

- Describe the basic imaging requirements for the adrenal glands and kidneys
- Name the major MR findings for each organ

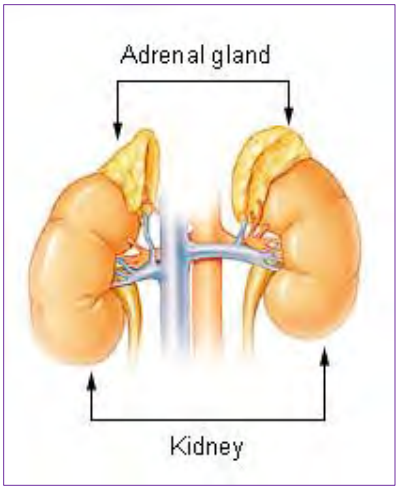

Figure 46. Anatomy of the adrenal glands and kidneys. Available at: Wikimedia.

MRI OF THE ADRENAL GLANDS

Overview

The adrenal glands are a type of **endocrine** gland that sit atop each kidney in a hood-like, thin, triangular layer (**Figure 46**). Made up of two layers, the outer cortex and the inner medulla, the adrenal glands produce norepinephrine and epinephrine (adrenaline), as well as salts to maintain **electrolyte** balance.

MR evaluation of the adrenal glands is quick and accurate. Typically, adrenal MR studies are referred for evaluation of an indeterminate mass detected on either CT or ultrasound. Most often these masses are adrenal **adenomas**, a common benign adrenal mass. MRI is useful for differentiating benign masses from neoplasms that have metastasized to the adrenal gland, such as from the lung. Adrenal gland MRI typically does not require the use of a GBCA, which substantially reduces exam time. Adrenal MRI is a relatively comfortable and quick exam for the patient.

In- and Out-Of-Phase Imaging

For characterization of adrenal masses, MR has higher specificity than CT because of the use of in-phase and out-of-phase imaging techniques. Recall that in- and out-of-phase imaging is a type of gradient-echo imaging, typically a T1 spoiled GRE (SPGR). “Spoiled” in this instance means that the residual transverse magnetization characteristic of GRE pulse sequences is dephased by an RF pulse just prior to the next slice-excitation pulse. Dephasing the residual magnetization yields a T1-weighted image instead of a mixture of T2* and T1. Recall that once the image weighting is set, tissue contrast is obtained by collecting image data at TE times when fat and water signals are in the same phase (in-phase) as well as in the opposed phase (out-of-phase).

Fat **precesses** at a different frequency than water, a well-known phenomenon in MR. When one voxel contains protons of both fat and water, the rotation of fat protons is faster than the rotation of water protons by approximately 220Hz at 1.5T. This means that every 2.3msec, the fat and water protons will alternate between being in-phase and out-of-phase. When in-phase, the fat and water signals combine to yield stronger, therefore higher, overall signal displayed in the image. Approximately 2.3msec later (at 1.5T), the fat and water protons are exactly opposed to the other, yielding a weaker, slightly fat-saturated image.

Obtaining a single SPGR in-phase set of images followed by an out-of-phase series requires less than five minutes of “table time.” These images are able to characterize lesions as adenomas with high specificity and sensitivity. Using out-of-phase techniques, adenomas lose signal intensity by 10% or more between in- and out-of-phase images (**Figure 47**). All imaging parameters, except for the TE, must be identical for in- and out-of- phase acquisitions, that is, the same TR, field-of-view, slice thickness, intersection gap, bandwidth, flip angle, etc. Advances in pulse sequence design and gradient performance have made 3D in- and out-of-phase SPGR imaging possible in a single breath-hold. Using thin slices to acquire both in- and out-of-phase images in a single breath-hold increases both the resolution and SNR of the images.

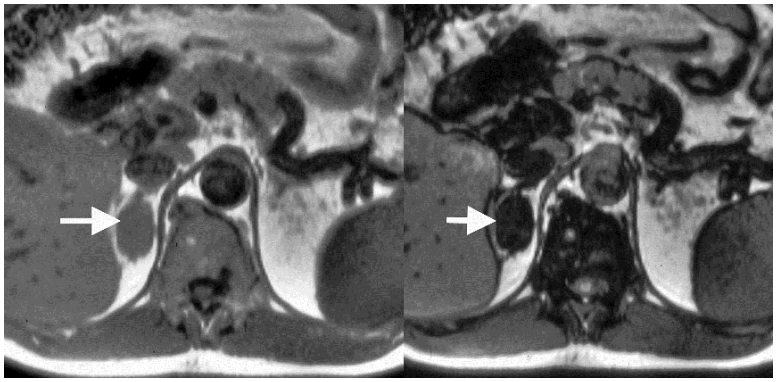

Figure 47. The adrenal adenoma located in the right adrenal gland (arrows) loses a substantial amount of signal between the (A) in-phase and (B) out-of-phase images.

Courtesy of James P. Earls, MD.

Slice Thickness and Fat Saturation

Because the adrenal glands are thin structures and adrenal lesions may be quite small, thin sections — typically 4-5mm slices — are optimal when performing adrenal MRI. Fat saturation is useful but can also be a hindrance. The retroperitoneal fat provides good internal contrast, making the adrenals easy to see, so employing fat saturation may actually make it more difficult to visualize subtle abnormalities. However, if the technologist wants to prove that a lesion in the adrenals contains macroscopic amounts of fat, it is best to perform a T1W GRE series both with and without fat saturation; any bulk fat-containing lesions, such as a myolipoma, will lose signal on the fat-saturated series.

MRI Findings

The major findings of adrenal MRI reveal cysts, hemorrhage, and adrenal carcinomas, such as **myolipoma** and **pheochromocytoma**. T2-weighted images are useful when evaluating these pathologies and therefore are included as a standard adrenal protocol. It should be noted that when pheochromocytoma is suspected, imaging should not be limited to only the adrenal area but used throughout the entire abdomen and pelvis since cancerous cells typically migrate from the adrenals to other areas in the **peritoneum**. Given these clinical circumstances, T2-weighted imaging and in- and out-of-phase imaging is useful, although it is not helpful for the most common indication for adrenal MRI, the characterization of adrenal adenomas. As mentioned earlier, the preferred sequence for imaging adenoma is a T1-weighted in- and out-of-phase gradient echo sequence in conjunction with a “spoiler” pulse.

Imaging of the adrenals should be fast and painless for the patient while yielding high diagnostic information. A sample adrenal MRI protocol can be found at the end of this material.

NOTES

MRI OF THE KIDNEYS

The kidneys are bean-shaped organs located posteriorly at the bottom of the rib cage, one on each side of the spine (**Figure 48**).Their primary function is to filter waste products and extra water from blood. Each day the kidneys filter approximately 200 quarts of blood, removing approximately two quarts of waste in the form of urea and extra water that when combined form urine, which then moves from the kidneys through the ureters and into the bladder.

The kidneys also play an important role in maintaining proper blood pressure and their role is two-fold: the kidneys cause the arteries and veins to constrict, and they increase the circulating blood volume. Pathologies like renal artery **stenosis** that prevent the proper amount of blood from flowing into the **nephrons**, the basic cell unit of the kidney, signal the nephrons to release hormones that cause an increase in blood pressure. Left uncontrolled, this "**nephrogenic hypertension**" can lead to other serious cardiovascular conditions such as stroke.

Renal MR imaging is most commonly performed to evaluate an indeterminate renal mass visualized on another imaging modality. Occasionally a mass seen on CT cannot be fully diagnosed, and the patient is referred for MR evaluation.

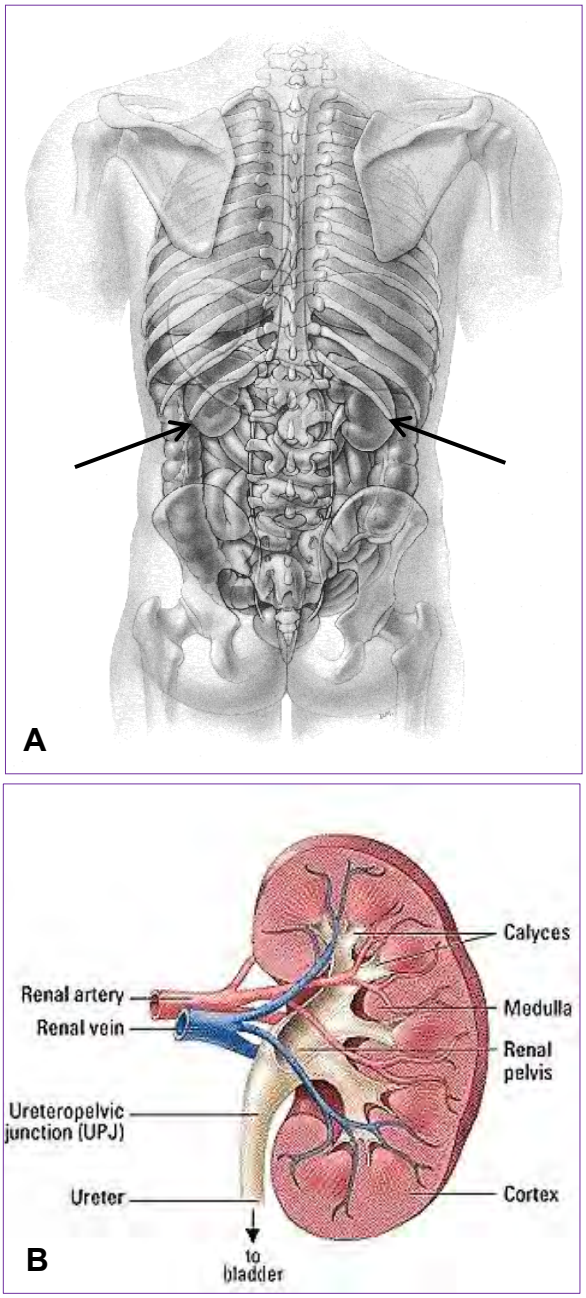

Figure 48. (A) The kidneys are often positioned relatively high within the abdomen. Most MRI protocols include a combination of axial and coronal imaging. (B) Anatomy of the kidney.

Used with permission of LifeArt.

While CT remains the workhorse for evaluating suspected renal masses, iodine-based contrast agents can stress compromised kidneys more than GBCAs. Patients with moderate to severe kidney disease or an allergy to CT iodine-based contrast agents may be contraindicated for CT imaging but may be appropriate for contrast-enhanced MRI.

Renal MR is performed in a similar manner to renal CT. Pre- and postcontrast images are essential for evaluation of the enhancement of masses, and the tissue contrast information differentiates cysts from solid masses (**Figure 49**). T2-weighted pulse sequences and fat saturation techniques are used to evaluate the **histological** composition of masses and other pathology.

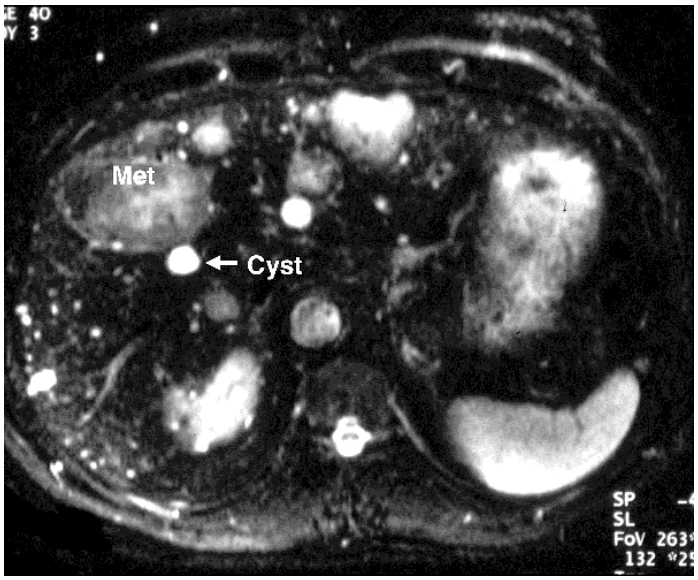

Figure 49. T2-weighted liver MR in a patient with both benign liver cysts and solid liver metastases. A properly selected TE helps differentiate cysts from solid masses. Most liver protocols use a TE of approximately 100msec for this purpose.

The one disadvantage of renal MR compared to CT is the relative insensitivity of MR to calcified stones in the collecting system and ureters. Since calcified stones do not contain water, there are virtually no useful protons for MR imaging and therefore where calcium exists, a black void appears in the image.

Imaging Parameters

Renal MRI protocols are simple and typically can be performed in 25 minutes or less. A T2W FSE/TSE sequence is acquired in two planes, axial and coronal, followed by a pre- and dynamic postcontrast T1W series performed as a breath-hold in a similar manner to the liver protocol previously discussed. It is best to use thin slices — 4 - 5mm is optimal — depending on the patient's breath-holding ability. The precontrast images can be subtracted from the postcontrast images to produce a **subtraction series,** excellent for determining the degree of enhancement of a mass or indeterminate lesion.

In addition to imaging the renal parenchyma, MR is an excellent tool for evaluating the renal vascular system, especially for visualizing the main renal arteries in cases of suspected nephrogenic hypertension and for evaluating the renal veins in cases of suspected **thrombosis** or tumor extension. Using 3D T1-weighted techniques, both 2D axial slice data and 3D MR angiography and **venography** can be performed (**Figure 50**).

Figure 50. Multiphase 3D GRE contrast-enhanced study. (A) Diagnostic 2D images for evaluation of organs and other anatomy, as well as 3D angiographic data. (B) Arterial anatomy. (C) Venous structures.

MRI Findings

Renal Cell Carcinoma

Renal cell carcinoma (RCC) is the most common type of renal malignancy. Renal cells are solid masses that typically are hyperintense on T2-weighted sequences and hypointense on T1-weighted sequences. Enhancement occurs following GBCA administration and is best demonstrated by reviewing the subtracted data series. Even subtle areas of enhancement not apparent on postcontrast images become obvious on subtraction imaging.

MRI is also very useful for staging renal cell carcinomas because the size and location of the primary tumor can be easily depicted (**Figure 51**). MRI is an excellent method for evaluation of not only localized cancer but for tumor extending beyond the kidney itself, either by direct extension into the renal vein or into the inferior vena cava (IVC) or for depicting **renal hilar lymphadenopathy**. The suspicion of renal metastasis to the liver, bone, and other structures can be easily depicted when imaging the abdomen and pelvis. A sample renal MRI protocol can be found at the end of this material.

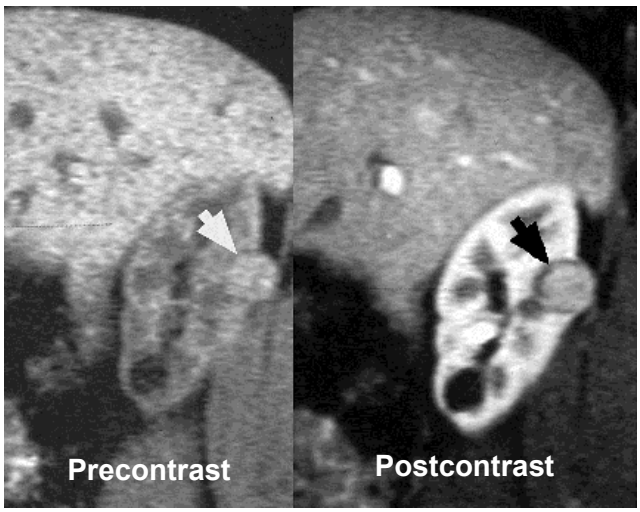

Figure 51. T1W GRE images depict a small solid renal cell carcinoma (arrow) that clearly enhances.

Angiomyelolipoma

Angiomyelolipomas (AML) are benign neoplasms of fat and **myeloid** tissue. Because AMLs are not cysts and clearly demonstrate contrast enhancement, they are often mistaken for renal cell carcinomas. The use of out-of-phase techniques or frequency-selective fat saturation may be helpful in depicting the fat or fat/water mixtures associated with these lesions, helpful in accurately characterizing AML and distinguishing them from renal cell carcinomas.

Hemorrhage

MRI can typically differentiate among simple renal cysts, hemorrhagic cysts, and renal cell carcinoma. Simple renal cysts will appear rounded, are **homogeneous**, and are hypointense on T1W imaging. Hemorrhagic cysts will appear medium-to-hypointense. Renal cell carcinoma will also exhibit areas of higher intensity due to the characteristic of hemorrhage in general.

SUMMARY

Although CT remains the primary modality for imaging the kidneys, MRI continues to play a significant role for evaluating kidney-specific pathologies.

NOTES

Tom Schrack, BS, ARMRIT
Fairfax Radiological Consultants
Fairfax, VA

MRI OF THE SMALL BOWEL

After completing this section, the reader should be able to:

- Describe the signs and symptoms of inflammatory bowel disease and the two major types of pathology
- Explain the preparation required for MR enterography
- Discuss the major applications and findings for MR enterography

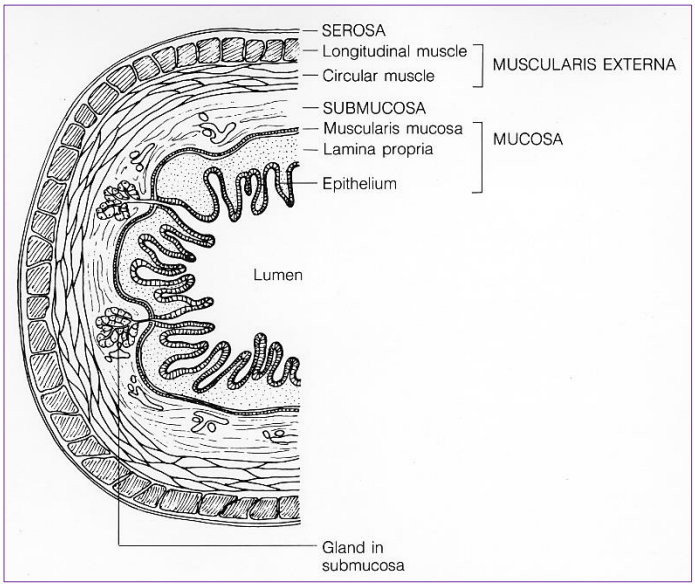

Figure 52. Illustration of the layers of the colorectal area.

Courtesy of the National Cancer Institute and available at Wikimedia Commons.

OVERVIEW

It is estimated that 1.4 million people in the US have a form of **inflammatory bowel disease** (IBD). IBD is an umbrella term for two distinct diseases, ulcerative colitis and Crohn's disease. IBD is a marked abnormal immune response to food and certain bacteria that results in the inflammation of the intestinal tract. The peak onset of IBD is from 15-30 years of age, though it can present at any age. Inflammatory bowel disease should not be confused with irritable bowel syndrome or IBS, which does not involve inflammation of the intestinal tract[18].

Crohn's Disease

Crohn's disease is marked by chronic inflammation of any part of the large or small bowel; however, it is most prevalent at the **terminal ilium**, the junction of the small and large bowel, and all layers of the bowel can be affected (**Figures 52 and 53**).

Symptoms of Crohn's include abdominal pain, diarrhea, bloating, cramping, loss of appetite, and weight loss. Rectal bleeding is also a common symptom. Complications of Crohn's disease can result in a mild to severe blockage of the bowel due to severe bowel swelling. Blockages can sometimes lead to the formation of artificial communication channels, referred to as **fistulas** that can form between loops of bowel, from the bowel into the peritoneum, or from the rectum into the vagina[19].

Ulcerative Colitis

Ulcerative colitis shares similar symptoms with Crohn's disease but is a separate disease classification. Ulcerative colitis differs from Crohn's disease in that it is limited to the large bowel, and inflammation is limited to the mucosa, the innermost layer of the large bowel.

Symptoms of ulcerative colitis include diarrhea and bloody stools. Symptoms range from mild to severe, requiring colostomy, but can be marked by periods of time where there are no symptoms at all.[20]

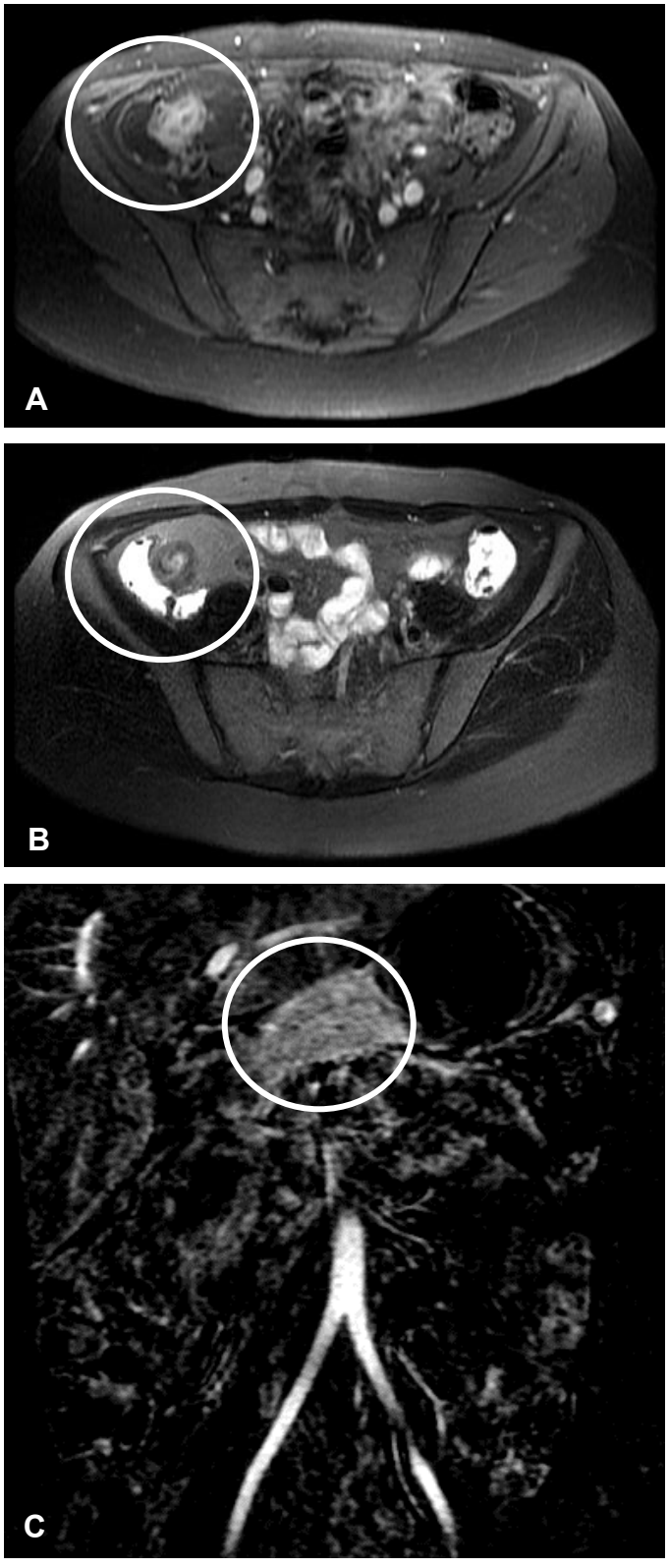

Figure 53. Enterography of a 29-year-old female. (A) Postcontrast axial T1-weighted image. (B) Fat-suppressed axial T2W at the same level. Both images demonstrate inflammatory thickening of the ileum consistent with Crohn's Disease (circles). (C) Postcontrast 3D subtraction demonstrates thickening of the jejunal loop (circle).

THE ROLE OF MRI

Traditionally patients with IBD are followed by imaging with CT. However, given that pediatric patients can suffer with IBD, as well as continuing efforts to reduce long-term radiation dose during serial imaging to monitor and stage disease, MR is playing an increasing role in the evaluation of the bowel, especially of the small bowel. While the high degree of spatial resolution provided by CT typically makes it the modality of choice for large bowel imaging, both MR and CT have been found to have similar imaging sensitivities for small bowel imaging.[21] MR **enterography** is used to evaluate the health of the small bowel.

Figure 54. MOVIE. Multiphase CINE loop (FIESTA) of a 29-year-old female following ingestion of 1000mL oral contrast (barium sulfate) and just prior to receiving 1mL of glucagon IM. Note lack of motility of the terminal ileum.

To view this movie, click here: YouTube.com/ICPMEducation.

Patient Preparation

Patients require special preparation before undergoing MR enterography. Typically the patient should be kept NPO (nothing by mouth) for 4 hours prior to imaging. Approximately 90 minutes before the exam time, the patient is given an oral contrast, usually a barium-sulfate suspension. Whole milk is an adequate substitute if the patient can drink it more easily or if the barium solution is otherwise not available or contraindicated. 1200mL of oral contrast is typically the optimal amount. However, 900mL of oral contrast may be adequate for patients with serious symptoms or for smaller or younger patients.

In order to quiet the bowel's peristalsis, a glucagon injection is highly effective. However, if the protocol calls for imaging the small bowel in a multiphase **cine** loop specific to observing the bowel peristalsis, the glucagon is not given until the after cine series is complete.

MR Protocols

The enterography imaging protocol typically involves coronal single-shot imaging with fat saturation followed by axial T2-weighted imaging also with fat saturation. Multiphase imaging through the moving bowel is effective for evaluating areas of abnormal peristalsis. Lastly, gadolinium-based contrast is indicated for MR enterography as sections of inflamed bowel will enhance with contrast media. The movie (**Figure 54**) shows typical inflammatory thickening of Crohn's disease and lack of motility of the terminal ileum.

SUMMARY

MRI has emerged as effective tool for imaging the small bowel, especially in the diagnosis and management of inflammatory bowel disease.

NOTES

Tom Schrack, BS, ARMRIT
Fairfax Radiological Consultants
Fairfax, VA

MRI OF THE FEMALE PELVIS

After completing this section, the reader should be able to:

- Name the primary MRI findings of the female pelvis, including pelvic floor weakness
- Discuss obstetrical and fetal imaging when exposure to ionizing radiation must be avoided
- Respond appropriately to the patient given the sensitive nature of the female pelvic MRI exam

OVERVIEW

While ultrasonography is the first-line imaging modality for evaluation of most benign disorders of the female pelvis, MR imaging is playing an increasingly important role. The advantages of MRI include a more global assessment of the pelvis, multiplanar imaging that can be reproduced more reliably than ultrasound, and capacity for tissue specificity.

Several technological developments have had a significant impact on MR imaging of the female pelvis. High-channel phased-array coils have substantially improved SNR, allowing a smaller field-of-view and increasing resolution. Higher gradient performance results in shorter scanning times and sharper images due to shorter echo-spacing times. Lastly, advances in pulse sequence design permit higher and more varied tissue contrast (**Figure 55**).

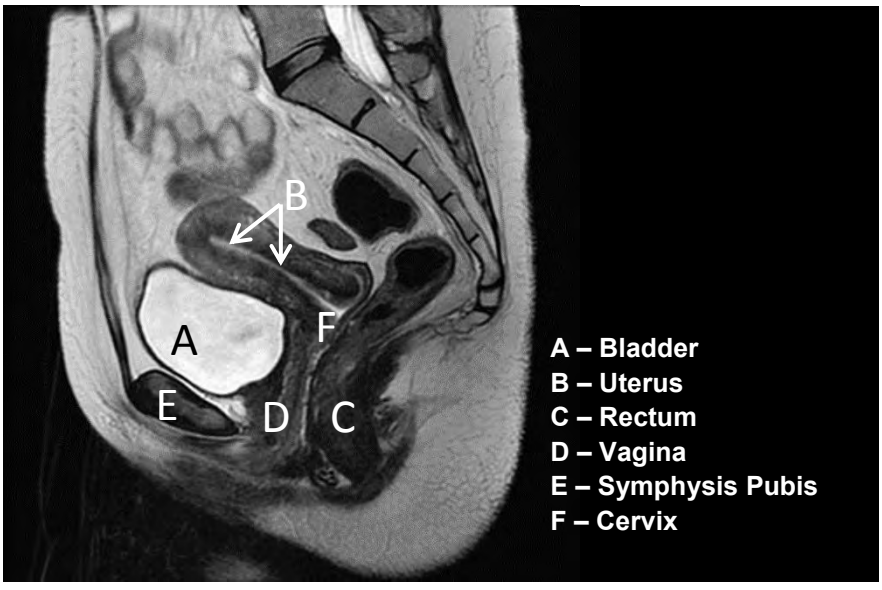

Figure 55. Sagittal image of the female anatomy.

IMAGING PARAMETERS

The standard pelvic imaging protocol consists of axial T1-weighted images of the pelvis and 3-plane T2-weighted images centered on the uterus. T1-weighted images provide information for tissue characterization as well as evaluation of lymphadenopathy, while T2-weighted images provide the best depiction of the zonal anatomy of the uterus and **adnexa.**

FSE/TSE techniques significantly decrease scan time compared to older spin echo techniques. For certain applications like evaluation of **fibroids**, even faster imaging with ultrafast T2W sequences (fast imaging employing steady-state acquisition [FIESTA, GE Healthcare] or fast imaging with steady-state precession [FISP, Siemens]) techniques results in a time-efficient protocol that offers excellent resolution. Rapidly acquired FIESTA/FISP images also provide prenatal evaluation of complex fetal abnormalities. Sample dynamic pelvis and female pelvis MRI protocols can be found at the end of this material.

CONTRAST ENHANCEMENT

A gadolinium-based contrast agent is administered as necessary for characterization of adnexal masses, and subtraction techniques are used to evaluate areas of contrast enhancement. Out-of-phase and fat saturation techniques provide greater tissue specificity in the diagnosis of fat-containing tumors like **dermoids** or **lipoleiomyomata**. 3D T1W gradient echo sequences provide contiguous 2mm slices of the pelvis in approximately 20 seconds, allowing dynamic imaging and generation of high-quality MR perfusion images. The 3D datasets also provide high-quality multiplanar reconstruction in an infinite number of projections. This can be helpful for preoperative planning for **myomectomy** or **embolotherapy** of fibroids.

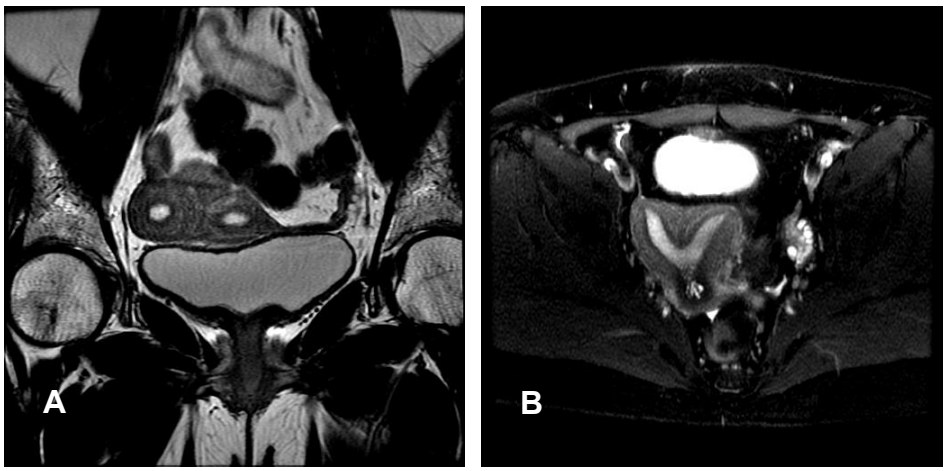

Figure 56. Patient with bicornuate uterus. (A) Axial T2 with fat suppression. (B) Coronal T2 without fat suppression.

MRI FINDINGS

Congenital Uterine Anomalies

Congenital uterine **anomalies** occur in 5% of the general female population. MRI is performed when ultrasound is technically inadequate, indeterminate, or if cervical or vaginal malformations are suspected. MRI depicts the fundal contour of the uterus, important in the distinction of **septate** from **bicornuate** uterus (**Figure 56**). MRI may identify a rudimentary horn in a patient with a **unicornuate** uterus, which often requires surgical removal if it does not communicate with the endometrial cavity.

MRI is also used to identify the presence and degree of **agenesis** of the vagina, cervix, and uterus when transvaginal ultrasound may be impossible to perform. It is important that the slice orientation be carefully suited to the patient's particular anatomy. Slice orientations should follow the plane of the **uterine stripe** in both the short axis and perpendicular long axis views (**Figure 57**).

Fibroids

Uterine fibroids are noncancerous neoplasms that occur in the uterine wall. It is estimated that as many as 80% of all adult women in the United States has a uterine fibroid. While the vast majority of women experience no symptoms from uterine fibroids as many as 25% experience symptoms severe enough to require treatment.[22] Symptoms include heavy menstrual bleeding, lengthy menstrual periods, moderate to severe pelvic pain, and urinary and bowel difficulties.[23] Treatment options range from hormone therapy to hysterectomy.

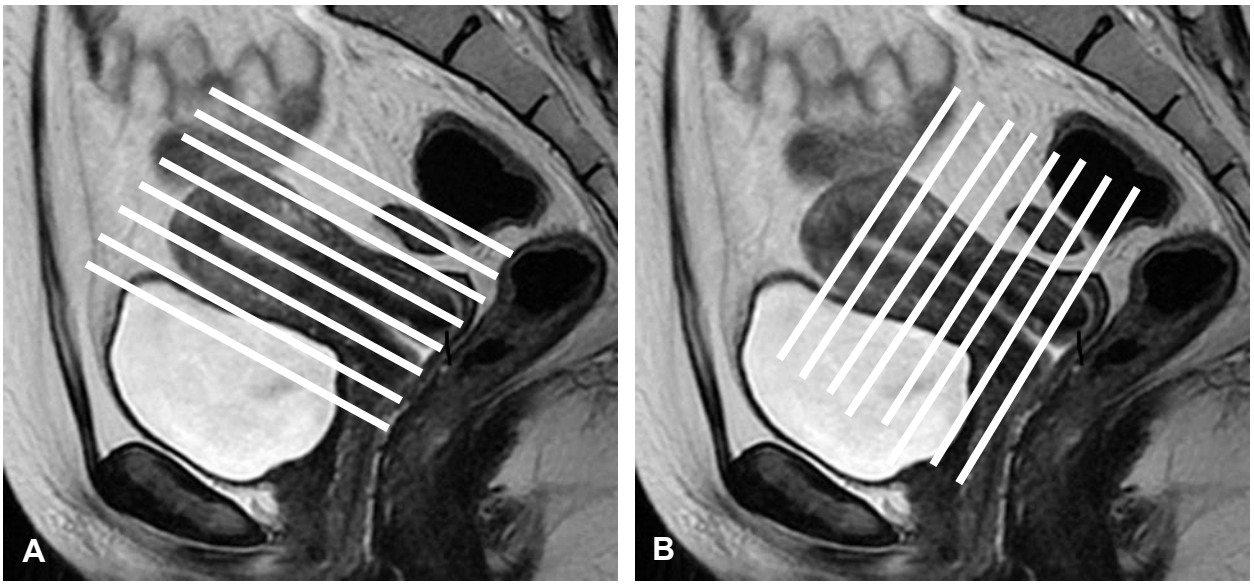

Figure 57. Proper slice orientation when imaging the uterus for uterine anomalies. Slices should be angled. (A) Parallel (long axis) and (B) perpendicular (short axis) to the uterine stripe.

MRI is beneficial in preoperative characterization of the size and location of fibroids for women who elect uterus-sparing myomectomy. This is particularly true for women with a markedly enlarged uterus with multiple fibroids. MR imaging also serves as a useful adjunct for differentiating fibroids from other pelvic pathology like solid adnexal masses.

Transcatheter Uterine Artery Embolization

Transcatheter uterine artery embolization (UAE) is an option for treatment of women with symptomatic fibroids. Contrast-enhanced MRI aids in identifying those women who will respond to such therapy. Several recent studies have described the postembolization appearance of fibroids with gadolinium-enhanced MRI[24,25] (**Figure 58**).

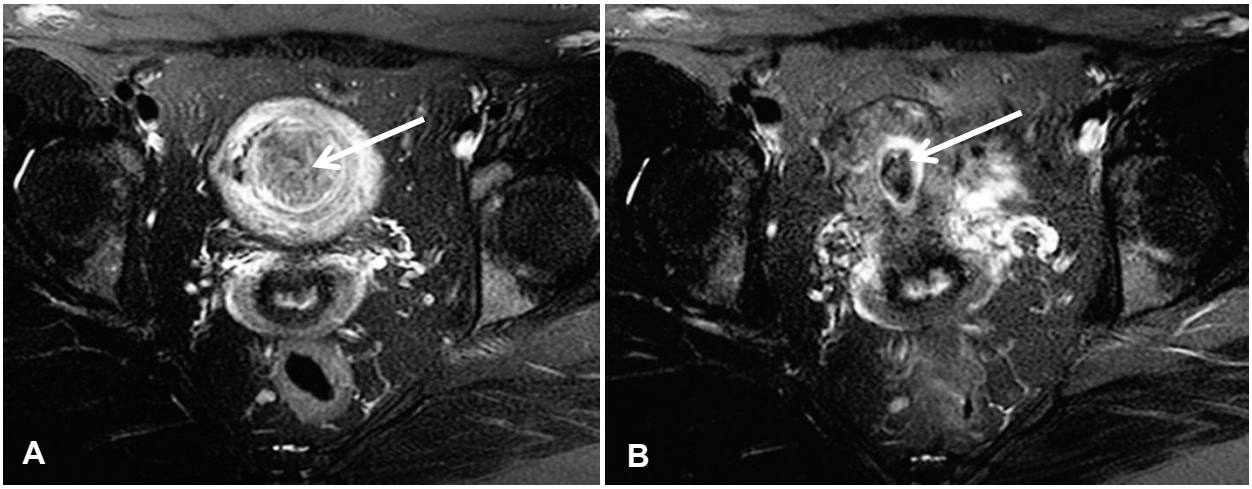

Figure 58. 42-year-old female with a large uterine fibroid. (A) Axial T2-weighted fat-suppressed image of fibroid pre-embolization; fibroid measures 35.2mm. (B) Axial T2-weighted fat-suppressed image after embolization; fibroid measures 13.4 mm.

MR-guided Focused Ultrasound Ablation of Uterine Fibroids

In 2004, the FDA cleared a non-surgical treatment method for uterine fibroids using high-frequency focused ultrasound (FUS) under MRI-guidance.[26] High-frequency ultrasound beams can be focused to a high degree of precision. When transmitted to human tissue, the absorbed energy is converted to heat. With the optimal amounts of energy transmission and time duration, enough heat can be generated to damage and destroy the targeted tissue. Focused ultrasound ablation is a viable non-surgical uterine-sparing treatment option for patients where hormone therapies have failed and who are facing hysterectomy.

In order to precisely target the patient's fibroids, real-time imaging is required. MRI provides excellent image quality and tissue contrast to allow highly accurate images of the uterus and fibroids without the use of ionizing radiation. Moreover, because tissue T1 and T2 times vary with changes in tissue temperature, MRI provides excellent contrast during the procedure to distinguish treated and non-treated tissue, providing real-time feedback to the administering physician.

During the procedure, the patient is positioned prone on the MRI table. The FUS equipment is housed inside the patient table. The patient is imaged using a standard high-resolution MRI protocol. After the images are reviewed and the ablation procedure planned, high-frequency ultrasound beams are transmitted to the patient in short "bursts" called **sonications** that last approximately 20 seconds.[27] The length of the procedure depends on the size and number of fibroids requiring treatment. Patients may experience mild discomfort following the procedure but generally do not require any convalescence.

Adenomyosis

Adenomyosis refers to the presence of misplaced endometrial glands and **stroma** in the uterine wall, with adjacent **myometrial hyperplasia**. The uterus becomes thickened when the endometrial tissue, which normally lines the uterus, moves into the outer walls of the uterus. If symptoms are severe, hysterectomy is considered the definitive therapy, and therefore it is important to differentiate adenomyosis from the presence of fibroids.

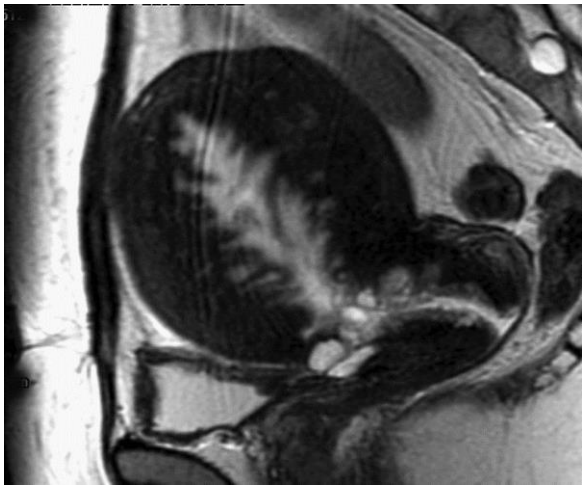

Figure 59. Sagittal T2-weighted FSE image depicts an enlarged uterus with diffuse adenomyosis. There is diffuse thickening of the junctional zone, and high signal intensity fluid-filled glands are seen to extend from the endometrium.

The most useful distinguishing features of adenomyosis include an ill-defined border, **contiguity** with the endometrium, and minimal mass effect. Diagnosis of adenomyosis is best made on T2-weighted images. Criteria for diagnosis include focal or diffuse thickening of the junctional zone greater than 12mm, low-signal intensity lesion adjacent to the junctional zone, and low-signal intensity myometrial mass (**Figure 59**).

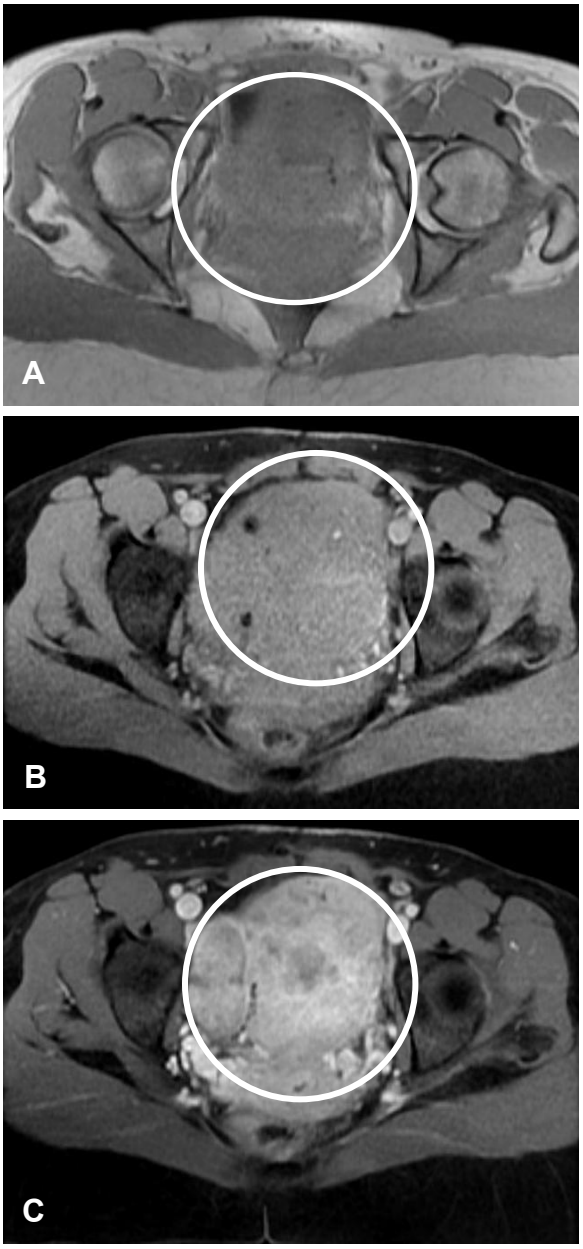

Figure 60. Axial imaging of a 49-year-old female with several large uterine fibroids. (A) Axial non-FAT SAT SPGR. (B) Same location with frequency-selective fat saturation. (C) Same location postcontrast with FAT SAT. The largest fibroid (circle) measures 4.2 x 5.4 x 4.2cm. Note how the use of fat saturation, particularly post contrast, increases conspicuity of tissue.

Dermoids

Dermoids are common benign ovarian neoplasms that frequently contain fat, a histologic marker used to advantage on MRI. Fat is bright on non-fat saturated imaging and is easily distinguished from the bright signal of abnormal tissue when a fat saturation technique is used. Using both fat saturated and non-fat saturated techniques can distinctively show if tissue is fat or a positive finding.

Findings include fat content within a cyst, fat-water chemical shift artifact, low-signal intensity calcification or “teeth,” and soft tissue nodules. Several techniques can confirm the presence of fat within a dermoid, including out-of-phase imaging and frequency-selective fat saturation, commonly referred to as “chemical fat saturation.”

Fat saturation is accomplished by exciting the proton spins of fat that precess 220Hz (at 1.5T) from water with a very finely tuned, or ”selective”, RF pulse. This “pre-saturation” RF pulse places only the fat spins into the transverse plane. Any signal coming from these spins is ignored. Immediately thereafter, a water-selective RF pulse excites the water spins. As the water spins are placed into the transverse plane, any fat spins still in the transverse plane are forced into the negative longitudinal plane and therefore produce no signal.

The technologist should remember that with out-of-phase imaging there must be relatively equal numbers of fat and water molecules to suppress the signal; therefore a mass that is primarily composed of fat may not suppress, and frequency-selective fat saturation may be necessary. Conversely, out-of-phase imaging may detect mixtures of fat and water that may not contain sufficient fat to show signal intensity loss by frequency-selective fat saturation (**Figure 60**).

Endometriosis

Endometriosis is the presence of actively growing and functioning endometrial tissue outside of the uterus. The usual appearance of an **endometrioma** is of high-signal intensity on T1 and low signal on T2. This phenomenon is believed to be secondary to repeated bleeding into the endometrioma, resulting in a high concentration of blood components that shorten T2. Endometriomas may also exhibit high-signal intensity on T2, but this appearance is nonspecific and may be seen in hemorrhagic functional cysts. Small hemorrhagic endometriotic deposits in the pelvis are often most apparent on T1-weighted fat-saturated images.

Endometrial Carcinoma

Endometrial carcinoma often presents as isointense on T1-weighted imaging compared to normal myometrium. However, on T2-weighted imaging, endometrial carcinoma usually appears hyperintense versus normal myometrium. Fat saturation techniques are useful in increasing the tissue contrast between the two. Contrast-enhanced images will typically demonstrate heterogeneous signal enhancement.[28]

Cervical Carcinoma

Approximately 12,000 American women were diagnosed with cervical cancer in 2013 in the United States, and most were younger than 55. Each year approximately 4,000 women die of this disease.[29] Among female cancers in the USA, cervical cancer ranks fifth.[30]

Cervical cancer is almost always caused by the human papilloma virus (HPV). Diagnosis of and death rates from cervical cancer have been falling steadily since the Pap smear became available in the US in the 1940s.[31,32]

Unlike other gynecological cancers, ultrasonography is not the preferred imaging modality for cervical cancer. MRI and CT are both superior and are complementary imaging options. MRI offers excellent soft tissue contrast, while CT offers higher spatial resolution. Generally MRI is indicated for evaluating tumor size and extent of tumor invasion.[33, 34]

As with imaging of the bladder, the role of MRI in the evaluation of cervical cancer is in staging the extent of cancer. Though typical treatment includes a total hysterectomy, follow-up therapies are tailored to those patients with higher grade staging. For example, a higher grade aggressive cervical tumor may require pre-operative radiation treatments as well as lymph node removal. Treatment for a lower grade cervical tumor typically would require pre-operative radiation treatments with lymph node sampling instead of excision.[35]

As with imaging of any cervical/uterine anomaly, high resolution imaging is angled to the plane of the cervix, which is most easily determined on the sagittal view. Usually T1W, T2W (usually fat-saturated), and T1W postcontrast imaging are performed. Cervical carcinoma often demonstrates as hypointense-to-isointense signal on T1-weighted imaging. On T2W, the carcinoma displays a heterogeneous as well as homogeneous signal characteristic.

Except for bladder imaging, all pelvic imaging requires the bladder be emptied just prior to the start of the exam, which will reduce ghosting from fluid moving within the bladder. Dynamic contrast-enhanced imaging is essential for the evaluation and staging of cervical tumors. Following gadolinium injection, cervical carcinoma usually demonstrates mildly heterogeneous enhancement[36] (**Figure 61**).

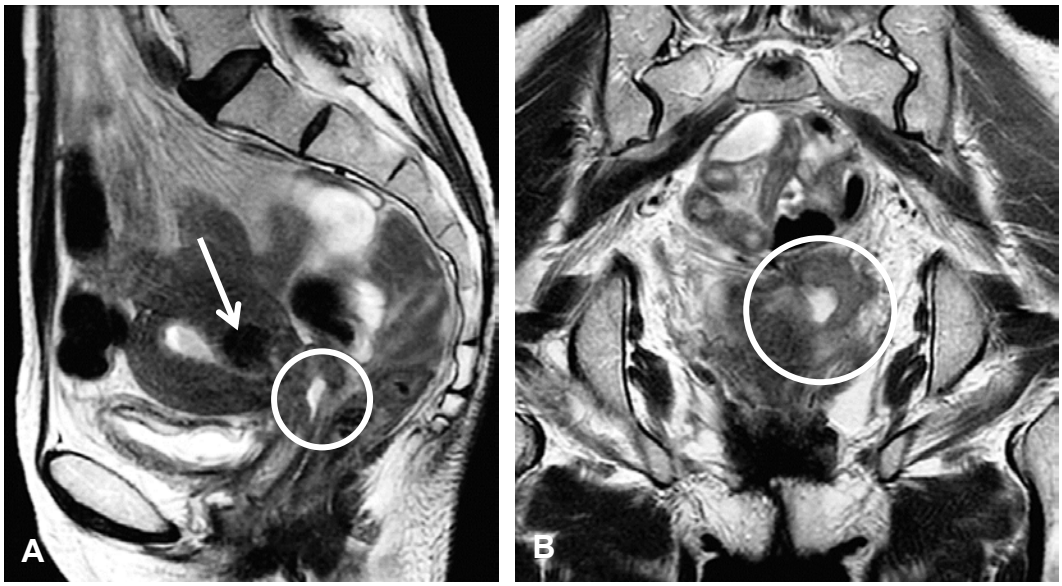

Figure 61. (A) Sagittal and (B) coronal non-fat-suppressed T2-weighted images of a 64-year-old female with a moderate-sized uterine fibroid (arrow) and cervical mass (circles).

OBSTETRICAL AND FETAL IMAGING

Obstetrical and fetal MR imaging are becoming more common. Many studies have shown the utility of MR for characterizing adnexal and uterine masses in the pregnant patient for whom ultrasound is indeterminate and where ionizing radiation must be avoided.

Appendicitis in the Pregnant Patient

A useful application of MRI in the pregnant patient is for the evaluation of the appendix. Appendicitis can lead to sepsis if left untreated. Symptoms typical of appendicitis include severe right lower quadrant pain, and a blood test to check for an elevated white cell count usually aids in diagnosis. However, in the pregnant patient, white blood counts may be naturally elevated.

Ultrasound assessment of the appendix in a pregnant woman may be inadequate due to interference from the enlarged abdominal cavity. Fortunately, MRI has proven to be an effective alternative for visualizing the appendix (**Figure 62**). Ultrafast imaging techniques are now fast enough to "freeze" abdominal motion and at the same time limit the amount of radiofrequency pulses to the fetus. While no adverse effects to the fetus have been shown with MRI, it is recommended that the amount of radiofrequency used while scanning the pregnant patient be limited in order to reduce the specific absorption rate. The most effective method for reducing SAR is to adopt gradient echo pulse sequences instead of long RF-echo-based sequences like FSE and TSE.

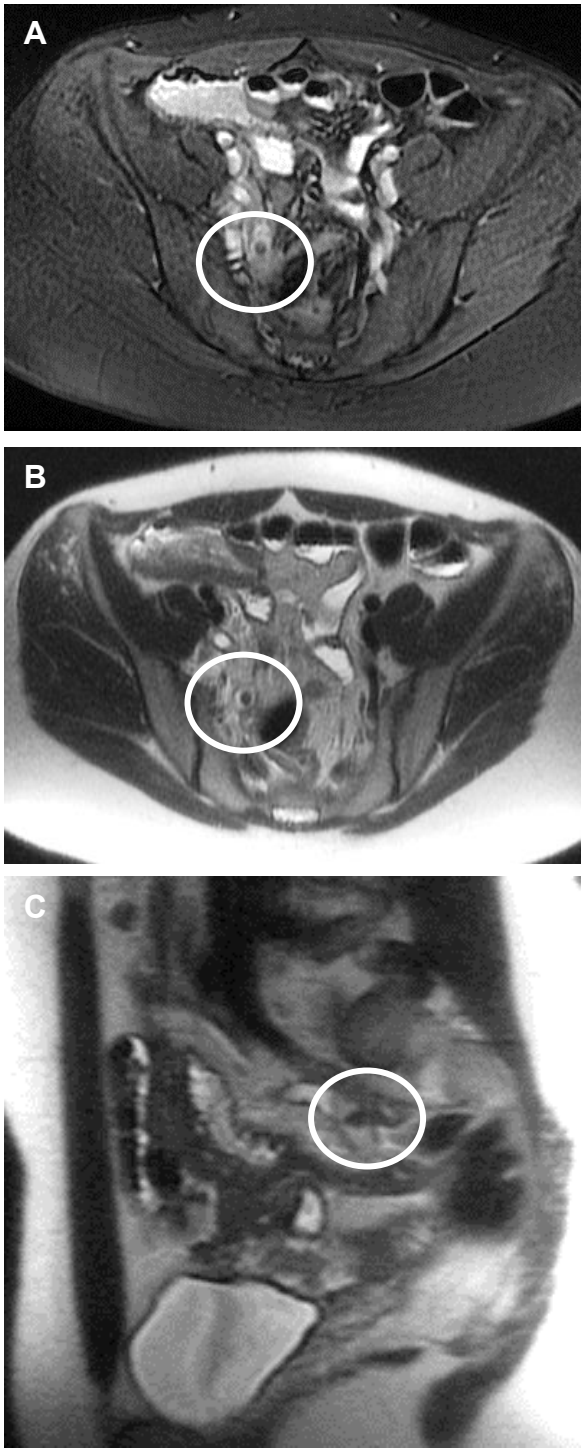

Figure 62. 25-year-old female in the first trimester of pregnancy presenting with lower right quadrant pain. (A) Axial T2W with fat saturation. (B) T1W non-fat saturated. (C) Sagittal SSFSE. Circles demonstrate the dilated tubular structure characteristic of acute appendicitis.

Fetal Imaging

As with obstetrical MRI, fetal MRI is also becoming more common.

Cerebral anomalies account for 9% of all fetal isolated anomalies and 16% of cases with multiple anomalies,[37] one example among many possible congenital anomalies. The greatly increasing number of surviving premature neonates increases the need for investigation, diagnosis, and treatment. Fetal intervention is feasible, increasing positive outcomes. Examples are surgical intervention for **ventriculomegaly** and congenital diaphragmatic hernia while the baby is still *in utero.* **Figures 63 and 64** are examples of congenital anomalies *in utero*.

Figure 63. Fetal imaging of 20-week-old with suspected congenital diaphragmatic hernia. (A) Coronal T2W image. (B) Sagittal T2W image confirms near-complete herniation of the liver into the right hemithorax (circles).

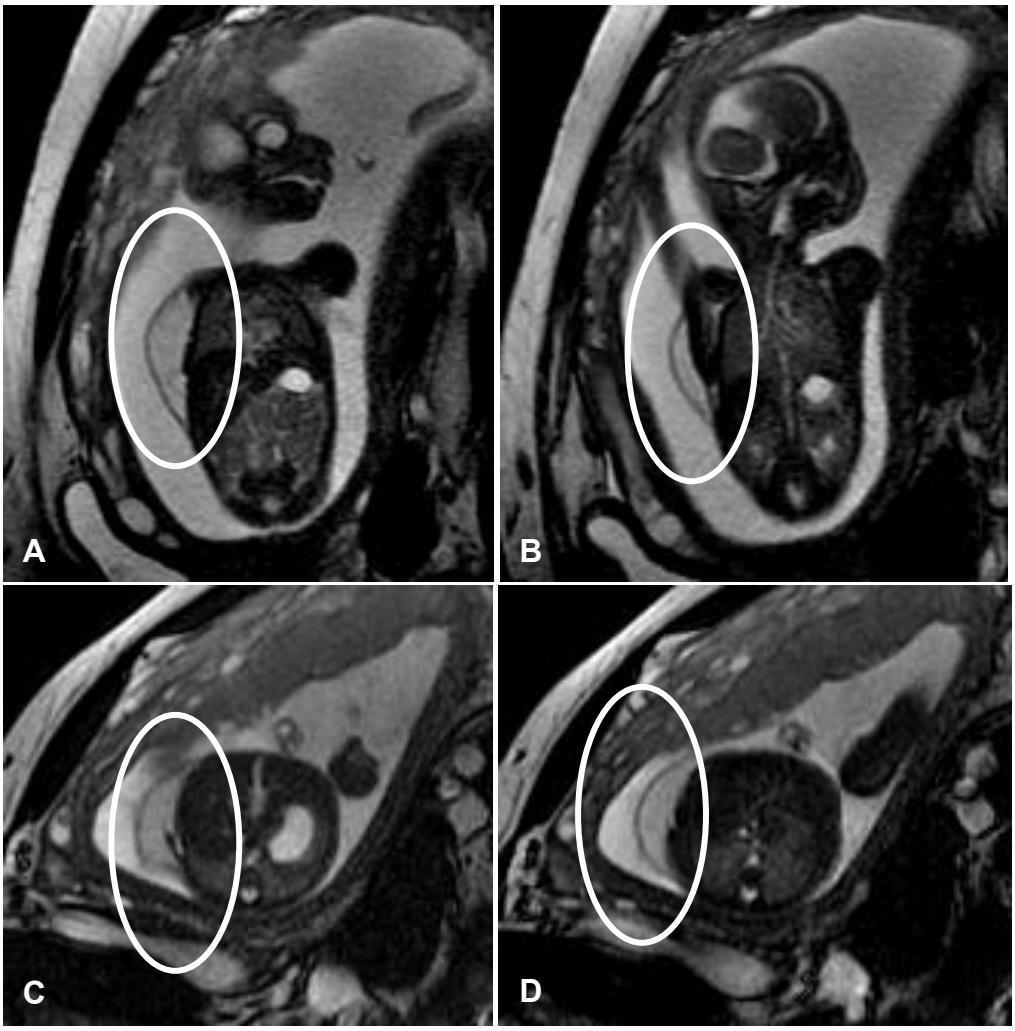

Figure 64. Fetal imaging of a 22-week-old with suspected upper extremity hygroma, a benign congenital lymphatic lesion. Images A and B are coronally aligned and demonstrate cystic hygroma (circles). Images C and D are aligned axially to the fetus.

MR has been shown to be a useful adjunct to ultrasound in the prenatal detection and characterization of these complex fetal anomalies. While ultrasonography is the stalwart of fetal imaging, it does have limitations. Ultrasound does not provide adequate visualization of the **cerebral sulci,** and evaluation of the **corpus callosum** can be challenging. Biometric measurements of, for example, the posterior **cranial fossa** are often inconsistent or unreliable on ultrasound at any stage of fetal development. Due to the rapid imaging time afforded by ultrafast T2 pulse sequences like single-shot FSE/TSE (SS-FSE/TSE) sequences, MRI of the fetus is easily performed and diagnostic, with decreased artifacts secondary to fetal motion because of technological advances of MR hardware and software (**Figure 65**).

The safety of fetal imaging is always of paramount concern. Although there have been no reports of adverse effects from performing fetal MRI at any stage in fetal development, both the National Radiological Protection Board and the FDA recommend *not* imaging during the first trimester.[38] In addition, limiting the specific absorption rate is highly recommended. The use of extremely rapid SS-FSE/TSE techniques delivers the least amount of SAR to the fetus and is therefore the most often used imaging technique.

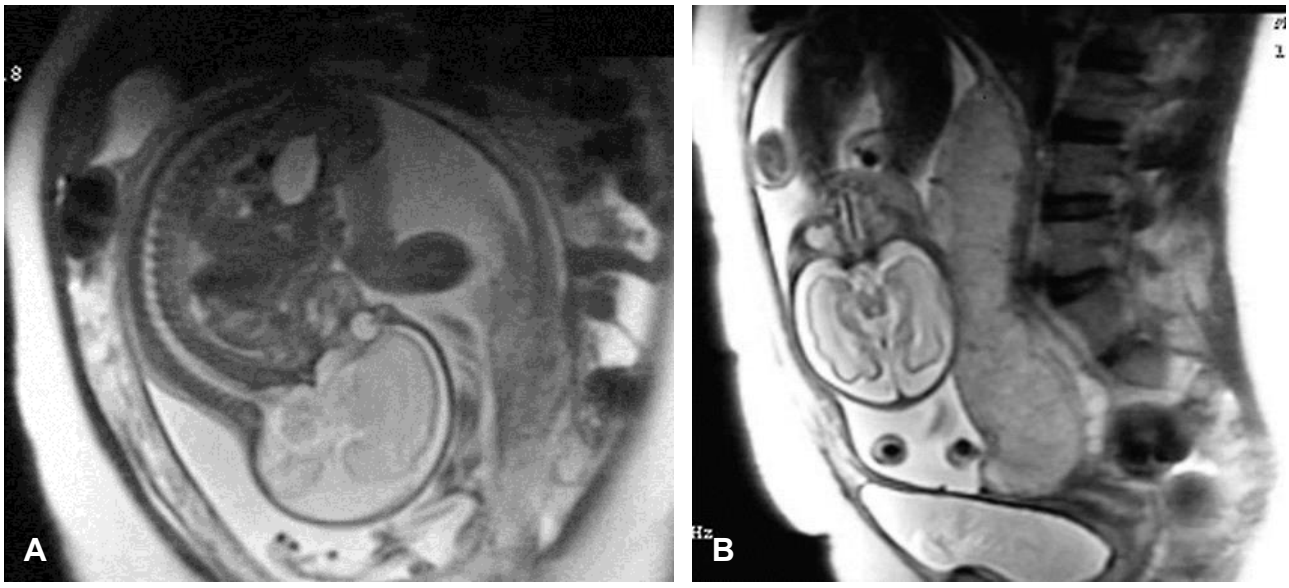

Figure 65. Fetal imaging in utero using single-shot FSE/TSE in (A) sagittal and (B) coronal anatomic planes. Note lack of motion due to very rapid scanning, yet spatial detail remains relatively robust.

Patient Positioning and Care

Much like other imaging applications that require heightened appreciation of the patient's apprehension, imaging of the fetus requires a great deal of sensitivity for the mother, who is understandably anxious about the health of her child. To lessen the mother's stress, it is recommended that the mother be screened only for MRI safety; a complete history as to why the MRI is being performed should be avoided. All relevant diagnostic history, eg, gestational age, most recent ultrasound reports, and consultation with the referring physician should be known before the patient arrives for the MRI exam.

Care must be taken to position the mother safely and comfortably. For imaging of a later-stage fetus, the mother should be positioned on the table in the decubitus position (on her side). This reduces stress on the lower back and prevents constriction of the abdominal aorta. To further aid in relaxing the mother, most fetal imaging is done *without* breath-holding. Single-shot techniques are typically fast enough to freeze not only respiratory motion but fetal motion as well.

Fetal Imaging Techniques

MR imaging of the fetus is straightforward:

- Image the entire fetus using a *large* FOV with all 3 planes **orthogonal** to the fetus.
- Image using a *smaller* FOV for the region of interest like the brain. Again, image in all 3 planes to the anatomy of the fetus.
- A long TE and short TE single-shot FSE/TSE provide excellent tissue contrast.
- EPI-based diffusion-weighted imaging is fast and highly diagnostic.
- Be sure the images are reviewed in real time to ensure diagnostic quality.

The challenges of fetal imaging involve the movement of the fetus between image acquisitions. When motion occurs, the prescribed locations will not be correctly displayed, and new localization scout views may be required. If the fetus moves again, several scans may be required just to localize. Affectionately known as "the baby chase," frequent movement typically occurs in the early developmental stages as by the mid-latter third trimester, the fetus is unable to move as freely.

Contrast-enhanced MRI is not used for fetal imaging. Gadolinium-based contrast agents have been shown to cross the placenta where the agent is ingested by the fetus. The GBCA is then excreted into the amniotic fluid, and the cycle continues. Given the developmental stages of the kidney, the use of a GBCA poses a significant risk to the fetus.

PELVIC FLOOR WEAKNESS

Pelvic floor weakness is common in middle-aged and elderly **parous** women, and pelvic floor **prolapse** occurs in roughly 50% of females who have had children. Pelvic floor weakness also affects males but to a far lesser extent.

Commonly these patients present with stress incontinence, incomplete defecation, and chronic constipation. Women can also present with uterine prolapse, which may require surgery. For patients for whom complex surgical repair may be required for multi-compartmental involvement, MRI is an essential pre-surgical tool.

For pelvic floor imaging of both women and men, MRI offers superior resolution for evaluation of soft tissues compared to ultrasound. Using ultrafast and high-resolution T2W sequences, assessment of the pelvic floor and organs has become possible in a dynamic fashion. Several breath-held sets of images can be obtained, one at each of several different degrees of pelvic straining. Dynamic MRI reliably detects descent of the pelvis, demonstrating all pelvic organs and pelvic floor musculature, essential information for both diagnosis and surgical planning.

Pelvic Floor MRI Examination

This exam is very quick, usually 15 minutes or less, and sensitive handling of the patient is required. While a contrast agent is not needed, the exam requires the patient's rectum to be filled with a water-soluble ultrasound gel that displays bright signal to enhance image contrast. Approximately 120cc of room-temperature gel is injected into the rectum via a standard enema tip. Once the gel is in place, the enema tip is removed. The exam typically requires high-resolution imaging in two planes, most commonly axial and coronal, and acquired at the beginning of the exam.

The diagnostic portion of the evaluation occurs at the end of the exam when the patient is instructed to strain, pushing the gel out during the high-resolution dynamic imaging portion of the evaluation. Pulse sequences typically used are FIESTA/true-FISP or single-shot FSE/TSE. A single mid-line sagittal image is acquired in multiphases. When displayed in a cine loop, the displacement of the pelvic organs can be observed in detail and precise measurements can be made. **Figure 66** shows pelvic floor images demonstrating normal and abnormal placement of pelvic organs.

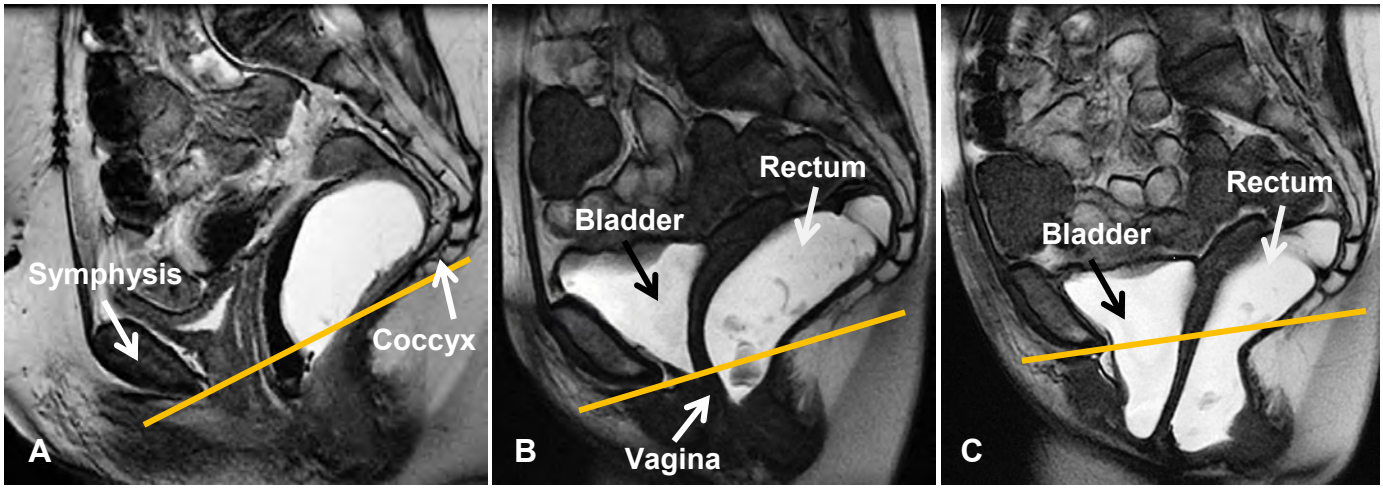

Figure 66. (A) Sagittal FIESTA image of 53-year-old female with normal positioning of internal pelvic organs above the pelvic floor. The line from inferior symphysis to the bottom of the coccyx indicates the boundary of the pelvic floor. (B, C) Sagittal FIESTA images of 55-year-old female (B) at rest and (C) after "push". Note the moderate prolapse of the rectum, inferior vagina, and mild prolapse of the bladder at rest on Image B. Note the severe prolapse at full "push" on Image C, where the rectum, vagina, and bladder are all nearly completely below the pelvic floor boundary.

Again, this exam requires the utmost sensitivity to the patient to maintain her privacy and dignity. The exam should be explained in detail prior to the beginning of the evaluation. A private, reserved bathroom must be available to the patient immediately afterward. While MRI of the pelvic floor is a fast, virtually pain-free, and highly diagnostic evaluation, few MR facilities offer this application because of the nature of the exam.

SUMMARY

MRI plays a pivotal role in the diagnosis and staging of many pelvic pathologies. The inherent ability of MRI to produce different image contrasts of the same tissue compared to adjacent tissue makes MRI a valuable adjunct to ultrasonography.

NOTES

Tom Schrack, BS, ARMRIT
Fairfax Radiological Consultants
Fairfax, VA

MRI OF THE BLADDER

After completing this section, the reader should be able to:

- Describe the role of MRI as an adjunct to ultrasonography for bladder imaging
- Discuss imaging techniques required for visualization of the bladder and bladder wall

OVERVIEW

Evaluation and staging of bladder cancer for both women and men is typically done using ultrasonography. However, the use of MRI is occasionally used as an adjunct tool when US is inconclusive, perhaps because of body habitus or lack of adequate tumor visualization.

Accurate tumor characterization is extremely important in bladder cancer. Tumor management is based on the findings provided by imaging whether by ultrasound or MRI. Superficial bladder tumors can be treated less invasively along with neoadjuvant therapies. Extensive and invasive tumors are treated more aggressively with surgery and chemotherapy.

IMAGING PROTOCOLS

MRI of the bladder consists of high resolution imaging in the sagittal, axial, and coronal planes. An important difference between imaging for the bladder and the rest of the pelvis is that in bladder imaging, *the bladder should be full*. Fluid in the bladder distends the bladder wall as well as provides good tissue contrast for visualization of pathologies in the bladder wall.

Dynamic contrast-enhanced MRI is essential for evaluation of the bladder. Images are acquired during the arterial phase about 20 seconds after injection, and the venous phase immediately following the arterial phase. Dynamic imaging in this fashion aids in the delineation of tumor margins in the bladder wall.

SUMMARY

While typically not used as first-line imaging when assessing or staging bladder cancer, MR imaging serves as a useful adjunct for visualization of the bladder and bladder wall.

Tom Schrack, BS, ARMRIT
Fairfax Radiological Consultants
Fairfax, VA

PROSTATE MRI

After completing this section, the reader should be able to:

- Identify the anatomy and describe the function of the prostate gland
- Explain the basic sequences for prostate imaging
- Describe MRI prostate findings and the utility of MRI-guided prostate biopsy
- Respond appropriately to the patient given the sensitive nature of the prostate MRI exam

OVERVIEW

The most obvious and significant role for MRI in a male-specific pelvic application is the imaging of the prostate gland, and prostate cancer is by far the most common indication for male pelvic MRI.

One in 35 of US men will die of prostate cancer, the second most common cancer after skin cancer. It is the second leading cancer death in men after lung cancer. In 2014, it is estimated that more than 233,000 men will be diagnosed with prostate cancer and 29,480 men will die from prostate cancer. About 1 in 7 men will be diagnosed with prostate cancer in their lifetime[39].

However, most men diagnosed with prostate cancer will not die from the disease. Due in part to advances in early detection, the five-year survival rate for men with prostate cancer is nearly 100%. The relative 10-year survival rate is nearly 99%, while the 15-year survival rate is about 94%.[40]

The sequences used for pelvic imaging are virtually the same for men as for women. Obviously the internal organs of the male and female pelvis are different, but imaging protocols, pulse sequences, and image weighting vary little by gender.

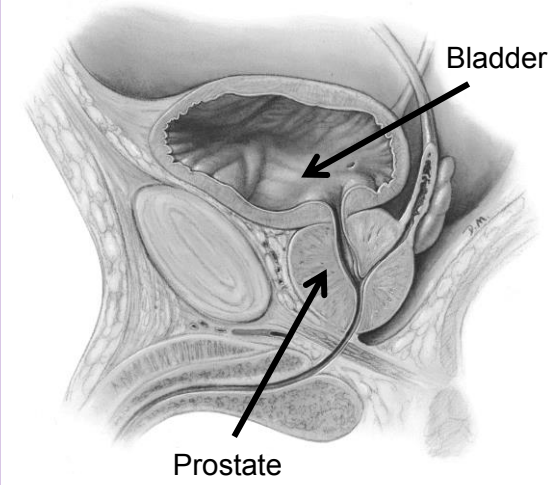

Figure 67. Bladder and prostate anatomy. The prostate has a variable position, sometimes leaning anteriorly or slightly posteriorly. Coronal MR imaging is best performed in the oblique coronal plane, tilted to coincide with the vertical axis of the prostate.

Used with permission of LifeART.

ANATOMY

The purpose of the prostate gland is to secrete seminal fluid, mixing with sperm and fluids from the seminal vesicles to produce semen.

The region of interest in prostate MRI includes the prostate gland itself (**Figure 67**), which is segmented into three zones — the central zone, the transitional zone, and the peripheral zone — as well as the seminal vesicles (**Figure 68**). The role of MRI is to evaluate tumor extension, either **extracapsular** or direct seminal vesicle invasion.

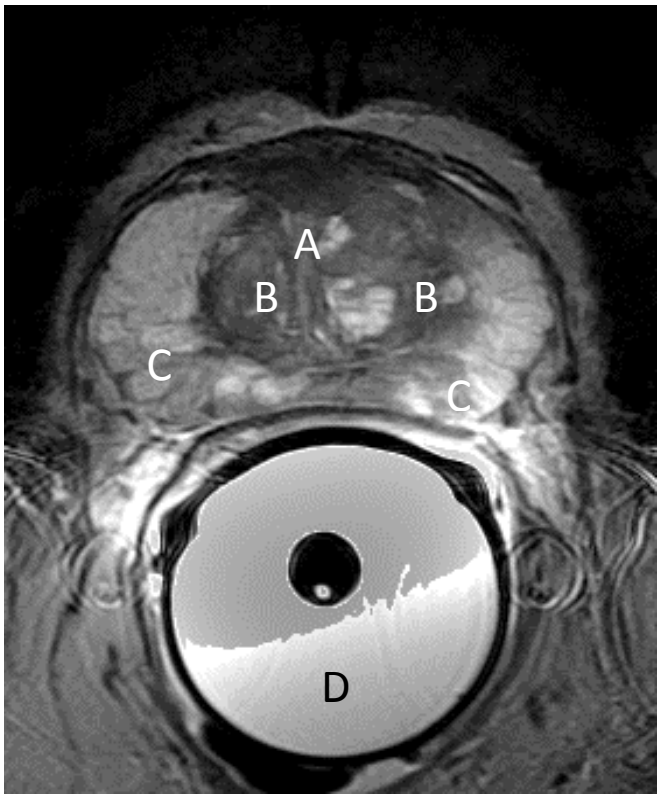

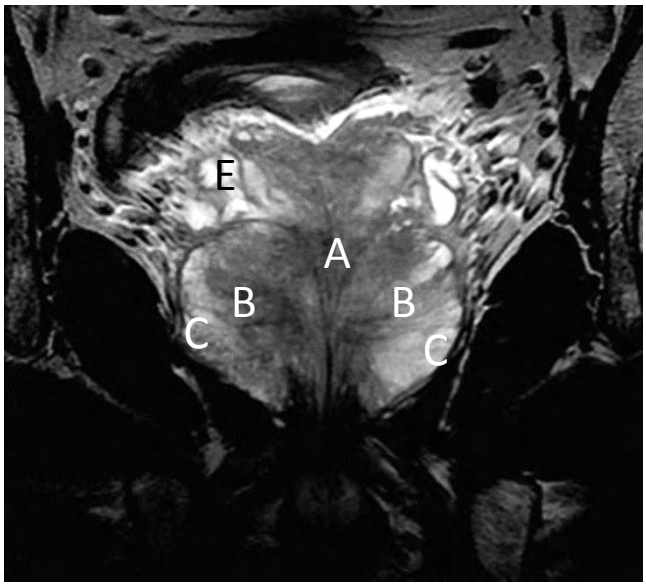

A - Transitional Zone
B - Central Zone
C - Peripheral Zone
D - Fluid-filled reservoir of endorectal coil
E - Seminal Vesicles

Figure 68. Prostate anatomy. (A) Axial view. (B) Coronal view.

3.0T CONSIDERATIONS

Signal-to-noise ratio and spatial resolution must especially be considered when imaging the prostate gland. For these reasons, imaging at 3.0T with its inherent high SNR is the field strength of choice for diagnosis and staging of prostate cancer. However, it should be noted that as with other applications imaged at 3.0T, artifacts such as chemical shift and peristalsis will be more prevalent. Even with the potential for increased artifacts, 3.0T imaging offers the best opportunity for high-signal, high spatial resolution imaging of the prostate gland.

Figure 69. Axial T1W of a patient 4 weeks post-biopsy. Note the residual blood in the left peripheral zone (circle). The exam did not proceed and was rescheduled for 4 weeks later.

PATIENT HISTORY OF BIOPSY

If the patient has had a previous biopsy, a minimum of six to eight weeks should separate biopsy and MR imaging to allow any residual blood from the biopsy to resolve. Blood in the prostate can obscure, or worse, mimic carcinoma (**Figure 69**).

At the time of the exam, the patient's **prostate-specific antigen** (PSA) level, **Gleason score**, biopsy date, and radiation and hormonal therapy history should be noted. This information is extremely useful for the radiologist when interpreting the MR images since prostate gland image contrast may be altered by radiation or hormone and neoadjuvant therapy.

STANDARD IMAGING PROTOCOL

The typical prostate protocol consists of axial, sagittal, and coronal T2W imaging without fat saturation. Because high spatial resolution is required, the slice thickness is thin, usually ≤3.0mm.

Diffusion-weighted Imaging

Diffusion-weighted imaging of the prostate is often a standard imaging sequence. **Apparent diffusion coefficient** (ADC) maps are extremely useful for showing restricted diffusion in cancerous prostate tissue (**Figure 70**). The use of parallel imaging not only increases SNR but greatly decreases potential geometric distortion common in some DWI imaging.

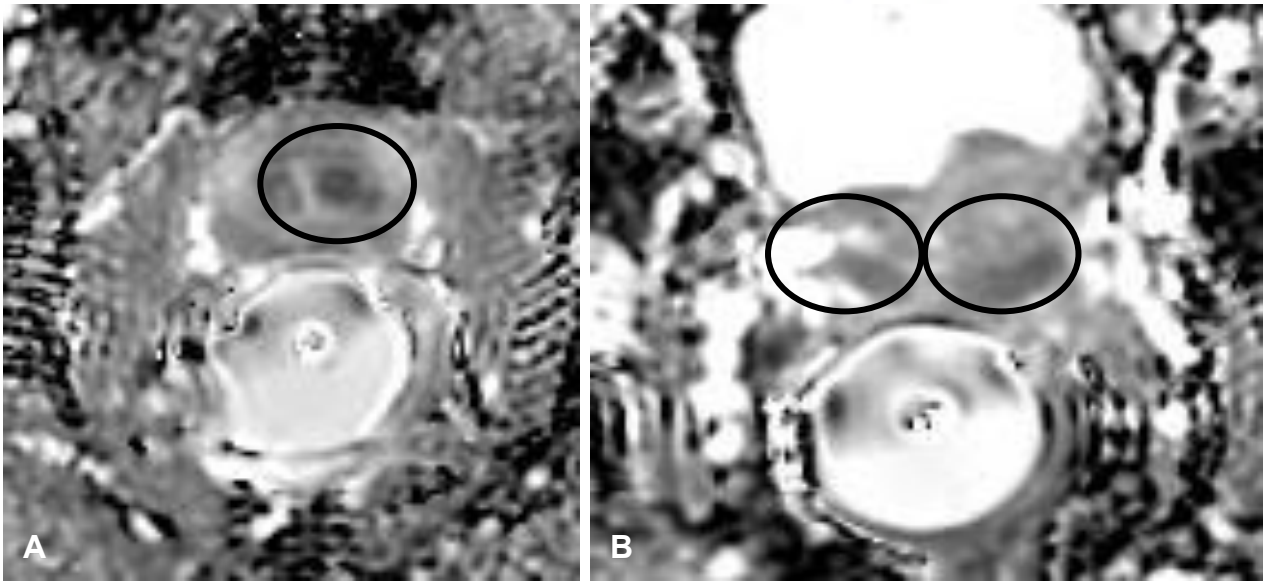

Figure 70. Apparent diffusion coefficient (ADC) map of the prostate. B-value for both diffusion sequences is 650. (A) Area of hypointense signal indicates restricted but normal diffusion in the central gland of a 67-year-old male. (B) Areas of hypointense signal indicate restricted and abnormal diffusion of the peripheral zone in a 72-year-old male.

Endorectal Coil

The prostate gland is optimally imaged using an inserted endorectal coil in conjunction with the pelvic phased-array coil, allowing for evaluation of the entire pelvis for possible cancer involvement and providing high spatial resolution images of the prostate with high SNR. Just as with female breast and pelvic floor MRI, the patient should be treated with extra sensitivity, and the exam should be explained in detailed prior to beginning the evaluation.

The endorectal coil uses an inflated bulb to hold it in place. A water-soluble lubricant must be used for insertion, but care must be taken in determining how much gel to use because the lubricant will produce a bright signal. Applying too much lubricant can result in excessive ghosting caused by rectal spasms; using too little gel can make insertion painful.

The coil should be inserted so that the coil element is seated just posterior to the prostate gland. The bulb should be inflated to the patient's tolerance level, usually 90-110mL of air but no more than 120mL. Instead of air, some facilities will use a fluid such as water or CT oral contrast solutions to inflate the balloon. The use of a fluid decreases susceptibility effects from tissue-air interfaces and may increase the local overall SNR.

It should be noted that some facilities do not use the endorectal coil. Other facilities may choose to use the coil for diagnosis but not for surgical planning, particularly if a 3.0T scanner is available.

MRI FINDINGS

Benign Prostate Hyperplasia

Most prostate cancers occur in the peripheral zone but are not uncommon in other zones. The central zone is most commonly associated with **benign prostate hyperplasia** (BPH) or enlarged prostate, a condition that often results in an acute need to urinate but with low yield. BPH is not always associated with cancer; however, cancer of the prostate can result in the same urinary dysfunction, making it important to have urinary changes medically evaluated without delay.

Prostate Cancer

The presence of prostate cancer (PCa) typically demonstrates as hypointense signal on T2-weighted imaging and is usually performed in all three planes orthogonal to the prostate gland (**Figures 71 and 72**). This sequence is also essential for BPH evaluation. Axial T1-weighted imaging through the pelvis is useful for evaluating **adenopathy** related to prostate cancer. **Figure 73** is a **movie** showing dynamic contrast acquisition of the prostate gland with rapid contrast uptake in the peripheral zone.

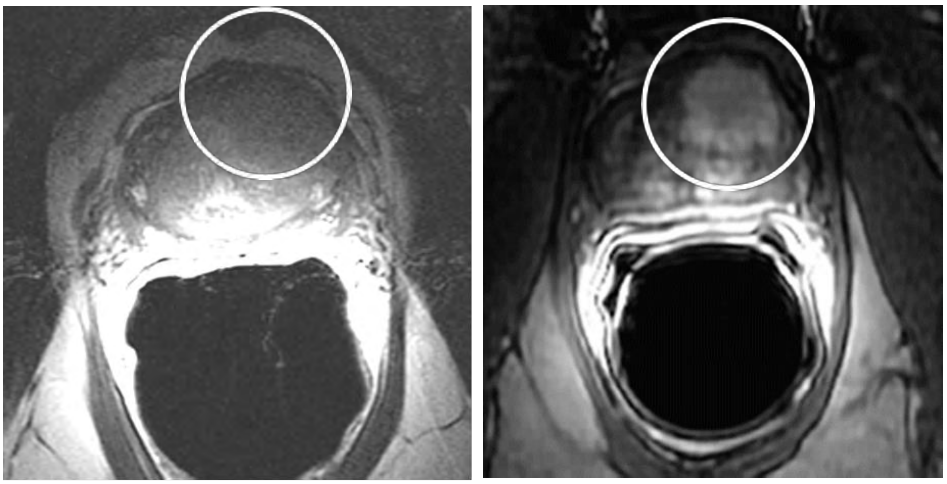

Figure 71. 65-year-old male. (A) Axial T1W shows a large central zone cancer. The circle indicates significant, hypointense tissue along the anterior wall. (B) Axial T1W image postcontrast enhancement of the same patient. Circle indicates rapid contrast uptake, indicative of a cancerous prostate gland.

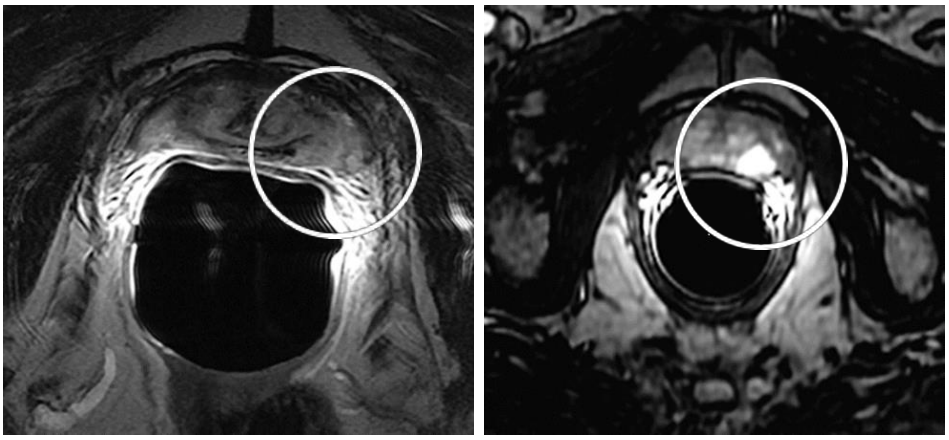

Figure 72. 77-year-old male. (A) Axial T2W. The circle indicates a recurrence in the mid-left peripheral zone posterior and lateral. (B) Postcontrast axial T2W image of the same patient. The circle indicates strong contrast uptake, indicative of prostate gland carcinoma.

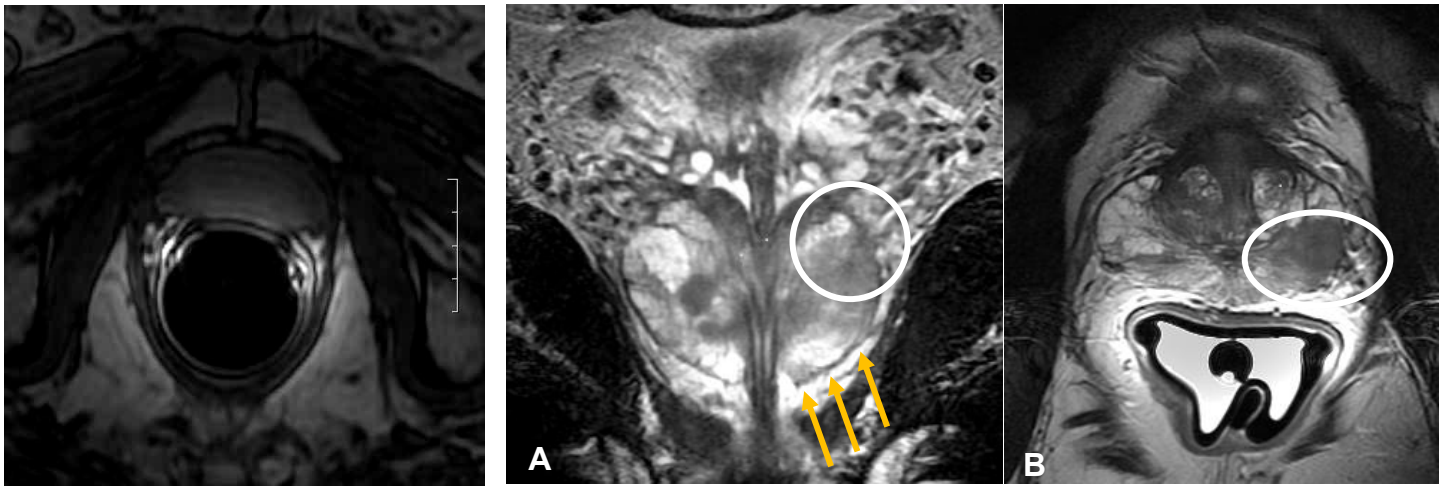

Figure 73 ***(above, left).*** **MOVIE**. Cine loop of dynamic contrast acquisition of the prostate gland. Note rapid contrast uptake in the left lateral peripheral zone vs normal prostate gland. To view this movie, click here:YouTube.com/ICPMEducation

Figure 74 ***(above, center and left).*** 64-year-old male with confirmed prostate cancer with capsular disruption. (A) Coronal T2W. The capsule is identified by the outer ring of fibrous hypointense signal (arrows). Disruption of the prostate capsule at the lateral base (circle) is demonstrated by the "break" in hypointense capsular ring. (B) Axial T2W demonstrating capsular extension of prostate cancer outward from the peripheral zone (circle).

Figure 75 ***(below).*** 64-year-old male with prostate carcinoma and seminal vesicle invasion. (A) Axial T2W. (B) Coronal T2W.

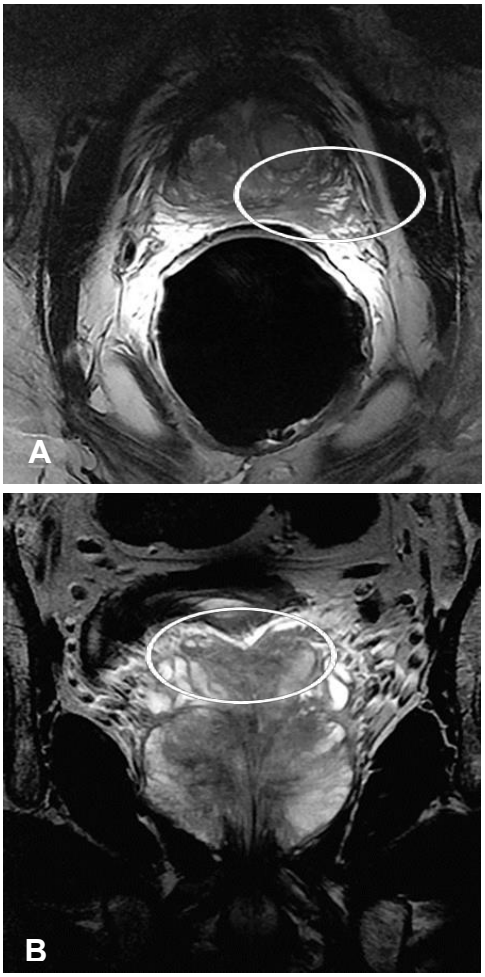

MRI findings of extracapsular extension include irregular bulge of the prostate margin, contour deformity with step-off or angulated margin, breach of the capsule with direct tumor extension, obliteration of rectoprostatic angle, and asymmetry of neurovascular bundles. Axial images are essential in the evaluation of extracapsular invasion (**Figure 74**).

Seminal Vesicle Invasion

As with cancer of the prostate gland itself, cancerous invasion of the seminal vesicles typically demonstrates as hypointense signal on T2-weighted imaging. Moreover, the cancerous invasion usually appears as a mass effect as it displaces normal seminal vesicle tissue (**Figure 75**).

Prostatitis

Prostatitis is an inflammation of the prostate gland and can be chronic or acute. Differentiating between prostate cancer and noncancerous prostatitis on MRI can be challenging since both conditions share many of the same signal characteristics, with low signal intensity of homogeneous tissue in the peripheral zone. Focal hypointense tissue signal that is not specific for cancer is the most common MR finding in chronic prostatitis.[41]

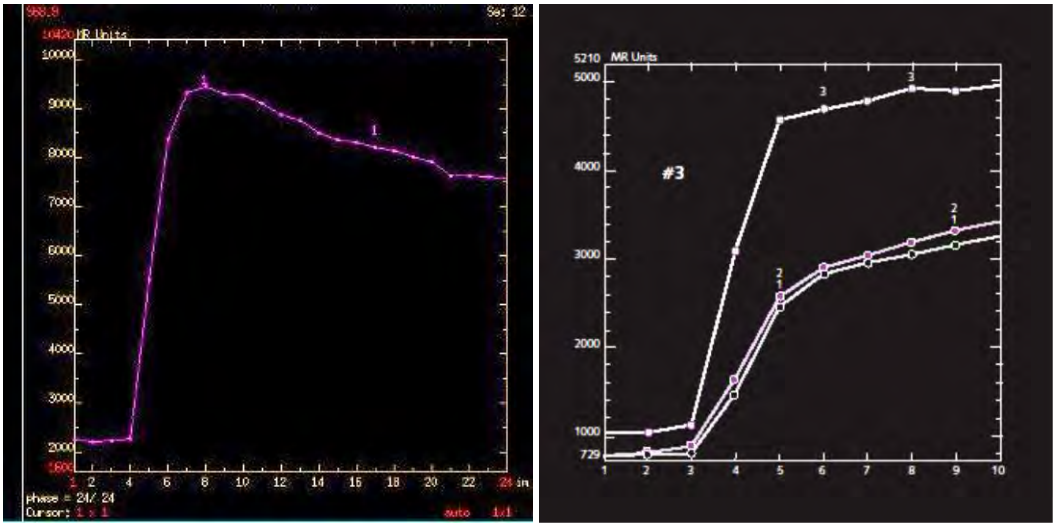

Figure 76. Signal enhancement ratio (SER) curves. Contrast update map indicates volume and rate of enhancement. Rapid wash-in/wash-out curves of SER maps can be an indicator for prostate cancer.

SIGNAL ENHANCEMENT RATIO

The role of contrast-enhanced MRI of the prostate gland is understood yet still challenging. Using GBCAs, normal, noncancerous prostate gland will show modest contrast uptake, just as a cancerous gland will. However, the use of **signal enhancement ratio** (SER) maps can be helpful for determining contrast-uptake differences between normal and cancerous tissue as a normal gland will enhance more slowly than a cancerous gland (**Figures 76 and 77**).

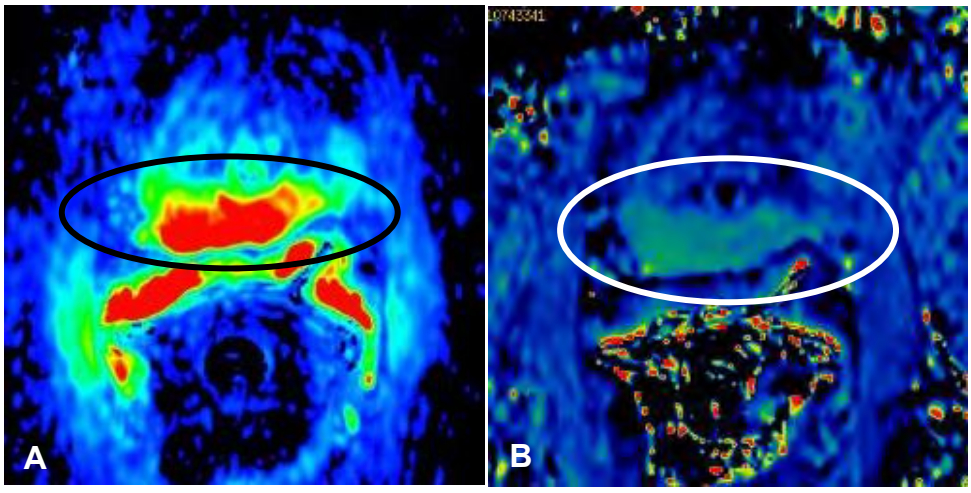

Figure 77. 72-year-old male. (A) Maximum slope of increase (MSI) map. (B) Signal enhancement ratio (SER) map. MSI map indicates areas that have a statistically higher degree of contrast enhancement than other areas of the prostate (circle). SER indicates an area that has a rapid degree of contrast wash-out as compared to other parts of the prostate (circle). Biopsy was positive for peripheral zone prostate cancer.

MR SPECTROSCOPY

MR spectroscopic (MRS) imaging has expanded the diagnostic assessment of the prostate beyond simple anatomic information. MRS provides metabolic information specific to the prostate through the detection of the cellular metabolites citrate, creatine, and choline. Information obtained from MRS allows an expanded assessment of tumor aggressiveness and risk of disease progression.

Typically high concentrates of choline and low concentrates of citrate are indicative of prostate gland carcinoma. However, normal prostate gland may display lower citrate concentrations following some hormonal therapies, such as androgen deprivation therapy, which helps slow the aggressiveness of prostate cancer when used in combination with radiation therapy[42] (**Figures 78 and 79**).

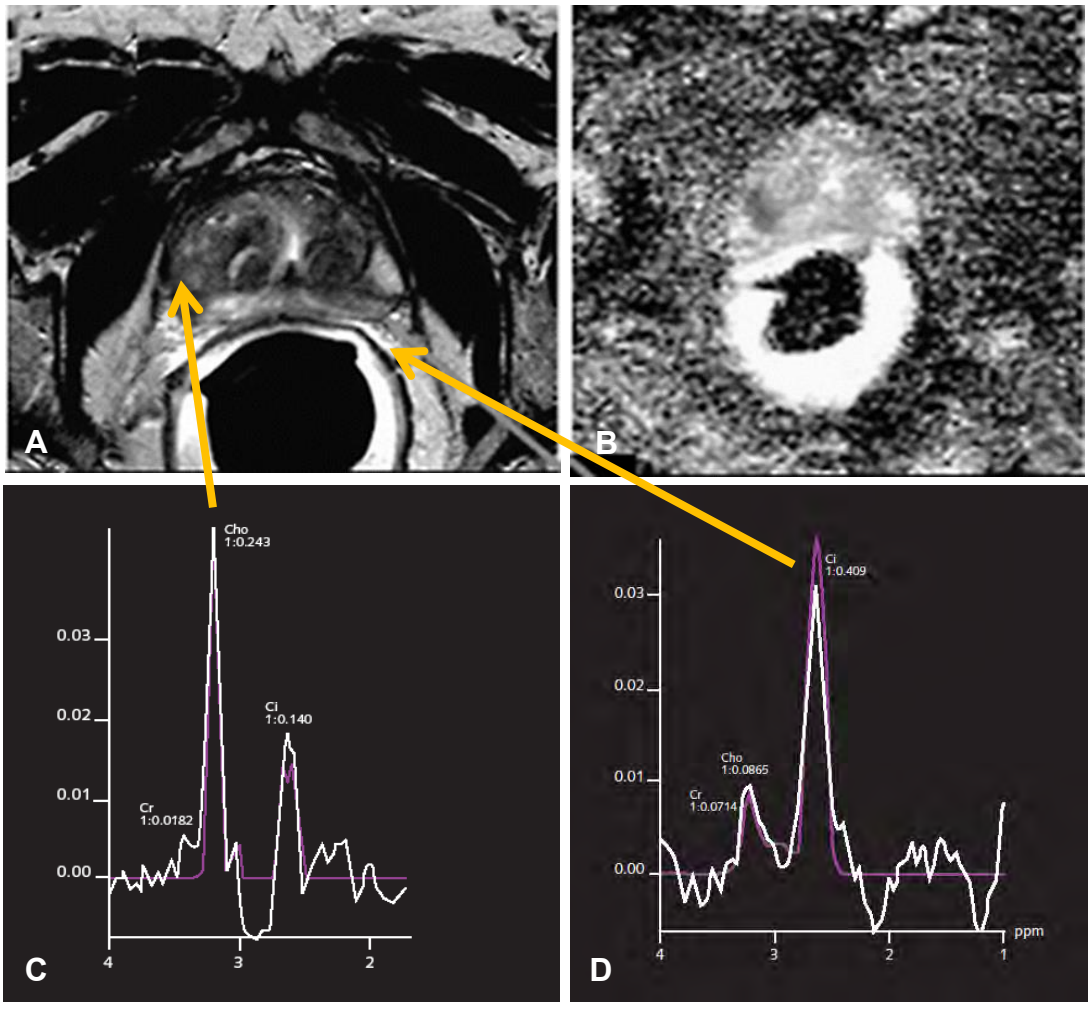

Figure 78. Prostate spectroscopy. (A) Axial T2W image. (B) Apparent diffusion coefficient map. (C, D) Spectrums of the areas indicated by the arrows. Note the high choline (C) and citrate (D) peaks, indicating prostate carcinoma.

Courtesy of Daniel J.A. Margolis, MD, UCLA.

In the localization of PCa, combined MRI and MRS demonstrate 91% specificity, the highest value obtained by a noninvasive method[43]. The combined use of MRI and MRS significantly improves evaluation of extracapsular spread and decreases interobserver variability, significantly increasing the value of MRI in the evaluation of prostate cancer.

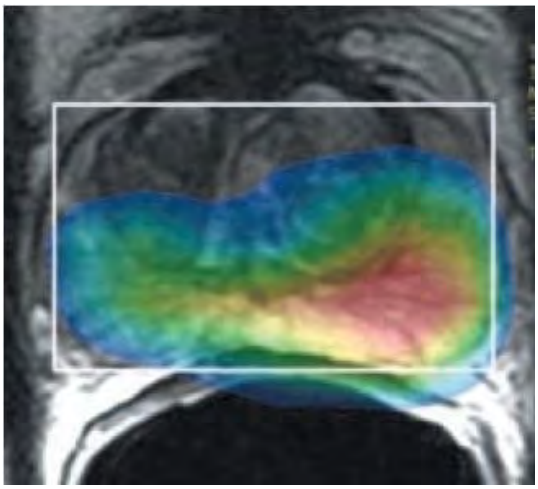

Figure 79. Prostate spectroscopy metabolite map showing high concentrations of choline (red).

Courtesy of GE Healthcare.

PROSTATE BIOPSY

Historically, prostate biopsy has been "blind," that is, the urologist or radiologist obtains tissue samples randomly and generally only in the peripheral zone, which is more easily accessed than the central zone. Since 70-80% of prostate cancers are found in the peripheral zone, 20-30% of prostate cancers are missed on initial standard biopsy.

These biopsy samples can underestimate positive results by sampling noncancerous tissue. Conversely, cancer findings that are "insignificant," as they often are in prostate cancer, could result in unnecessary radical surgery[44]. With targeted MR-guided prostate biopsy, the days of blind biopsy could become a thing of the past.

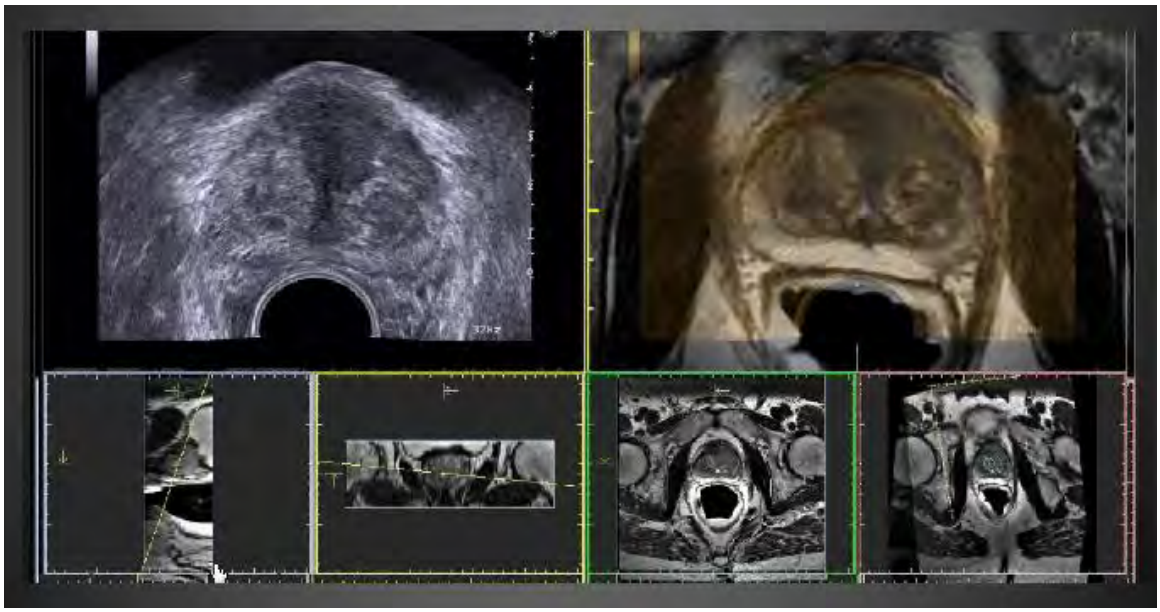

Figure 80. Transrectal ultrasound images fused with MR images allow for targeted biopsy under US guidance.

Courtesy of François Cornud, MD, Hôpital Cochin, Paris

Multiparametric imaging like T2W, diffusion-weighted, dynamic contrast-enhanced, and spectroscopic MRI not only aids in localizing the tumor, particularly anterior tumors, but allows for targeted biopsy using MRI guidance or a fusion of ultrasound and MRI images under ultrasound guidance (**Figure 80**).

Results of several studies have shown that targeted biopsy produces an increased yield, a decrease in the number of cores taken, and a decreased detection rate of insignificant cancers, potentially resulting in fewer unnecessary surgeries[45,46,47].

A sample prostate MRI protocol can be found at the end of this material.

SUMMARY

When performed with close attention to high spatial resolution and signal-to-noise ratio, MRI of the prostate provides highly detailed and useful information in the detection and staging of prostate cancer and benign prostate hyperplasia. However, high-quality prostate imaging is invasive in that it requires the use of an endorectal prostate coil, which may be physically and emotionally uncomfortable for the patient. Techniques such as prostate spectroscopy, diffusion-weighted imaging, and functional post-processing of dynamic contrast images into signal enhancement maps are useful additional tools in cancer evaluation of the prostate.

NOTES

Tom Schrack, BS, ARMRIT
Fairfax Radiological Consultants
Fairfax, VA

PELVIC MR IMAGING FOR ANAL-RECTAL CANCER

After completing this section, the reader should be able to:

- Identify the main anatomical structures of the anal-rectal area
- List the major imaging parameters for evaluating anorectal cancer
- Discuss the advantages of MRI vs CT in visualizing anorectal cancer
- Name typical MRI findings of the anal-rectal area

OVERVIEW

Colon and rectal cancer is the 4th most common form of cancer in the United States after prostate, breast, and lung cancer. Colorectal cancer represents 8.6% of all new cancer cases in the USA. The median age for a diagnosis of colorectal cancer is age 69. It is diagnosed in men more often than in women and in African Americans. In 2013, 45 out of every 100,000 people in the US were diagnosed with colorectal cancer.[48]

Significant progress has been made in increasing the five-year survival rate because of early detection, due in large part to increased public awareness of the disease and the effectiveness of treatment and survivability when the cancer is detected early. Diagnostic imaging plays an important role in the detection and staging of colorectal cancer.

CT has historically been the go-to imaging modality for *colorectal* cancer. While CT remains the first choice for imaging of the large bowel, MR is increasingly being used for diagnosis and staging of *anal-rectal* cancer (**Figure 81**).

PATIENT PREPARATION

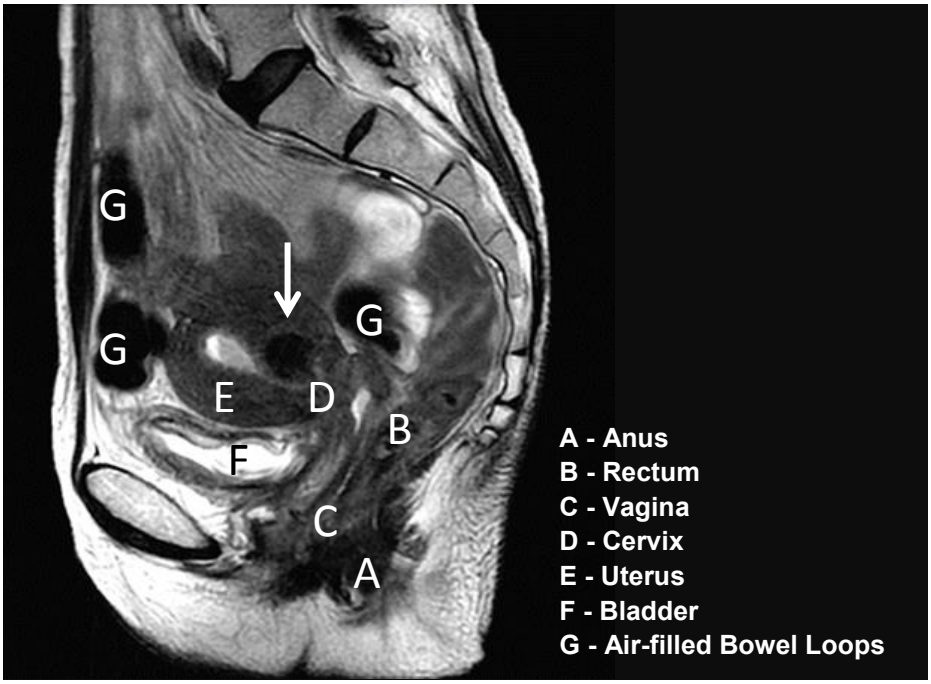

Figure 81. Anorectal anatomy. Note the uterine fibroid (arrow).

Patient preparation for this exam is not complicated. Typically, the patient is NPO for four hours prior to the exam. Neither a cleansing enema nor inter-rectal gel is required. To highlight image contrast, it is common for the rectum to be filled with a contrast medium, and typically water-soluble ultrasound gel is injected using a standard enema tip. Approximately 50mL of gel is inserted into the rectum, which provides excellent contrast between the walls of the rectum and tumor. Caution is required for the insertion of small rectal tips to ensure that no perforation or trauma to the mass occurs. The administration of glucagon is effective and recommended for relaxing quivering rectal muscles. For known anal cancers or cancers low into the anorectal verge, contrast-enhanced imaging is often indicated.

The patient is placed supine on the MR table and if possible enters the magnet bore feet-first to minimize claustrophobia. The typical exam takes no more than 30 minutes.

IMAGING PARAMETERS

The majority of anal-rectal cancer cases referred for MRI are patients with known or strongly suspected anal-rectal cancer. Therefore, MRI is typically used to evaluate and stage the cancer.

Spatial resolution is the paramount imaging requirement for anal-rectal cancer imaging. The key objective is to determine if the tumor margins have broken the rectal wall and invaded or advanced into the retroperitoneal spaces. GBCA administration is usually not required for rectal cancer staging but shows benefit for cancer that is localized in the anus.

Scan protocols for anorectal cancer typically include high-resolution sagittal and **oblique** axial T2-weighted imaging planes (**Figure 82**). It is important that the oblique axial plane is set to the long axis of the tumor in order to well visualize the tumor margins.

High-resolution T2-weighted imaging provides the most useful image contrast when imaging the anorectal area. Typically, three planes of imaging are acquired that are obliqued to be parallel and perpendicular to the tumor. If the tumor is multi-directional, angling to the plane of the rectum is preferred. Fat- and non-fat saturated imaging is typical.

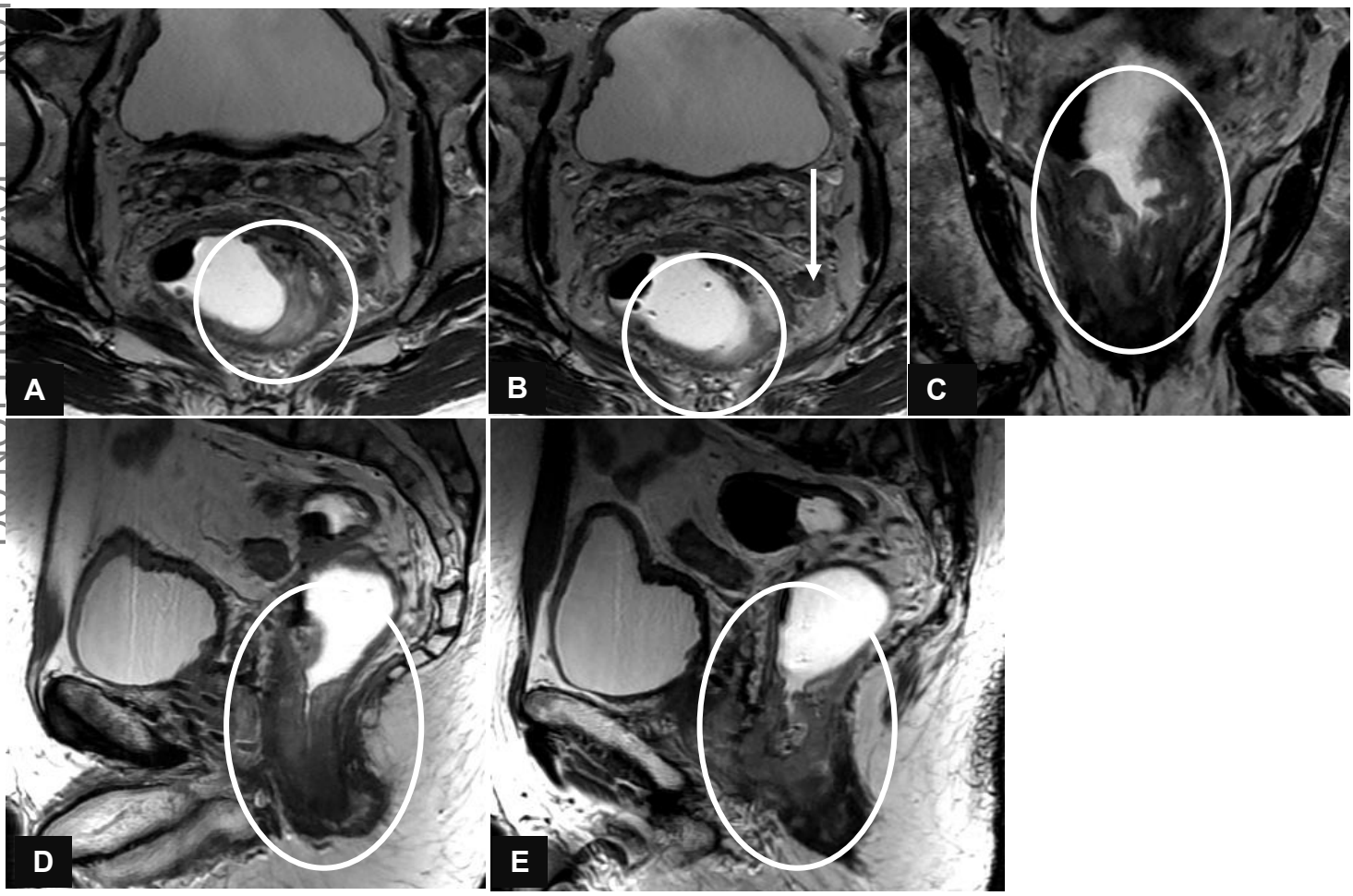

Figure 82. 80-year-old male with known rectal cancer undergoing MRI for cancer staging. (A, B) Axial T2W images indicating a tumor in the left rectal wall (circles). (B) Arrow indicates a mesorectal lymph node. (C) Coronal T2W. (D, E) Sagittal T2W.

High spatial resolution is key to the success of the exam. Imaging slices are thin, typically 3-4 mm with a high matrix. To provide the required SNR, the use of a local high-channel pelvic-array coil is essential. This coil provides higher SNR than does the body coil or other lower, four-channel array coils. See a sample scan protocol at the end of this material.

IMAGING AT 3.0T

Imaging at 3.0 T also provides a boost in SNR that allows for even greater resolution or faster scan times. Typically the use of contrast-enhanced MRI is not indicated if the tumor is located well into the rectum since the rectum will be easily definable from the tumor margins. However, if the tumor resides in the anal area or at the anal-rectal junction, GBCA administration will aid in defining tumor margins (**Figure 83)**.[49]

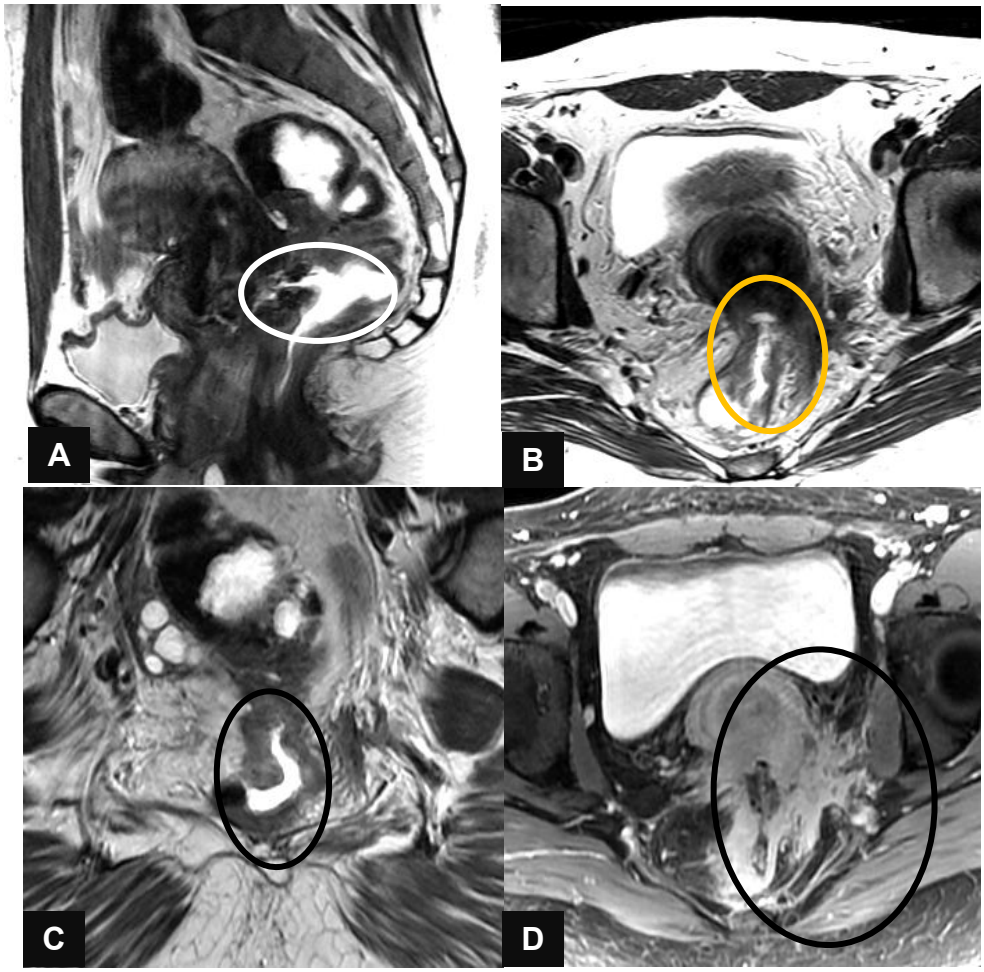

Figure 83. 30-year-old female with known anal-rectal cancer. 3.0T MRI demonstrates Stage 4 carcinoma with a rectal-vaginal fistula. (A) Sagittal T2W. (B) Axial T2W. (C) Coronal T2W image demonstrating tumor involvement. (D) Postcontrast, the tumor is shown to extend beyond the left border through the mesorectal fascia into the vagina, extending into the left sciatic notch.

MRI FINDINGS

MR imaging demonstrates not only the size and shape of the tumor but also its composition and extent. High-resolution images exhibit tissue distinctions of the mucosa and bowel wall, as well as the extent of tumor involvement into the pelvic cavity and any obstruction of the rectum. Axial imaging of the entire pelvis will reveal any adenopathy in the pelvis. Typically one plane of fat-saturated imaging (either chemical fat saturation or IR-pulse fat saturation) is performed to differentiate perirectal fat from potential cystic fluid and blood.

SUMMARY

Great progress has been made in increasing the five-year survival because of early detection due in large part to increased public awareness of the disease and the effectiveness of treatment and survivability when the cancer is detected early. Diagnostic imaging plays an important role in the detection and staging of colorectal cancer.

MR imaging of the anal-rectal area is a quick method for scanning and staging patients with known or suspected anorectal cancer. The exam provides images of high diagnostic value through high-contrast and high-resolution scanning. The exam is not difficult or invasive for the patient. There is little preparation required by the patient and IV contrast is typically not needed.

NOTES

SAMPLE LIVER MRI PROTOCOL (1.5T)

Parameter	3-Plane Localizer	Coronal SSFSE	AXIAL T2W Fat/Sat*	Axial In/Out Phase 2D	Axial FSPGR Triple Phase Fat/Sat Dynamic	Axial FSPGR Fat/Sat Portal Venous	Axial FSPGR Fat/Sat Equilibrium
Pulse Sequence	Gradient	SSFSE	FSE	Gradient	FSE	FSE	FSE
TE (msec)	min	140	80-100	IP = 2.1 OP = 4.2	min	min	min
TR (msec)	min	min	3-6000	150-250	min	min	min
Flip Angle				80	12	12	12
Options		Fast, SS, ASSET	FC, TRF, RT, Fast	ASSET	Zipx2, ASSET	Zipx2, ASSET	Zipx2, ASSET
Slice Thickness (mm)	10	6	6	2D=6	4-8	3-6	3-6
Slice Spacing (mm)	0	2	2D=1.5	2D=1.5	0	0	0
Sat Bands			S, I, Fat	S, I	Fat	Fat	Fat
Matrix	256x128	256x192	320x224	256x192	256x160	256x160	256x160
NEX	1	1	2	1	1	1	1

*Use respiratory triggering or a navigator to assist with respiratory artifact. Scan can be performed with breath-holds. See Optional Liver Sequences.

SAMPLE OPTIONAL LIVER MRI SEQUENCES (1.5T)

Parameter	3D Gradient In/Out 2-Point Dixon*	Axial Diffusion ** Non-breath-hold	Axial T2W Breath-hold
Pulse Sequence	Gradient	SW EPI	FSE
TE (msec)	TE1 = 2.3, TE2 = 4.6	Min	80-100
TR (msec)	Min	3500	2000-4000
Flip Angle	12	90	90
Options	ASSET	ASSET, EPI, Diff	TrF, Fast, ASSET, FR
Slice Thickness (mm)	4	6	6
Slice Spacing (mm)	0	1.5	1.5
Sat Bands			S, I, Fat
Matrix	256x160	132x160	256x192
NEX	1	10	1

* Reconstructs in- and out-of-phase images, as well as fat and water only images.
** Ramp Sampling = 1 B-value = 50,800 Diffusion Direction = S > 1

SAMPLE ADDITIONAL SEQUENCES FOR MRCP PROTOCOL (1.5T)

Parameter	Coronal HASTE 3D Thick Slab	HASTE 3D Thick Slab +20°	HASTE 3D Thick Slab -20°	Coronal 3D FSE*	Coronal 2D Thin Slice**
Pulse Sequence	SSFSE	SSFSE	SSFSE	FSE, Fast Reconstruction	SSFSE
TE (msec)	700-800	700-800	700-800	min ~700	350
TR	min	min	min	2-3 R to R	2000
Sat Bands	Fat	Fat	Fat	Fat	Fat
Options	Fast, SS	Fast, SS	Fast, SS	Zipx2, ASSET, RT, EDR, FR, MRCP	Fast, SS
Slice Thickness (mm)	40-60	40-60	40-60	1-1.4	3-4
Slice Spacing (mm)	0	0	0	0	0
Matrix	288x288	288x288	288x288	256x256	288x192
NEX	1	1	1	1	1

* Respiratory trigger – use respiratory bellows or a navigator.
**LOC before pause – split series into reasonable breath-holds for patient.

EOVIST PROTOCOL (1.5 and 3.0T)

Parameter	3-plane Localizer	Coronal SSFSE	Axial In-and Out-of-Phase	Dynamic Pre	Triple Phase Dynamic	PV	Diff	Equil	T2	Axial Delay	Coronal Delay
										15 and 20-min delay	
Pulse Sequence	GRE	SSFSE	GRE	FSPGR	FSPGR 3D	FSPGR 3D	GRE EPI	FSPGR 3D	FSE	FSPGR 3D	FSPGR 3D
TE (msec)	Min	140	IP=2.1 OP=4.2	Min	Min	Min		Min	80-100	Min	Min
TR (msec)	Min	Min	150-250	Min	Min	Min	3000-4000	Min	3000-6000	Min	Min
Flip Angle			80	12	12	12		12		12	12
Options		FAST, SS, ASSET	ASSET	ZIPx2, ASSET	ZIPx2, ASSET	ZIPx2, ASSET	ASSET	ZIPx2, ASSET	FC, TRF, RT, FAST	ZIPx2, ASSET	ZIPx2, ASSET
Slice Thickness (mm)	10	6	6	3-6	4-8	3-6	6	3-6	6	3-6	3-6
Slice Spacing (mm)	0	2	1.5	0	0	0	1.5	0	1.5	0	0
Sat Bands			SI	Fat	Fat	Fat	Fat	Fat	S, I, Fat	Fat	Fat
Matrix	256x128	256x192	256x192	256x160	256x160	256x160	128x160	256x160	320-x224	256x160	256x160
NEX	1	1	1	1	1	1	1	1	2	1	1

SAMPLE ADRENAL MRI PROTOCOL

	Scout	T1W (in-phase and out-of-phase)
Sequence	Ultrafast T2W (HASTE, SSFSE)	Fast GRE (FSPGR, FLASH)
Plane	Coronal	Axial
NEX	1	1
TR (msec)		150-250
TE (msec)	99	4.6 and 2.3 (at 1.5T)
Flip Angle	NA	70-90
Slice Thickness (mm)	8	4
Gap	2	1
Matrix	256x160	256x192
Options	Breath-hold	Breath-hold

SAMPLE RENAL MRI PROTOCOL

	Scout	T2W	T2W	T1W
Sequence	Ultrafast T2W (HASTE)	T2W (FSE/TSE, etc.)	T2W (FSE/TSE)	Fast GRE (FMPSPGR, FLASH)
Plane	Coronal	Axial	Coronal	Axial
NEX	1	2-3	2-3	1
TR (msec)		>2000	>2000	150-250
TE (msec)	99	102	102	4.6
Flip Angle	NA	NA	NA	70-90
Slice Thickness (mm)	8	5	5	5
Gap	2	0-2	0-2	0-2
Matrix	256x160	256x256	256x256	256x160
Options	Breath-hold	Fat Saturation	Fat Saturation	Breath-hold Fat Saturation

SAMPLE DYNAMIC PELVIS MRI PROTOCOL

	3D Gradient In/Out T2W	T1W	FIESTA (FISP)	FIESTA (FISP)
Sequence	FSE	FSE	FIESTA	FIESTA
Plane	Axial	Coronal	Sagittal	Sagittal
TR (msec)	4000	4000	min	min
TE (msec)	100	100	min	min
Slice Thickness (mm)	4.5	7	10	10
FOV (cm)	25	26	30	30
ETL	15	15		
Flip Angle			75	75
NEX	4	3	1	1
Phase	512	256	320	320
Frequency	384	192	320	320
Images/Loc			10 REST	10 PUSH

SAMPLE FEMALE PELVIS MRI PROTOCOL

	3-Plane Localizer	Sagittal T2W	Axial T1W	Axial T2W	Coronal T2W
Orientation	Feet first, supine	Feet first, supine	Feet first, supine	Feet first, supine	Feet first, supine
Coil	Torso phased-array	Torso phased-array	Torso phased-array	Torso phased-array	Torso phased-array
Plane	3 Planes	Sagittal	Oblique	Oblique	Oblique
Imaging Parameters					
Pulse Sequence	GRE	FSE	SPGR	FSE	FSE
Scan Timing					
Number of Shots	n/a	n/a	n/a	n/a	n/a
TE (msec)		120	In-Phase	120	120
TR (msec)		6000	250	6000	6000
TI (msec)	n/a	n/a	n/a	n/a	n/a
Flip Angle			70		
ETL		12-16		12-16	12-16
Options		NPW, VBw FC, EDR	NPW, EDR	NPW, VBw FC, EDR	NPW, VBw FC, EDR
Scanning Range					
FOV (cm)	48	22	28	20	20
Slice Thickness (mm)	8	4	5	5	5
Slice Spacing (mm)	2	1	0	1	1
Sat Bands		Anterior Inferior Superior	Anterior Inferior Superior	Anterior Inferior Superior	Anterior Inferior Superior
Acquisition Time					
Acquisition Matrix Frequency	256	256	256	256	256
Acquisition Matrix Phase	128	256	160	256	256
NEX	1	3	2	3	3
Phase FOV	1	1	1	1	1
Frequency Direction		S/I	R/L	R/L	S/I
Auto Center Frequency	Water	Water	Water	Water	Water
Autoshim	Yes	Yes	Yes	Yes	Yes

Notes

- Axial T1 images should start at the distal pole of the kidneys and end at the pubis symphysis.
- Axial T2W images should be prescribed perpendicular to the uterus.
- Coronal T2W images should be prescribed parallel to the uterus.

SAMPLE PROSTATE SCAN PROTOCOL USING ENDORECTAL COIL

	3-Plane Localizer	Axial T1W	Axial T2W	Oblique Coronal T2W	Sagittal T2W	Oblique Axial DWI
	Patient Position					
Orientation	Feet first, supine	Feet first, supine	Feet first, supine	Feet first, supine	Feet first, supine	Feet first, supine
Coil	Torso phased-array	Torso phased-array and endorectal	Torso phased-array and endorectal	Torso phased-array and endorectal	Torso phased-array and endorectal	Torso phased-array and endorectal
Plane	3 planes	Axial	Axial	Oblique Coronal	Sagittal	Oblique Axial
Imaging Parameters						
Pulse Sequence	GRE	SE	FSE	FSE	FSE	Diffusion-weighted EPI
			Scan Timing			
Number of Shots	n/a	n/a	n/a	n/a	n/a	1
TE (msec)	n/a	Minimum	120	120	120	min
TR	n/a	600	6,000	4,500	5,500	3000-4000
TI/b-value	n/a	n/a	n/a	n/a	n/a	1000
FA	n/a	n/a	90	90	90	n/a
ETL	n/a	n/a	12	12	20	n/a
Options	n/a	Res Comp, NPS	Flow Comp, NPW, VBw	Flow Comp, NPW, VBw	Flow Comp, NPW, VBw	Parallel Imaging
Scanning Range						
FOV (cm)	48	24-48	14	14	16	28
Slice Thickness (mm)	8	5	3	3	4	3
Slice Spacing (mm)	2	1	0	0	1	0
SAT Bands		Inferior/Superior Anterior/Posterior	Inferior/Superior Anterior/Posterior	Inferior/Superior	Inferior/Superior	none
Acquisition Time						
Acquisition Matrix Frequency	256	256	256	256	256	128
Acquisition Matrix Phase	128	192	192	192	256	128
NEX	2	1	4	4	3	6
Phase FOV	1	1	1	1	1	1
Frequency Direction		R/L	A/P	S/I	S/I	R/L
Auto Center Frequency	Water	Water	Water	Water	Water	Water
Autoshim	Yes	Yes	Yes	Yes	Yes	Yes

Notes

- When using a probe, be sure the probe lies flat against the prostate; if it is rotated, make the proper adjustments before continuing past the localizer scan.
- The T1W axial images should be placed from the bifurcation of the iliac arteries to the pubis symphysis.
- The T2W should cover from just above the seminal vesicle to just below the prostate gland.
- The use of a compression belt will help reduce respiratory effect.
- Make the patient as comfortable as possible by offering music and elevating the knees with a wedge or pillow.

SAMPLE ANAL-RECTAL MRI PROTOCOL

Parameter	Sagittal FIESTA (FISP, Balanced FFE)	Axial T1W Pelvis	Oblique-Axial T2W	Oblique-Coronal T2W	Oblique-Axial Fat Sat
Imaging Parameters					
Pulse Sequence	FIESTA	FSE	FSE	FSE	FSE
Plane	Sagittal	Axial	Oblique-axial	Oblique-coronal	Oblique-axial
TR	Min	500-600	3000	2400	3000
TE	Min	Min full	100	90	100
Slice thickness (mm)	5	6	3.5	3.5	4
FOV (cm)	30	26	20	20	20
ETL		5	21	19	21
FA	65				
NEX	4	3	4	4	4
Phase	320	288	384	288	288
Frequency	256	192	224	192	224

REFERENCES

1. University of California San Francisco website. Contrast extravasation. Available at: http://www.radiology.ucsf.edu/patient-care/patient-safety/contrast/iodinated/contrast-extravasation. Accessed November 1, 2013.
2. Colletti PM. Nephrogenic systemic fibrosis and gadolinium: a perfect storm. *AJR Am J Roentgenol.* 2008;191(4):1150-1153.
3. United States Department of the Interior website. What does water do for you? Available at: http://ga.water.usgs.gov/edu/propertyyou.html. Accessed October 30, 2013.
4. Widmark JM. Imaging-related medications: a class overview. Proc (Bayl Univ Med Center). 2007;20(4):408-417.
5. Jung JW, Kang HR, Kim MH, et al. Immediate hypersensitivity reaction to gadolinium-based MR contrast media. *Radiology*. 2012;264(2):414-422.
6. Prince MR, Zhang H, Zou Z, Staron RB, Brill PW. Incidence of immediate gadolinium contrast media reactions. *AJR Am J Roentgenol.* 2011;196(2):W138-143.
7. Prince MR, 2011.
8. Prince MR, 2011.
9. American College of Radiology website. ACR Manual on Contrast Media v9 2013.
10. American College of Radiology website. ACR Manual on Contrast Media v9 2013.
11. National Kidney Disease Education Program website. GRF MDRD Calculator for Adults. Available at: http://nkdep.nih.gov/lab-evaluation/gfr-calculators/adults-conventional-unit.shtml. Accessed November 7, 2013.
12. American College of Radiology website. ACR Manual on Contrast Media v9 2013.
13. American College of Radiology Website. Liver Imaging Reporting and Data System. Available at: http://www.acr.org/Quality-Safety/Resources/LIRADS. Accessed March 3, 2014.
14. American College of Radiology website. LIRADS archive. Available at: http://www.acr.org/Quality-Safety/Resources/LIRADS/Archive. Accessed March 3, 2014.
15. World Health Organization website. Hepatitis. Available at: http://www.who.int/topics/hepatitis/en/. Accessed March 3, 2014.
16. Memorial Sloane Kettering Cancer Center website. About liver metastases. Available at: http://www.mskcc.org/cancer-care/adult/liver-metastases-secondary-liver/about-liver-metastases. Accessed March 6, 2014.
17. Saich R, Chapman R. Primary sclerosing cholangitis, autoimmune hepatitis and overlap syndromes in inflammatory bowel disease. *World J Gastroenterol.* 2008;14(3):331-337.
18. Centers for Disease Control and Prevention website. Inflammatory bowel disease. Available at: http://www.cdc.gov/ibd/. Accessed March 3, 2014.
19. CDC website.
20. CDC website.
21. Siddiki HA, Fidler JL, Fletcher JG. Prospective comparison of state-of-the-art MR enterography and CT enterography in small-bowel Crohn's disease. *AJR Am J Roentgenol.* 2009;193(1):113-121.

22. National Uterine Fibroids Foundation. Statistics. Available at: http://www.nuff.org/health_statistics.htm. Accessed February 28, 2014.

23. Mayo Clinic website. Uterine fibroids. Available at: http://www.mayoclinic.org/diseases-conditions/uterine-fibroids/basics/symptoms/con-20037901. Accessed February 28, 2014.

24. Harman M, Zeteroğlu S, Arslan H, Sengül M, Etlik O. Predictive value of magnetic resonance imaging signal and contrast-enhancement characteristics on post-embolization volume reduction of uterine fibroids. *Acta Radiol.* 2006;47(4):427-435.

25. Livermore JA, Adusumilli S. MRI of benign uterine conditions. *Appl. Rad.* 2007;36(7).

26. FDA website. Medical devices: ExAblate®2000 System. Available at: http://www.fda.gov/medicaldevices/productsandmedicalprocedures/deviceapprovalsandclearances/recently-approveddevices/ucm080704.htm. Accessed February 28, 2014.

27. InSightec website. MR guided focused ultrasound therapy; ExAblate for treating uterine fibroids. Available at: http://us.insightec.com/ExAblate-uterine-fibroids.html. Accessed February 28, 2014.

28. Toprak U, Paşaoğlu E, Karademir MA, Gülbay M. Sonographic, CT, and MRI findings of endometrial stromal sarcoma located in the myometrium and associated with peritoneal inclusion cyst. *AJR Am J Roentgenol.* 2004;182(6):1531-1533.

29. Centers for Disease Control and Prevention. Cervical cancer statistics. Available at http://www.cdc.gov/cancer/cervical/statistics/. Accessed February 28, 2014.

30. American Cancer Society website. Cancer facts for women. Available at: http://www.cancer.org/healthy/findcancerearly/womenshealth/cancer-facts-for-women. Accessed February 28, 2014.

31. National Cancer Institute website. Cervical cancer. Available at: http://www.cancer.gov/cancertopics/types/cervical. Accessed February 28, 2014.

32. New York-Presbyterian/Weill Cornell Medical Center archives. George Papanicolaou: development of the Pap smear. Available at: http://weill.cornell.edu/archives/blog/2011/06/george-papanicolaou-development-of-the-pap-smear.html. Accessed March 3, 2014.

33. Scheidler J, Heuck AF. Imaging of cancer of the cervix. *Radiol Clin North Am*. 2002;40(3):577-590.

34. Sala E, Wakely S, Senior E, Lomas D. MRI of malignant neoplasms of the uterine corpus and cervix. *AJR Am J Roentgenol.* 2007;188(6):1577-1587.

35. Sala E, 2007.

36. Li XC, Shang JB, Wu XM, et al. MRI findings of uterine cervical cancer and value of MRI in preoperative staging [in Chinese]. *Nan Fang Yi Ke Da Xue Xue Bao.* 2007;27(3):352-354.

37. Ben Sira L, Garel C, Leitner Y, Gross-Tsur V. Prenatal imaging of the fetal brain--indications and developmental implications of fetal MRI [in Hebrew]. *Harefuah*. 2008;147(1):65-70, 93.

38. Abujudeh HH, Bruno MA, eds. Quality and Safety in Radiology. Oxford, UK: Oxford University Press; 2012:320.

39. American Cancer Society website. Prostate cancer. Available at: http://www.cancer.org/cancer/prostatecancer/detailedguide/prostate-cancer-key-statistics. Accessed March 3, 2014.

40. American Cancer Society website. Survival rates for prostate cancer. Available at: http://www.cancer.org/cancer/prostatecancer/detailedguide/prostate-cancer-survival-rates. Accessed March 3, 2014.

41. Shukla-Dave A, Hricak H, Eberhardt SC. Chronic prostatitis: MR imaging and 1H MR spectroscopic imaging findings--initial observations. *Radiology.* 2004;231(3):717-724.

42. Noworolski S. Prostate MR imaging. Paper presented at: Annual Scientific Assembly and Annual Meeting of the Radiological Society of North America, December 2, 2009; Chicago, IL

43. Kurhanewicz J, Sotto CK, Coakley F. Magnetic resonance anatomic and spectroscopic imaging of prostate cancer – current status. *PCRI Insights.* 2006;9(4).

44. Chun FK, Karakiewicz PI, Briganti A. Prostate cancer diagnosis: importance of individualized risk stratification models over PSA alone. *Eur Urol.* 2008;54(2):241-242.

45. Delongchamps NB, Peyromaure M, Schull A, et al. Pre-biopsy Magnetic Resonance Imaging and prostate cancer detection: comparison of random and MRI-targeted biopsies using three different techniques of MRI-TRUS image registration. *J Urol.* 2013;189(2);493-499.

46. Haffner J, Lemaitre L, Puech P, et al. Role of magnetic resonance imaging before initial biopsy: comparison of magnetic resonance imaging-targeted and systematic biopsy for significant prostate cancer detection. *BJU Int.* 2011 Oct;108(8 Pt 2):E171-178.

47. Mouraviev V, Pugnale M, Kalyanaraman B, et al. The feasibility of multiparametric magnetic resonance imaging for targeted biopsy using novel navigation systems to detect early stage of prostate cancer: The preliminary experience. *J Endourol.* 2013;27(7):820-825.

48. National Cancer Institute website. SEER stat fact sheets: colon and rectum cancer. Available at: http://seer.cancer.gov/statfacts/html/colorect.html. Accessed February 28, 2014.

49. Taylor FG, Swift RI, Blomqvist L, Brown G. A systematic approach to the interpretation of preoperative staging MRI for rectal cancer. *AJR Am J Roentgenol.* 2008;191(6):1827-1835.

Abbreviation Glossary

ADC	apparent diffusion coefficient
AML	angiomyelolipoma
A/P	anterior/posterior
ASSET®	array spatial sensitivity encoding technique (GE Healthcare)
B_0	the main magnetic field
BPH	benign prostate hyperplasia
CAD	computer-aided detection
CT	computed tomography
DTI	diffusion tensor image
DWI	diffusion-weighted imaging
EDR	extended dynamic range
eGFR	estimated glomerular filtration rate
EPI	echo-planar imaging
ERCP	endoscopic retrograde cholangiopancreatography
ESP	echo spacing
ETL	echo train length
FA	flip angle
FC	flow compensation
FFE	fast field echo
FFT	fast Fourier transform
FHN	focal nodular hyperplasia
FIESTA™	fast imaging employing steady-state acquisition (GE Healthcare)
FISP™	fast imaging with steady-state precession (Siemens Healthcare)
FLASH®	fast low angle shot (Siemens Healthcare)
FMPSPGR	fast multi-planar spoiled gradient echo
FNH	focal nodular hyperplasia
FOV	field-of-view
FR	fast recovery
FSE	fast spin echo
FSPGR	fast spoiled gradient echo
FUS	focused ultrasound
FSE	fast spin echo
GBCA	gadolinium-based contrast agent
GFR	glomerular filtration rate
GRE	gradient echo (also gradient-recalled echo)
HASTE™	half-Fourier acquisition single-shot turbo spin echo (Siemens Healthcare)
HCC	hepatocellular cancer

Hz	Hertz
IBD	inflammatory bowel disease
IBS	irritable bowel syndrome
IP	in-phase
IR	inversion recovery
IV	intravenous
IVC	inferior vena cava
LOC	localizer
LI-RADS®	Liver Imaging Reporting and Data System
MDRD	Modification of Diet in Renal Disease
mg	milligram
MIP	maximum intensity projection
mL	milliliter
mm	millimeter
MRA	magnetic resonance angiography
MRCP	magnetic resonance cholangiopancreatography
MRS	magnetic resonance spectroscopy
msec	millisecond – one-thousandth of a second
mTm	milliTesla per meter
NEX	number of excitations; also NSA
NPO	nothing by mouth
NPW	no phase wrap
NSA	number of signal averages; also NEX
NSF	nephrogenic systemic fibrosis
OP	out-of-phase or opposed-phase
PCa	prostate cancer
PSA	prostate-specific antigen
PSD	pulse sequence database
PV	peripheral vascular
rBW	receiver bandwidth
RCC	renal cell carcinoma
RES	reticuloendothelial cell system
Res Comp	respiratory compensation
RF	radiofrequency
R/L	right/left
ROI	region of interest
Rt	right
SAR	specific absorption rate

SE	spin echo
SER	signal enhancement ratio
S/I	superior/inferior
SNR	signal-to-noise ratio
SPGR	spoiled gradient echo
SS	single shot
SSFSE	single-shot fast-spin echo (also SSTSE, single-shot turbo spin echo)
SW EPI	susceptibility-weighted echo-planar imaging
T	Tesla
TE	echo time
T/m/sec	Tesla per meter per second
TOF	time-of-flight
TR	repetition time; time to recovery
TRf	tailored RF (radio frequency)
TSE	turbo spin echo
UAE	uterine artery embolization
US	ultrasound
µs	microsecond – one-millionth of a second
VBw	variable bandwidth
ZIP	zero-filled interpolation

GLOSSARY

aberrant
an abnormality, exception, or peculiarity; deviation from the normal or usual

adenocarcinoma
a cancerous neoplasm originating in glandular tissue that develops in the lining or inner surface of an organ

adenoma
a common, benign epithelial neoplasm; the tissue is abnormal but not considered cancerous

adenomatosis
a benign condition characterized by multiple glandular overgrowths; hepatic adenomatosis results when multiple adenomas appear simultaneously

adenomyosis
uterine thickening that occurs when endometrial tissue, which normally lines the uterus, moves into the outer muscular walls of the uterus

adenopathy
swelling or enlargement of the lymph nodes; also called lymphadenopathy

adnexa, uterine
structures most closely related structurally and functionally eg ovaries, and fallopian tubes

agenesis
failure of an organ to develop during embryonic growth and development

aliasing
a common artifact caused when the field-of-view selected is smaller than the area of tissue excited; also known as wrap-around

anaphylactoid reaction/ anaphylactic/anaphylaxis
a systemic or generalized hypersensitivity reaction from exposure of a sensitized individual to a specific antigen, like shellfish, nuts, or penicillin, which otherwise is harmless to non-sensitized individuals. Unlike an allergic reaction, anaphylaxis can result in complete airway obstruction, shock, and even death. An *anaphylactoid* reaction resembles anaphylaxis but does not involve an immunological mechanism; sometimes called *pseudoanaphylactic*.

angiography/angiogram
an image of arteries and/or veins in the body. In MRI, angiograms are projection images created from multiple images acquired with flow-sensitive imaging protocols. Depending on the sequence selected, MRA can measure both the flow of blood through the vasculature, as well as it direction and velocity.

angiomyelolipoma (AML)
benign renal neoplasm consisting of fat and myloid tissue

apparent diffusion coefficient maps (ADC)
a measure of the magnitude of diffusion of water molecules in a tissue; ADC maps are useful for showing restricted diffusion in cancerous prostate tissue

artifact
an image artifact is a structure not normally present but visible in an image caused by blood flow or other patient motion, chemical shift or magnetic susceptibility efforts, or hardware or software problems of the MRI scanner

ascites
the build-up of fluid in the space between the lining of the abdomen and abdominal organs called the peritoneal cavity; ascites results from high pressure in the blood vessels of the liver (portal hypertension) and low levels of the protein albumin

atrophy
the partial or complete wasting away of a part of the body or organ

benign prostate hyperplasia (BPH)
increased prostate size; often called “enlarged prostate”

bicornuate uterus
uterus with two “horns,” resulting in a heart-shaped uterus

bilirubin
a brownish-yellow substance found in bile, produced when the liver breaks down old red blood cells. It is removed from the body through the stool and gives stool its normal color.

bolus
in contrast-enhanced MRA, a dose of a gadolinium-based contrast agent given in order to deliver the agent to an area of interest in a predictable amount of time

caudate lobe
an independent part of the liver connected to the right lobe

cerebral sulci
the furrows between the cerebral gyri, which are winding "paths" on the surface of the cerebral hemispheres

chemical saturation
a specialized technique that selectively saturates fat or water protons prior to acquiring data; the suppressing of either water or fat signal by using an RF pre-pulse that has an excitation frequency bandwidth specific to the precessional frequency of fat or water; also chemical fat saturation

cholangiocarcinoma
cancer of the bile ducts inside and outside the liver

cholecystectomy
surgical removal of the gallbladder

cholecystitis
inflammation of the gallbladder

choledocholithiasis
presence of a stone in the common bile duct

cine
a series of rapidly recorded multiple images taken at sequential cycles of time and displayed in a dynamic movie display format

cirrhosis
chronic liver disease in which healthy tissue is replaced by scarring characterized by inflammation and degeneration that often leads to jaundice, ascites, and hepatic death; causes of cirrhosis include hepatitis C, fatty liver, and alcohol abuse

compartment syndrome
as a result of severe contrast extravasation, diminished perfusion distal to the IV site due to swelling of the fascial planes

contiguity/contiguous
in imaging, when slices are adjacent, that is, without space in-between them

creatinine
byproduct of normal breakdown of creatine phosphate in the body; serum creatinine levels are used as a measurement of kidney function

Crohn's disease
an inflammatory bowel disease that results in chronic inflammation of any part of the large or small bowel, most prevalent at the terminal ileum. Symptoms are abdominal pain, diarrhea, bloating, cramping, loss of appetite, weight loss, and rectal bleeding. Crohn's can be managed medically but in severe cases may require surgery.

cyst
an abnormal sac that contains gas, fluid, or semi-solid material

dermoid
a type of fat-containing tumor

dielectric effect
a dielectric effect is caused by local eddy currents due to the increased conductivity of body tissue. In liver MRI, a dielectric effect is usually seen on images of the left lobe of the liver and is more prominent at 3.0 T. Manufacturer supplied dielectric pads placed between the patient and the anterior coil may help with artifacts.

diffuse
spread out or disseminated, as opposed to focal

diffusion-weighted imaging (DWI)
an acquisition technique that generates images with intensities that depend in part on the microscopic motion of water molecules

dilatation
also dilation; stretching or enlarging an opening

double duct sign
dilatation of both the pancreatic and bile ducts

echo-planar imaging (EPI)
similar to fast/turbo spin echo, multiple lines of *k*-space are acquired after each excitation using a gradient reversal to form an echo and at a much faster rate. EPI is the fastest of the gradient echo-based scanning protocols, although resolution and image quality may be lower than that of standard images

echo spacing
the time between successive echo read-out gradient pulses

edema
the observable swelling from the accumulation of fluid in body tissues

elastography
an imaging modality using ultrasound or MRI that maps the properties of soft tissue based on tissue stiffness indicating the presence of abnormal tissue

electrolyte
in the human body, primarily sodium, potassium, magnesium, calcium, chloride, and bicarbonate that in fluid dissociates into ions capable of conducting electrical current; constitutes a major force in controlling fluid balance in the body

embolotherapy
used in pre-operative management of highly vascular neoplasms by occluding the artery

end-expiratory
the most quiescent part of the respiratory cycle

endocrine gland
glands that secrete hormones into the bloodstream; includes the pituitary, thyroid, parathyroid, adrenal glands, and the thymus

endometrioma
circumscribed mass of ectopic endometrial tissue

endometriosis
the presence of actively growing and functioning endometrial tissue outside of the uterus

enterography
imaging of the small and large bowel

equilibrate
to keep in balance or in equilibrium

extracapsular
situated out the capsule or capsule lining

extracellular
literally, outside of a cell or cells, as opposed to *intracellular*

extravascular
literally, outside of the vessel, as opposed to *intravascular*

extravasation, contrast
the unintended or accidental infiltration of extravascular fluid into intravascular space

fascia/fascial
a band or sheet of fibrous connective tissue that envelops, binds, or separates muscles, organs, and other soft structures of the body

fast Fourier transform (FFT)
an efficient method for calculating the frequency content (the Fourier transform) of a digital signal; first described in 1965, it is universally used in MR image reconstruction

fibroid
noncancerous neoplasms in the uterine wall

fibrosis
formation of excess fibrous tissue as a reparative or reactive process; similar to scarring

field-of-view
area of tissue to be imaged

fistula
an abnormal connection or passageway between an organ, vessel, intestine, or other structure, caused by injury, surgery, infection, or inflammation; inflammatory bowel disease can lead to the creation of fistulas between one loop of intestine and another

focal
pertaining to a focus or foci, as opposed to diffuse

focal nodular hyperplasia (FNH)
a benign and common liver neoplasm that frequently displays a central scar or fibrovascular core

ghost/ghosting
in MRI, image artifact where a shifted copy of the object or “ghost” appears elsewhere in the image; commonly caused by patient motion in echo-planar imaging

Gleason score
a classification of adenocarcinoma of the prostate by evaluation of the pattern of glandular differentiation; the tumor grade is numbered on a scale of 1 to 5

gradient amplitude
the range that a gradient field can change from high to low; measured in milliTesla per meter

gradient echo (GRE)
MR signal that appears following the rephasing of spins by a gradient reversal in a gradient echo pulse sequence, which consists of an RF excitation pulse of 90° or less followed by pulses or reversals of magnetic field gradients; unlike spin echo, GRE has no refocusing 180° pulse after the initial excitation

hemangioma
benign tumor consisting primarily of dilated or newly formed blood vessels

hemochromatosis
a rare metabolic disorder caused by deposit of iron-containing substances, especially hemosiderin, and usually affecting the liver and pancreas

hemosiderosis
excessive deposit of hemosiderin, an iron-containing protein that results from disorders of iron metabolism and breakdown of red blood cells

hepatic adenoma
benign liver lesion that is clinically significant as liver adenomas tend to be symptomatic

hepatic steatosis
a condition where fat is stored in the liver; also known as fatty infiltration of the liver

hepatitis
a viral infection characterized by irritation or swelling of liver cells causing inflammation of the liver; often a result of the hepatitis virus, other infections, or alcohol abuse

hepatocellular carcinoma (HCC)
a primary malignancy that arises from the liver; commonly seen in patients with cirrhosis but occasionally seen in an otherwise normal liver; also known as hepatoma

hepatocyte
a liver cell

hepatorenal syndrome
acute renal failure in people with liver or biliary tract disease

heterogeneous
composed of parts of different kinds; incongruous; not homogeneous

histological/histology
the microscopic study of cells and tissues

homogeneous
having a common property throughout; essentially alike; not heterogeneous

hyperplasia
abnormal multiplication of cells

inflammatory bowel disease
umbrella term for ulcerative colitis and Crohn's disease

in-phase imaging
when fat and water protons resonate at the same frequency within the same voxel; controlled by TE in a GRE pulse sequence

iodinated contrast agent
iodine-based contrast agents are used in CT scanning; they may be classified as ionic or nonionic

induration
an abnormally hard spot

***k*-space**
the domain in which the information from each phase-encoding step is placed during a pulse sequence. Each "filled in" line of *k*-space corresponds to each phase-encoding step; once the required amount of *k*-space is filled, image reconstruction with a Fourier transform can begin

lactic acidosis
a type of metabolic acidosis caused by an accumulation of lactic acid, typically due to lack of oxygen to the tissue

lipoleiomyomata
a type of fat-containing tumor

lymphadenopathy
enlarged lymph nodes; a disease process that affects a lymph node(s)

magnetic susceptibility
the ability of a material to become magnetized

maximum intensity projection (MIP)
a projection image that is obtained from a 3D data set by selecting the maximum intensity along lines or rays that cut through the 3D image volume

metastasis/metastatic
also called secondary cancer; a malignant tumor that has spread from another organ (primary site) affected by cancer

myeloid
tissue primarily found in the red bone marrow but also present in the liver and spleen

morphology/morphological
the outward appearance and internal form and structure of an organism

myolipoma
a rare, benign neoplasm consisting mainly of fat cells

myomectomy
removal of a fibroid from the uterus through the vagina

myometrium
the middle layer of the uterine wall that is muscular and comprises the bulk of the organ

navigator device
a navigation pulse usually placed at the diaphragm or dome of the liver that tracks a patient's respiratory cycle and triggers the sequence to acquire data during the expiratory phase

neoplasm
abnormal mass of tissue due to neoplasia, an abnormal proliferation of cells

nephrogenic hypertension
hypertension caused by factors originating in the kidney, eg, renal artery stenosis

nephrogenic systemic fibrosis (NSF)
a rare but serious condition that has been associated with the use of gadolinium-based contrast agents in patients with kidney disease

nephron
basic cell unit of the kidney

oblique angle
a plane that is not a multiple of 90°, as opposed to an orthogonal angle, which is a right angle

opacification
to make opaque; impenetrable by light, as opposed to transparent

orthogonal angle
a right angle, as opposed to an oblique angle, which is not a multiple of 90°

out-of-phase/opposed-phased imaging
when fat and water protons precess at 180° from each other within the same voxel; controlled by TE in a GRE pulse sequence

pancreas divisum
the most common anatomic variant of the pancreas resulting from failure of fusion of the dorsal and ventral pancreatic ducts. May be associated with an increased prevalence of acute pancreatitis. MRCP has been shown to have up to 100% accuracy for detection of pancreas divisum.

pancreatitis
inflammation of the pancreas; acute pancreatitis presents suddenly, while chronic pancreatitis is characterized by recurring or persistent pain

parallel imaging
imaging sequences that shorten acquisition time by calculating sensitivity maps of the individual elements of a phased-array coil. The sensitivity maps are used to under-sample areas of *k*-space thereby reducing acquisition time

paramagnetic
having a small but positive magnetic susceptibility; the tendency of magnetic dipoles to align with an external magnetic field. Gadolinium has paramagnetic properties.

parenchyma/parenchymal
the specific tissue of an organ as opposed to connective or supporting tissue

parous
having given birth one or more times

peristalsis
the series of muscle contractions that occur in the digestive tract, moving food through the digestive system, urine from the kidneys into the bladder, and bile from the gallbladder into the duodenum

peritoneum
the serous membrane that forms the lining of the abdominal cavity

phased-array coil
any set of small receiving-element coils aligned in unison yet connected to individual receivers that provide the SNR of a single smaller coil yet the coverage of a single large coil

pheochromocytoma
a rare, usually benign adrenal tumor

pixel
smallest discrete part of a digital image (2D) display; from "picture element"

precess/precession
the "wobbling" rotation of a spinning object; the spin axis of the precessing object describes a cone-shaped path

primary sclerosing cholangitis (PSC)
a disease of the bile ducts that causes inflammation and subsequent obstruction of bile ducts both at an intrahepatic and extrahepatic level

prolapse
a condition in which an organ is misaligned or slips out of place, eg the uterus or rectum

prostate-specific antigen (PSA)
a protein produced by the cells of the prostate gland, normal range is 0 – 3.9. PSA velocity is a marked increase in PSA within a short time of period, even if the PSA itself falls within the normal range.

prostatitis
inflammation of the prostate gland; can be chronic or acute

pseudocyst
an accumulation of fluid in a cyst-like structure

quiescent
being quiet, still, or at rest

radiofrequency (RF)
the frequency of radio waves that oscillate in the range of around 3kHz to 300 GHz. RF signal in MRI is produced by the transmit and receive coils that generate and receive electromagnetic fields.

receiver bandwidth (rBW)
a range of frequencies used to sample the MR signal and a parameter that is under the control of the scan operator

relaxivity
the ability of magnetic compounds, like gadolinium-based contrast agents, to increase the relaxation rate of water protons in the surrounding tissue to improve tissue contrast

renal cell carcinoma (RCC)
the most common type of kidney cancer that originates in the small tubes that transport waste from the blood to the urine

renal hilar lymphadenopathy
disease of the lymph nodes specific to the adrenal glands and the renal hilar regions; the renal pedicle is the hilum (depression around the point of entrance or exit) of the kidney

respiratory trigger/triggering
acquisition of image data timed to the patient's respiratory cycle measured by placing air-filled bellows over the patient's abdomen. The expansion and contraction of the bellows allow the pulse sequence to acquire phase-encoding steps during the most quiescent (end-expiratory) period of the respiratory cycle, therefore greatly reducing respiratory ghosting.

rise time
the time required for a gradient to reach a specified amplitude, most often in microseconds

saturation
a tissue state where the longitudinal magnetization of the tissue cannot fully recover before being excited by the next slice-excitation RF pulse. Saturation typically occurs when the selected TR is far shorter than the tissue T1 time. Most frequently used to suppress fat signal from appearing in the image and to aid in the suppression of motion artifacts.

scan delay
the time needed for contrast material to arrive at the area of interest for best arterial enhancement; used for dynamic imaging

scout image
a quick set of data acquired in multiple planes to assist in planning subsequent sequences

sensitivity
ability of an imaging technique to determine whether there is pathology

septate, septation
when referring to the uterus, a divided uterus

shimming
technique used to eliminate inhomogeneity in the main magnetic field, B_0. Shimming is performed prior to certain exams by measuring and adjusting the main magnetic field with additional coils installed in the scanner and called active shimming. Passive shimming uses small pieces of metal to adjust the magnetic field when the magnet is installed.

signal enhancement ratio (SER)
a measurement of contrast uptake over time in a specific anatomical region

signal-to-noise ratio (SNR)
amount of true signal relative to the amount of random background signal (noise) on an image

slew rate
the overall gradient performance as a function of gradient amplitude and gradient rise time; described in units of Tesla per meter per second

sonication
a short burst of high-frequency ultrasound beam

spatial resolution
the most critical of the three primary requirements of a highlight diagnostic MRI exam: spatial resolution, SNR, and image contrast. Spatial resolution defines how much detail can be captured in an image and is dependent on the matrix size acquired; the smaller the voxel size, the higher the spatial resolution.

specific absorption rate (SAR)
the RF power absorbed per unit of mass of an object, measured in watts per kilogram (W/kg)
FDA SAR limits

- 4 W/kg averaged over the whole body for any 15-minute period
- 3 W/kg averaged over the head for any 10-minute period
- 8 W/kg in any gram of tissue in the head or torso for any 5-minute period
- 12 W/kg in any gram of tissue in the extremities for any 5-minute period

specificity
the ability of an imaging technique to determine what the specific pathology is

spin echo
MR signal that appears due to the rephasing of spins by a 180° refocusing pulse that follows the initial 90° RF pulse in a spin echo pulse sequence

stenosis
abnormal narrowing of a vessel

stroma
connective, functionally supportive framework of a cell, tissue, or organ

subtraction series
the subtraction of precontrast images from postcontrast images

surface coil
a receive-only coil that serves as a receiving antenna and collects the signal from excited protons, then carries that signal back into the RF subsystem for analysis and conversion into *k*-space. Surface coils are designed for a specific anatomical part and come in all shapes and sizes, as well as single- and multi-coil designs.

temporal resolution
how rapidly an image data set is acquired; as temporal resolution decreases, spatial resolution increases

terminal ileum
the most distal part of the small intestine

thrombosis
formation of a blood clot inside a blood vessel

time-of-flight imaging (TOF)
a pulse sequence that makes stationary materials appear dark on the image, while moving tissues such as blood show up bright due to flow-related enhancement. The resulting image shows only flowing blood which in turn provides an outline of the blood vessels.

tri-phasic flow velocities
when arterial blood flow moves in three distinct phases: fast forward, short reverse, then fast forward; becomes more prominent the farther away from the heart

ulcerative colitis
an inflammatory bowel disease that is limited to the large bowel (unlike Crohn's disease) and affects only the lining of the colon

unicornuate uterus
normal uterus, that is, with one “horn”

urticaria
a skin condition characterized by welts or wheals that itch intensely and can be caused by an allergic reaction, infection, or stress; commonly called *hives*

uterine stripe
the mucous membrane (endometrium) that lines the uterus

vasculopathy
any disease or disorders of the blood vessels

venography/venogram
x-ray visualization of the veins, especially the veins of the leg

venous contamination
in an MRA image, unwanted signal of veins typically due to mistiming the arrival of the contrast bolus

ventriculomegaly
a brain condition that occurs when the lateral ventricles become dilated

volume averaging
the incomplete visualization of anatomy in an image due to a slice thickness that is greater than the anatomy itself; also known as partial volume effect

voxel
volume of tissue corresponding to a pixel on an MR image; from “volume element”